Preparation of the Implementation Plan of AASHTO Mechanistic-Empirical Pavement Design Guide (M-EPDG) in Connecticut: Phase II – Expanded Sensitivity Analysis and Validation with Pavement Management Data

Prepared By: Iliya Yut, James Mahoney and Donald A. Larsen, P.E.

February 8, 2017

Report Number: CT-2293-F-17-1

SPR-2293

Connecticut Transportation Institute
School of Engineering
University of Connecticut

Prepared For:
Connecticut Department of Transportation
Bureau of Policy and Planning
Research Information Systems Unit
Research Section

Michael Connors
Assistant Planning Director

Disclaimer

This report [article, paper or publication] does not constitute a standard, specification or regulation. The contents of this report [article, paper or publication] reflect the views of the author(s) who (are) responsible for the facts and the accuracy of the data presented herein. The contents do not necessarily reflect the views of the Connecticut Department of Transportation or the Federal Highway Administration.

Acknowledgements

This report was prepared by the University of Connecticut, in cooperation with the Connecticut Department of Transportation and the United States Department of Transportation, Federal Highway Administration. The opinions, findings and conclusions expressed in the publication are those of the author(s) and not necessarily those of the Connecticut Department of Transportation or the Federal Highway Administration.

Standard Conversions

SI* (MODERN METRIC) CONVERSION FACTORS

APPROXIMATE CONVERSIONS TO SI UNITS

Symbol	When You Know	Multiply By	To Find	Symbol
		LENGTH		
in	inches	25.4	millimeters	mm
ft	feet	0.305	meters	m
yd	yards	0.914	meters	m
mi	miles	1.61	kilometers	km
		AREA		
in^2	square inches	645.2	square millimeters	mm^2
ft^2	square feet	0.093	square meters	m^2
yd^2	square yard	0.836	square meters	m^2
ac	acres	0.405	hectares	ha
mi^2	square miles	2.59	square kilometers	km^2
		VOLUME		
fl oz	fluid ounces	29.57	milliliters	mL
gal	gallons	3.785	liters	L
ft^3	cubic feet	0.028	cubic meters	m^3
yd^3	cubic yards	0.765	cubic meters	m^3
		NOTE: volumes greater than 1000 L shall be shown in m^3		
		MASS		
oz	ounces	28.35	grams	g
lb	pounds	0.454	kilograms	kg
T	short tons (2000 lb)	0.907	megagrams (or "metric ton")	Mg (or "t")
		TEMPERATURE (exact degrees)		
^oF	Fahrenheit	5 (F-32)/9 or (F-32)/1.8	Celsius	^oC
		ILLUMINATION		
fc	foot-candles	10.76	lux	lx
fl	foot-Lamberts	3.426	$candela/m^2$	cd/m^2
		FORCE and PRESSURE or STRESS		
lbf	poundforce	4.45	newtons	N
lbf/in^2	poundforce per square inch	6.89	kilopascals	kPa

APPROXIMATE CONVERSIONS FROM SI UNITS

Symbol	When You Know	Multiply By	To Find	Symbol
		LENGTH		
mm	millimeters	0.039	inches	in
m	meters	3.28	feet	ft
m	meters	1.09	yards	yd
km	kilometers	0.621	miles	mi
		AREA		
mm^2	square millimeters	0.0016	square inches	in^2
m^2	square meters	10.764	square feet	ft^2
m^2	square meters	1.195	square yards	yd^2
ha	hectares	2.47	acres	ac
km^2	square kilometers	0.386	square miles	mi^2
		VOLUME		
mL	milliliters	0.034	fluid ounces	fl oz
L	liters	0.264	gallons	gal
m^3	cubic meters	35.314	cubic feet	ft^3
m^3	cubic meters	1.307	cubic yards	yd^3
		MASS		
g	grams	0.035	ounces	oz
kg	kilograms	2.202	pounds	lb
Mg (or "t")	megagrams (or "metric ton")	1.103	short tons (2000 lb)	T
		TEMPERATURE (exact degrees)		
^oC	Celsius	1.8C+32	Fahrenheit	^oF
		ILLUMINATION		
lx	lux	0.0929	foot-candles	fc
cd/m^2	$candela/m^2$	0.2919	foot-Lamberts	fl
		FORCE and PRESSURE or STRESS		
N	newtons	0.225	poundforce	lbf
kPa	kilopascals	0.145	poundforce per square inch	lbf/in^2

*SI is the symbol for the International System of Units. Appropriate rounding should be made to comply with Section 4 of ASTM E380.
(Revised March 2003)

Technical Report Documentation Page

1. Report No. CT-2293-F-17-1	2. Government Accession No. N/A	3. Recipient's Catalog No.
4. Title and Subtitle Preparation of the Implementation Plan of AASHTO Mechanistic-Empirical Pavement Design Guide (M-EPDG) in Connecticut: Phase II – Expanded Sensitivity Analysis and Validation with Pavement Management Data		5. Report Date February 8, 2017 6. Performing Organization Code
7. Author(s) Iliya Yut, James Mahoney and Donald A. Larsen, P.E.		8. Performing Organization Report No. CAPLAB 01-2017
9. Performing Organization Name and Address University of Connecticut Connecticut Transportation Institute 270 Middle Turnpike, U-5202 Storrs, Connecticut 06269-5202		10 Work Unit No. (TRIS) N/A 11. Contract or Grant No. CT Study No. SPR-2293 13. Type of Report and Period Final Report January 2015 – June 2016
12. Sponsoring Agency Name and Address Connecticut Department of Transportation 2800 Berlin Turnpike Newington, CT 06131-7546		14. Sponsoring Agency Code SPR-2293
15. Supplementary Notes Prepared in cooperation with the U.S. Department of Transportation and Federal Highway Administration		

16. Abstract

The study re-evaluates distress prediction models using the Mechanistic-Empirical Pavement Design Guide (M-EPDG) and expands the sensitivity analysis to a wide range of pavement structures and soils. In addition, an extensive validation analysis of the accuracy of the M-EPDG model predictions was conducted using CTDOT's Pavement Management Information System (PMIS) data. The major findings indicate:

(1) Overall, the Pavement-ME software has capability of running multiple simulation projects simultaneously, thus accelerating sensitivity analyses.

(2) The PMIS in Connecticut was found to report overestimated extent of linear cracking, most likely, due to built-in settings of the processing algorithms.

(3) The statistical analysis of predicted and reported distress values indicated poor accuracy of Pavement-ME predictions regarding fatigue and thermal cracking in Connecticut. On the other hand, longitudinal cracking, IRI, and rutting predictions were found correlated with PMIS-reported values.

(4) This study confirmed that an increase in the level of detail for asphalt material properties could lead to an increase in accuracy for longitudinal cracking prediction.

17. Key Words M-EPDG, composite pavements, sensitivity analysis, M-EPDG Implementation	18.Distribution Statement No restrictions. This document is available to the public through the National Technical Information Service, Springfield, Virginia 22161. The report is available on-line from National Transportation Library at http://ntl.bts.gov.

19. Security Classif. (of report) Unclassified	20. Security Classif. (of this page) Unclassified	21. No. of Pages 146	21. Price
Form DOT F 1700.7 (8-72)	Reproduction of completed page authorized		

Table of Contents

List of Figures

List of Tables

List of Acronyms and Abbreviations

AADTT	Average Annual Daily Truck Traffic
AASHTO	American Association of State Highway and Transportation Officials
AC	Asphalt Concrete
ACACPCC	AC-on AC on PCC
ACBIND	AC layer binder performance grade
ACOLBIND	AC Overlay Binder performance grade
ACPCC	AC on PCC
ANOVA	Analysis of Variance
ARAN^{TM}	Automatic Road Analyzer
CTDOT	Connecticut Department of Transportation
CTI	Connecticut Transportation Institute
DOT	Department of Transportation
EB	Resilient modulus of granular base
ES	Resilient modulus of subgrade
ESB	Resilient modulus of granular subbase
FHWA	Federal Highway Administration
FWD	Falling Weight Deflectometer
HAC	Thickness of AC layer
HACOL	Thickness of AC overlay layer
HBASE	Thickness of granular base
HMA	Hot Mixed Asphalt
HMILL	Milled-off thickness of existing AC layer
HPCC	Thickness of PCC slab
HSB	Thickness of granular subbase
IRI	International Roughness Index
LTPP	Long-Term Pavement Performance
M-EPDG	Mechanistic-Empirical Pavement Design Guide
NAC	New AC
NCHRP	National Cooperative Highway Research Program
NWP	Non-wheelpath
PCC	Portland Cement Concrete
PG	Performance Grade
PMIS	Pavement Management Information System
PR	Pre-overlay performance rating of the existing surface
PSA	Total percent slabs repaired after restoration
PSB	Combined percent slabs cracked and repaired before restoration
SHRP	Strategic Highway Research Program
SPR	SP&R =State Planning and Research
TAP	Technical Advisory Panel
TOTRUTEXIST	Total rutting in existing AC-on-PCC pavement
UConn	The University of Connecticut
VCD	Vehicle Class Distribution
WIM	Weigh-in-Motion
WP	Wheelpath

Executive Summary

Introduction

This report summarizes background information, the research methodology, and major findings from the SPR-2293 project, which encompasses the second phase of the preparation for implementation of the Mechanistic-Empirical Pavement Design Guide (M-EPDG) by the Connecticut Department of Transportation (CTDOT). This study by the Connecticut Transportation Institute at the University of Connecticut expanded the sensitivity analysis conducted under the first phase (SPR2274) to a wider range of pavement structures and subgrade soils. In addition, an extensive validation analysis of the accuracy of the M-EPDG distress model predictions was conducted with the use of CTDOT Pavement Management Information System (PMIS) data.

The two main objectives of this study were (1) to include flexible and composite pavements on thinner base/subbase with variable quality as well as uncertain distributions of vehicle classes and (2) ability of M-EPDG software to predict pavement performance at a higher level of detail (Level 2) using PMIS inputs.

Methodology

The research approach for this project included (1) sensitivity analysis of M-EPDG inputs with both M-EPDG 1.1 (the last publically available) and Pavement-ME (most recent commercial) software packages, (2) evaluation of PMIS inputs to be used for validation of M-EPDG distress predictions, and (3) evaluation of accuracy of the Pavement-ME predictions based on PMIS data.

Altogether, over 600 simulation runs of design software were conducted for three types of pavements (new AC, AC on PCC and AC-overlaid AC on PCC) in the three climatic zones in Connecticut. Three levels of input values (high, base, and low) were evaluated with regard to traffic (truck traffic volume and vehicle class distribution), pavement structure (layer thickness), and material properties (e.g., AC binder performance grade and volumetrics as well as unbound material moduli), and rehabilitation parameters (e.g., existing surface rating and percent PCC slabs repaired). Based on the results of statistical analysis, an importance ranking was assigned to each input based on its contribution to the variability in predicted distress outcome.

The PMIS data included location, layer thicknesses, and traffic design level for 48 pavement sections (177 0.1-mile segments), whereas the subgrade properties were extracted from the national M-EPDG database. The performance data for those sections included crack lengths and orientations, average IRI, and average rutting per segment. The multiple correlation analysis was conducted to evaluate reasonability of annual deterioration trends and relationships between PMIS inputs and reported pavement performance.

The accuracy of Pavement-ME distress predictions were evaluated by the analysis of a correlation between predicted and reported distress values. This analysis included performing a two-sample Kolmogorov-Smirnov test for normality of distributions, followed by the analysis of

the significance of Pearson's correlation between datasets of predicted and reported distress values

Conclusions on Sensitivity Analysis of Pavement-ME Inputs

Overall, the new Pavement-ME software allows for faster runs of simulation projects, although having a more complicated structure of the reports. The Pavement-ME sensitivity runs mostly yielded similar rankings of design input importance compared with that of the M-EPDG runs, with the following observations worth noting:

- The Pavement-ME longitudinal cracking model for new AC pavements is much more sensitive to input changes as compared with the M-EPDG software.
- For thicker AC-overlaid AC on PCC pavements, the Pavement-ME analysis yielded on average much lower sensitivity of cracking predictions to all input as compared with M-EPDG software. In addition, for this pavement type, the Pavement-ME analysis yielded larger effects of subgrade and pre-overlay pavement surface condition on rutting and IRI as compared with M-EPDG software.
- For AC-overlaid PCC pavements, cracking sensitivity rankings were noticeably different between the Pavement-ME and M-EPDG prediction models. This included finding of zero sensitivity for the transverse (thermal) cracking model and an enormously high (up to 2300%) variation in longitudinal cracking predictions. This does exclude reflective cracking as the Pavement-ME software counts that type of cracking as slab cracking.

Accuracy of PMIS Performance Data

- The analysis of pavement performance data generated by the WiseCrax^{TM} software was complemented by the visual evaluation of distresses directly from the Photolog pavement surface images. The following are the most significant findings from the analysis:
- It appears that PMIS reports overestimate the extent of linear cracking in all directions, possibly because of built-in settings of the processing algorithms. In particular, the factor of overestimation was slightly larger with respect to longitudinal cracking for data collected with laser cameras used on CTDOT van 8 whereas the strobe system (CTDOT van 7) significantly overestimated transverse cracking.
- The analysis of annual deterioration trends indicated that visual assessment of the images is likely to be closer than the automated method to "ground truth."
- Although alligator cracking has never been reported by the WiseCraxTM system, it is deemed feasible and advantageous to develop a transfer function to estimate the alligator cracking in percent area from the total linear cracking length. This is important because the alligator cracking is one of the major distress outputs in Pavement-ME analysis.

Validation of Accuracy of Pavement-ME Predictions

- Extensive analysis of distributions along with multiple correlation analysis of predicted and reported distress values generally indicated poor accuracy of Pavement-ME predictions regarding cracking with the exception of longitudinal cracking, IRI, and AC layer rutting. This difference was made more evident by the way cracks are categorized

in the Pavement-ME software as compared to CTDOT's Pavement Management software.
- Analysis of the influencing factors on the accuracy of Pavement-ME predictions revealed pavement type having the highest influence on bias in prediction of all distresses, followed by construction type (new or rehabilitation).
- It has been confirmed that an increase in the level of detail for asphalt material properties can lead to an increase in accuracy for longitudinal cracking prediction.

Recommendations

The following studies and activities are proposed for the next phase (Phase III) of the implementation of M-EPDG in Connecticut:

- Develop a database of vehicle class distributions based on the average daily traffic data for the set of pavements used in this project, and use this data in the calibration phase.
- Determine master curves for typical AC binders historically used in Connecticut (PG 64-22, PG 64-28, and AC-20) and use this information in the calibration phase.
- Calibrate AC layer rutting, Longitudinal Cracking, and IRI models on the set of pavements used in the validation analysis.
- Use Level 2 data for traffic and asphalt material data in order to increase the accuracy of the Pavement-ME distress predictions.

CHAPTER 1 Introduction

This report summarizes background information, the research methodology, and major findings from the SPR-2293 phase II project for implementation of the Mechanistic Empirical Pavement Design Guide (M-EPDG). This project was performed for the Connecticut Department of Transportation (CTDOT) by a research team from the Connecticut Transportation Institute at the University of Connecticut (UConn). The study re-evaluates M-EPDG prediction models using both M-EPDG version 1.1 software (formerly available on-line) and the most recently released commercial Pavement-ME software and expands the sensitivity analysis to a wider range of pavement structures and subgrade soils. In addition, an extensive validation analysis of the accuracy of the M-EPDG model predictions is conducted with the use of CTDOT Pavement Management Information System (PMIS) data.

Under the phase I project (SPR-2274), the research team conducted a limited sensitivity analysis for thick flexible and composite pavements. The initial range of design inputs was based on design traffic levels and asphalt mix volumetric properties as specified by CTDOT construction specifications. The traffic distribution parameters and unbound material modulus values were adopted at default Level 3, which had the lowest level of detail of the three levels of hierarchy provided by the M-EPDG software. In addition to the limited sensitivity analysis, an example validation of the distress predictions was attempted using the Long Term Pavement Performance (LTPP) data from the Special Pavement Studies (SPS) project 9A located on Route 2, in Lebanon, CT [2]. The main products of the initial research were (1) a comprehensive step-by-step implementation plan for M-EPDG, (2) recommendations on the use of hierarchical levels for traffic and material data collection, and (3) suggestions on the calibration of the M-EPDG predictive models to local Connecticut conditions.

The second phase of the project, which is summarized in this report, included expanded range of inputs to address uncertainties in the distribution of vehicles of a particular AASHTO class (e.g., single-unit trucks, single-axle trailers and others) on both the limited and unlimited access routes in Connecticut. The subgrade inputs included the weaker subgrade soils and poorly graded subbase materials that are typically found on these types of roadways. In addition, the following three scenarios of pavement design were included in the sensitivity analysis: (1) thinner asphalt pavements (4-9 inch asphalt pavements), (2) asphalt-overlaid asphalt-on-Portland cement concrete and (3) asphalt-overlaid repaired Portland cement concrete pavements. Lastly, the research team used a wider range of inputs from the Department's pavement management database for validating M-EPDG distress predicting models.

Objectives

The second phase of the preparation for implementation of M-EPDG in Connecticut under SPR-2293 study targets two main objectives:

1. Expand the sensitivity analysis of M-EPDG inputs to include thinner flexible and composite pavements on weaker subgrade (8-12 inch bases) with uncertain traffic volumes. This is in comparison to SPR 2274, which used asphalt pavement thicknesses of 8-12 inches and bases of 10-18 inches.
2. Validate M-EPDG distress predictive capabilities using State level of input hierarchy (Level 2).

Organization of the Report

The first Chapter of this report presents the problem statement and lists the objectives of this study. Chapter 2 provides an updated literature review on M-EPDG implementation efforts nationwide, supported by a Bibliography (Appendix A). Chapters 3 and 4 present the methodology and compare the sensitivity analyses of design inputs conducted with M-EPDG version 1.1 and Pavement-ME software packages, respectively. Chapter 5 provides the results of an evaluation of pavement characteristics and performance data available within the CTDOT PMIS in order to validate its applicability for use with Pavement-ME design software. Chapter 6 discusses the accuracy of PMIS performance data as generated from CTDOT WiseCrax™ distress reports. The validation of Pavement-ME prediction models in terms of accuracy and potential for their successful calibration is discussed in Chapter 7. Lastly, Chapter 8 provides a summary of major findings as well as recommendations for the next phase of M-EPDG implementation efforts in Connecticut. The supporting PMIS data for Chapters 5 and 6 are located in Appendices B and C, respectively. Appendix D contains Pavement-ME inputs and outputs to support the discussion in Chapter 7.

CHAPTER 2 Literature Review

Introduction

This chapter summarizes findings from literature pertinent to the objectives of the project. The next few sections review the state of the art in implementing AASHTO Mechanistic Empirical Pavement Design Guide (M-EPDG) on a national scale. The emphasis is made on local calibration efforts and the use of Pavement Management Data to validate M-EPDG predictions of distresses for flexible and composite pavements. A comprehensive bibliography can be found in Appendix A.

Nationwide M-EPDG Validation and Calibration Efforts

The M-EPDG employs prediction of the distresses in pavement layers through the correlation of the load- and temperature-related engineering stresses with measured values of cracking, rutting, faulting, and roughness [4]. The inputs of physical properties of asphalt, Portland cement concrete (PCC), granular bases, and subgrade are required for computing the stresses. The in-situ distress measurements, on the other hand, are provided by the LTPP distress data collected from hundreds of test pavement sections spread throughout the mainland U.S. and Canada. The M-EPDG manuals recognize the limitations of the M-EPDG in terms of adequacy of distress predictions. Those limitations originate in the inability of the LTPP dataset to be truly representative of the large variety of traffic, climate, and subgrade soil conditions that exist. In addition, the LTPP dataset does not reflect the extent of the variability in pavement material properties nationwide [4]. Therefore, the local calibration of the M-EPDG predictive models is highly recommended where the disparities between measured and predicted distresses are significant [4, 5]. A Guide for Local Calibration of M-EPDG has been developed under NCHRP Project 01-40B [5].

The calibration of the M-EPDG distress prediction models can be made through the M-EPDG software user interface by adjusting the regression coefficients in the M-EPDG predictive models [3, 4]. However, the abundance of required inputs and large number of coefficients in the statistical models complicate this task. A recent AASHTOWare® customer survey has indicated that only nine (9) out of 52 users have completed their calibration efforts, while another 20 agencies have the calibration process underway [6]. It should be noted that over the last three years, the publically available evaluation version 1.1 of the M-EPDG has been decommissioned and replaced by commercial software called Pavement ME [7]. Quite a few agencies that started implementing M-EPDG earlier and wanted to transition from M-EPDG 1.1 to Pavement ME reported differences in sensitivity rankings between the two packages, as well as calibration issues with the latter [8]. Most of the calibration studies report using M-EPDG 1.1 version, apparently because they already have had it in place and, most likely, because of easier access to the calibration coefficients as compared with Pavement ME [9-15]. Some state DOTs (e.g., Oregon, North Carolina New Mexico Iowa, and Louisiana) turn to research teams at local universities [10, 12, 15-17]. Other agencies (e.g., Colorado, Georgia, Idaho, and Arizona) employ Applied Research Associates, Inc., who is an official AASHTO contractor for this matter, to conduct implementation and calibration of the commercial Pavement-ME prediction models [18-21].

Challenges and Solutions for Validating M-EPDG Predictions

To reduce the cost of performing calibration, it is feasible to decrease the amount of inputs and optimize a desired level of input detail through a sensitivity analysis [3, 4]. Previous studies in Connecticut and other states have found that inputs related to truck traffic and the asphalt properties are the most influencing factors for the majority of distresses in flexible pavements [3, 8-15]. For overlaid flexible and composite pavements, pavement condition of a rehabilitated surface has been found to have an overwhelming effect on the outcome predicted by the M-EPDG [3, 10, 11].

Traffic Data

Reliable vehicle classification and axle load distributions are crucial for adequately modeling the effect of traffic on the distresses, for all types of pavement. Such data are usually generated from the Weigh-in-Motion (WIM) load and axle counts [4, 7]. Some agencies have invested significant time and resources into generating M-EPDG traffic inputs by employing WIM stations, even on non-Interstate roads [11, 12, 14, 19, 21]. However, most calibration studies only reported using traffic counts from their pavement management data in conjunction with the fixed M-EPDG default distribution values [8-10, 13, 15]. Note that there is an argument about the sensitivity of M-EPDG predictions to the axle load distribution input [8, 15]. Ultimately, it can be beneficial to go beyond the average annual daily truck traffic (AADTT) levels and explore the sensitivity of variable default traffic distributions offered by the M-EPDG, for a variety of road functional classes, as it has been attempted in this project.

Material Characterization

To achieve a greater precision in distress predictions, it is desired to measure both strength and stiffness of bound and unbound pavement layers [4]. Over the last two decades, many material tests have been developed under the Strategic Highway Research Program (SHRP), with the potential to be included into M-EPDG [4]. However, in most cases the material information from the time of construction is not available in the M-EPDG format, especially for older roads in New England, and, particularly, in Connecticut. Most of the other agencies reported using a combination of LTPP data, typical agency values, and Level 3 default values offered by the M-EPDG [9, 10, 13, 15, 20, 21].

The most advanced level of material characterization has been reported, for instance, by Iowa, North Carolina, and Colorado studies [8, 12, 19]. In Iowa, hot mix asphalt (HMA) mix design information from 4000 construction projects was available, while granular material and soil properties were tested under a special task [8]. In North Carolina and Colorado, most of the effort was invested in laboratory testing to verify twelve typical asphalt mix designs [12, 19]. The subgrade soil properties were developed using a geographic information system (GIS) to superimpose location and material properties retrieved from a National Soil Database for use with M-EPDG, generated under NCHRP project 09-23A [12, 24]. For granular base, the Level 3 default values were used in the absence of testing data [12].

Existing Pavement Condition

For the efficient calibration of the M-EPDG, predicted and measured distress values should be first compared to determine the magnitude of prediction error [4, 5]. The distress data can be ultimately retrieved from a Pavement Management Information System (PMIS), which exists in the vast majority of the U.S., including Connecticut. In particular, distress data from the research

road testing facilities in Minnesota (MnRoad) and Alabama (National Center for Asphalt Testing) has been instrumental in calibrating M-EPDG distress models [22, 23].

One challenge of using PMIS data for M-EPDG calibration is to match the units of distress used in the M-EPDG to the units reported by an agency [8-13]. For example, the LTPP distress manual distinguishes between linear units for longitudinal and transverse cracking and area percentage for alligator cracking, whereas CTDOT reports linear units for all types of cracking [25]. Some other challenges include matching definitions of distress severity [10], separating rutting in individual layers from the total rutting in a pavement structure [8, 9], and differentiating between thermally induced and joint reflection transverse cracking [8]. Lastly, the amount of cracking reported by an automated pavement survey system may differ from windshield survey results [9, 25].

Selecting Candidate Sections from PMIS

To increase the accuracy of M-EPDG distress predictions, it is crucial to select a set of existing pavement sections that adequately represents typical site conditions (i.e., climate, traffic, and subgrade). The selected candidate sections should also reflect, as much as possible, the variety of local pavement layer thicknesses, layer material properties, and existing pavement surface conditions. The number of sections and the range of existing pavement structure and material inputs vary considerably between the reporting agencies [8-15]. For example, the NCHRP project 1-40B report prescribes a minimum of 20 to 30 test sections to be selected for the calibration of rutting and alligator cracking models, respectively [5]. Depending on the prevalent pavement type and size of their State, the agencies have chosen between 20 to 40 new HMA pavements, 5 to 35 new PCC pavements, and 5 to 35 composite/rehabilitated pavements for the validation and calibration studies [8-15]. It has been noted that most of the reviewed calibration studies included LTPP sections from the national calibration datasets in conjunction with PMIS sections [8, 9, 12, 15]. All studies based their selection criteria mostly on the completeness of the PMIS data and a geographic location. Some studies targeted specific pavement structures [9], specific materials [12], or specific road use [14].

Use of Non-Destructive Deflection Testing to Generate M-EPDG Inputs

Non-destructive measurement of pavement deflections by Falling Weight Deflectometers (FWD) has been extensively used by the majority of the transportation agencies in the U.S. for evaluation of the structural capacity of pavements, since 1980 [26]. The FWD employs measuring deflections due to peak impact load generated by dropping a known weight from a known height. A set of 5 to 7 transducers record deflections under the plate and up to 60 inches from the load center, in 12-in. increments. Under the LTPP program, the FWD data was used to evaluate the structural integrity of a pavement system as a whole, as well as for backcalculating individual pavement layer elastic moduli [27, 28]. The iterative methods for moduli backcalculation incorporated in MODCOMP and EVERCALC software have been reported as most successful in analyzing non-linear pavement response in LTPP sections with minimal error [20]. Therefore, the M-EPDG recommends using backcalculated moduli of unbound layers as Level 2 inputs [3]. The Federal Highway Administration (FHWA) initiated case studies of the use of FWD data and analysis with M-EPDG as early as 2006 [29] Most recently, new backcalculation techniques have been explored to use FWD-measured deflections for directly predicting parameters of master curves for asphalt mixes [30]. The so-called damage master

curves allow backcalculating the initial (as constructed) dynamic modulus of HMA (E*) from the FWD-based values at the time of testing [4, 30].

The backcalculation results, however, should be used with caution. Quite a few factors may affect modulus values backcalculated from the FWD. One such factor would be an asphalt quality deficiency resulting from non-uniform temperatures of the asphalt mat during construction (also known as thermal segregation) [31]. In addition, pavement age and longitudinal wheelpath cracking may significantly influence performance of surface asphalt layers as measured by FWD on LTPP sections [32]. Lastly, a seasonal variation in backcalculated moduli in 50 LTPP sections across the U.S. and Canada was found to be highly correlated with asphalt surface temperature [33].

CHAPTER 3 Expanded Sensitivity Analysis with M-EPDG Version 1.1 Software

Introduction

Per the original proposal, the expanded sensitivity analysis was to be performed using commercially available AASHTO Pavement-ME software. However, at the start of the analysis the software had not been delivered to UConn. To avoid delays in the project schedule, the research team decided to proceed with the last updated public domain version 1.1 of the M-EPDG software to perform the sensitivity analysis. Once the AASHTO Pavement-ME software became available, the sensitivity analysis was performed again. The results of the second analysis are reported in Chapter 4.

Scope of the Sensitivity Runs

The sensitivity analyses of the M-EPDG predictive models in Phase II include a wider range of inputs as recommended by the Technical Advisory Panel (TAP) in the previous phase of the project. Accordingly, the new set of input includes variable vehicle class distributions (VCD) for the fixed AADTT values (see Table 3.1) obtained from the M-EPDG traffic option tables. Three pavement design types are evaluated, namely, asphalt concrete (AC) pavement on weak subgrade soil, AC-overlaid composite pavement (AC over AC/PCC), and overlaid repaired PCC pavement (AC over PCC). In SPR 2274, the sensitivity analysis was performed for AC-overlaid-AC and will not be discussed in this phase of the project.

Table 3.1. Definition of Vehicle Class Distributions (VCDs) used for traffic analysis

Vehicle Class	Vehicle Class Percentage		
	VCD 1 (Low) Bus >2% Multi-trailer <2%	VCD 2(Base) Bus >2% Multi-trailer <2%	VCD 3 (High) Bus >2% Multi-trailer <2%
Class 4	2.9	3.3	1.3
Class 5	56.9	34.0	8.5
Class 6	10.4	11.7	2.8
Class 7	3.7	1.6	0.3
Class 8	9.2	9.9	7.6
Class 9	15.3	36.2	74.0
Class 10	0.6	1.0	1.2
Class 11	0.3	1.8	3.4
Class 12	0.3	0.2	0.6
Class 13	0.4	0.3	0.3

The "one-at-a-time" approach to sensitivity analysis was implemented, first, by creating baseline designs with average input values for each of three climatic zones (defined by geographic areas) in Connecticut as established under the SPR-2274 project. Next, a high and low value for each evaluated input was substituted, respectively, to create designs for the sensitivity analysis. The three climatic input files (Climate I, II, and III for shore, inland, and high hills zones, respectively) were created by the interpolation of the temperature, precipitation, and wind data as shown in Table 3.2. Note that insufficient data was available for weather stations (Poughkeepsie,

NY, and Pittsfield, MA) in the vicinity of Litchfield County (northwestern Connecticut). Therefore, the data from Westfield, MA, and Springfield, MA stations was used for simulating Climate III (high hills). The elevation and ground water table data were interpolated for each climate as well.

Table 3.2. Summary of the M-EPDG climatic data

Climate ID	Climate Name	Weather Station Locations	Elevation [ft]	Depth of Groundwater Table [ft]
Climate I	SHORE	Bridgeport, CT New Haven, CT Groton, CT	11	10
Climate II	INLAND	Hartford, CT Willimantic, CT	18	10
Climate III	HILLS	Westfield, MA Springfield, MA	415	10

Tables 3.3 through 3.5 summarize ranges of design inputs used during Phase II for AC, AC overlaid composite, and AC-overlaid repaired PCC designs, respectively. The ranges of layer thicknesses and unbound material types were finalized during the project kick-off meeting with the TAP. The corresponding binder type and aggregate gradation values were taken from Section M.04 of the CTDOT specifications for bituminous concrete (See Appendix E). Altogether, 320 simulation runs were conducted using M-EPDG v.1.1 software to create a dataset of inputs and outputs for the statistical analysis.

Table 3.3. Design inputs for Phase II sensitivity analysis of AC pavements

Truck Traffic over Design Life, (million ESALs*)	Asphalt Layer Thickness, (in.)	Binder Performance Grade	Base Thickness, (in.)	Base Modulus, (psi)	Subbase Thickness, (in.)	Subbase Type	Subgrade Type
1.9 (Low) 4.8 (Baseline) 12.1 (High)	4 (Low) 7 (Baseline) 9 (High)	PG 64-22 (Baseline) PG 76-22 (High)	4 (Low) 6 (Baseline) 8(High)	20,000 (Low) 25,000 (Baseline) 30,000 (High)	8 (Low) 10 (Baseline) 12 (High)	A-2-6 (Low) A-2-4 (Baseline) A-3 (High)	A-7-5 (Low) A-6 (Baseline) A-3 (High)

* Each traffic level will be evaluated with the three variable vehicle class distributions from Table 3.1

Table 3.4. Design inputs for Phase II sensitivity analysis of AC-overlaid composite and AC overlaid repaired PCC pavements

Truck Traffic over Design Life, (million ESALs *)	Asphalt Overlay Thickness, (in.)	Overlay Binder Performance Grade	Existing AC Thickness, After Milling (in.)	Existing PCC Thickness, (in.)	Percent Slabs cracked before restoration, (%)	Percent Slabs cracked after restoration, (%)	Subbase Thickness, (in.)	Subbase Type	Subgrade Type
1.9 (Low) 4.8 (Baseline) 12.1 (High)	3 (Low) 5 (Baseline) 7 (High)	PG 64-22 (Baseline) PG 76-22 (High)	2 (Baseline) 3 (High) 4 (Very High)	7(Low) 8(Baseline) 10(High)	30 (Low) 40 (Baseline) 50 (High)	0 (Low) 10 (Baseline) 20(High	8 (Low) 10 (Baseline) 12 (High)	A-2-6 (Low) A-2-4 (Baseline) A-3 (High)	A-7-5 (Low) A-6 (Baseline) A-3 (High)

* Each traffic level will be evaluated with the three variable vehicle class distributions from Table 3.1

Table 3.5. Rehabilitation inputs for AC overlays

Milled Thickness, (in.)	Existing Pavement Rating	Existing Total Rutting, (in.)
2 (Baseline) 1(Low) 0(Very Low)	Poor (Low) Fair (Baseline) Good (High)	0 (Low) 0.5 (Baseline) 1(High)

Evaluation of Outputs

The M-EPDG output values for major performance indicators (see Table 3.6) were evaluated for each pavement design type in two steps. First, a formal multivariate analysis of variability (ANOVA) was conducted using the F-statistics value to evaluate a contribution of the variation in each categorical input to the overall variability in an analyzed distress. Next, an importance ranking was assigned to each input based on the statistical significance of the corresponding F-statistics value on a logarithmic scale. The level of confidence $\alpha=0.05$ was chosen as a threshold for statistical significance, whereas each importance ranking represented an order of magnitude of the logF value (i.e., critical for $\log F>3$, high for $1\leq\log F\leq 3$, moderate for $0.5<\log F<1$, low for $0\leq\log F\leq 0.5$, and very low for $\log F<0$).

Table 3.6. Performance indicators for sensitivity analysis

Design Type/ Pavement Type	Performance Indicator Model
Newly Constructed (New) AC AC-overlaid AC on PCC AC-overlaid Repaired PCC	Longitudinal cracking (top-down fatigue) Alligator cracking (bottom-up fatigue) Thermal (transverse) cracking AC layer rutting Total rutting IRI

The next section presents the results of ANOVA and importance ranking for each distress/pavement design type accompanied by the interpretation of the results.

Statistical Analysis Results and Input Ranking

New AC Pavement

The sensitivity analysis of the distress prediction models for newly constructed AC pavement designs targeted the following inputs:

- Average annual daily truck traffic (AADTT)
- Performance grade of AC binder (ACOLBIND)
- Geographic location (CLIMATE)
- Resilient modulus of granular base (EB)
- Resilient modulus of subgrade (ES)
- Thickness of AC layer (HAC)
- Thickness of granular base (HBASE)
- Vehicle class distribution (VCD)

Tables 3.7 through 3.12 summarize sensitivity rankings of the above inputs for longitudinal cracking, alligator cracking, transverse cracking, AC layer rutting, total rutting, and IRI in that order. In addition, an overall (combined) importance ranking for cracking, rutting, and IRI predictions is summarized separately in graphical form (see Figures 3.1 through 3.3). The following are brief notes interpreting the major trends observed from the sensitivity ranking of M-EPDG inputs for new AC pavement design:

- The AC layer thickness (HAC) appears to be a critical factor for longitudinal and alligator cracking. It also highly affects rutting and IRI, while only moderately contributing to the variability in transverse cracking.
- The performance grade of AC binder (ACBIND) did not show a statistically significant effect on either longitudinal or alligator cracking, most likely, because of higher probability of cracking due to increase in AADTT or due to decrease in AC layer thickness. The major effect of AC binder grade on transverse cracking, rutting and IRI, is evident.
- As might be expected, traffic inputs (AADTT and VCD) are shown to have a high level of effect on all types of load-related distresses (longitudinal and alligator cracking, AC layer rutting and total rutting) and roughness (IRI). It is interesting to observe that the overall amount (number) of trucks (AADTT) shows an effect that is an order of magnitude higher than the truck class distribution.
- The moderate effect of geographic location (CLIMATE) on load-related cracking for new AC layers is contrasted by its higher effect on thermal (transverse) cracking, rutting and IRI.
- The subgrade material stiffness (ES) reported as resilient modulus of subgrade is shown to have the most prominent effect on predicted IRI values, and a high influence on load-related cracking and total rutting in a new AC pavement.
- The granular base thickness (HBASE) does not appear to be a factor in any distress prediction, which can be explained by a relatively high resilient modulus of base (EB=20 to 30 Ksi) used in the analysis. On the other hand, the effect of stiffness of base (EB) on the transverse cracking should not be neglected.

Table 3.7. ANOVA of inputs for the longitudinal cracking model in new AC pavement design

Order No.	Predictor Index	F	p-value	logF	Statistical Significance	Assigned Importance
1	HAC	2621.36	0.000	3.42	Yes	Critical
2	AADTT	29.4	0.000	1.47	Yes	High
3	ES	11.51	0.000	1.06	Yes	High
4	VCD	5.96	0.005	0.78	Yes	Moderate
5	CLIMATE	4.01	0.024	0.60	Yes	Moderate
6	EB	0.85	0.432	-0.07	No	Very Low
7	HBASE	0.35	0.705	-0.46	No	Very Low
8	ACBIND	0.07	0.798	-1.15	No	Very Low

Table 3.8. ANOVA of inputs for the alligator cracking model in new AC pavement design

Order No.	Predictor Index	F	p-value	logF	Statistical Significance	Assigned Importance
1	HAC	1464.52	0.000	3.17	Yes	Critical
2	AADTT	185.10	0.000	2.27	Yes	High
3	VCD	21.78	0.000	1.34	Yes	High
4	ES	19.37	0.000	1.29	Yes	High
5	CLIMATE	4.66	0.014	0.67	Yes	Moderate
6	ACBIND	2.07	0.156	0.32	No	Low
7	EB	0.57	0.570	-0.24	No	Very Low
8	HBASE	0.02	0.979	-1.70	No	Very Low

Table 3.9. ANOVA of inputs for the transverse cracking model in new AC pavement design

Order No.	Predictor Index	F	p-value	logF	Statistical Significance	Assigned Importance
1	CLIMATE	152.65	0.000	2.18	Yes	High
2	HAC	7.23	0.002	0.86	Yes	Moderate
3	ACBIND	5.20	0.027	0.72	Yes	Moderate
4	EB	2.82	0.068	0.45	No	Moderate
5	AADTT	0.00	1.000	n/a	No	Very Low
6	VCD	0.00	1.000	n/a	No	Very Low
7	ES	0.00	1.000	n/a	No	Very Low
8	HBASE	0.00	1.000	n/a	No	Very Low

Table 3.10. ANOVA of inputs for the AC rutting model in new AC pavement design

Order No.	Predictor Index	F	p-value	logF	Statistical Significance	Assigned Importance
1	AADTT	620.48	0.000	2.79	Yes	High
2	HAC	153.75	0.000	2.19	Yes	High
3	VCD	94.86	0.000	1.98	Yes	High
4	CLIMATE	82.41	0.000	1.92	Yes	High
5	ACBIND	52.59	0.000	1.72	Yes	High
6	ES	6.40	0.003	0.81	Yes	Moderate
7	HBASE	0.18	0.833	-0.74	No	Very Low
8	EB	0.00	0.999	n/a	No	Very Low

Table 3.11. ANOVA of inputs for the total rutting model in new AC pavement design

Order No.	Predictor Index	F	p-value	logF	Statistical Significance	Assigned Importance
1	AADTT	435.35	0.000	2.64	Yes	High
2	HAC	281.83	0.000	2.45	Yes	High
3	ES	102.87	0.000	2.01	Yes	High
4	VCD	101.79	0.000	2.01	Yes	High
5	ACBIND	23.88	0.000	1.38	Yes	High
6	CLIMATE	17.43	0.000	1.24	Yes	High
7	EB	0.23	0.795	-0.64	No	Very Low
8	HBASE	0.21	0.811	-0.68	No	Very Low

Table 3.12. ANOVA of inputs for the IRI model in new AC pavement design

Order No.	Predictor Index	F	p-value	logF	Statistical Significance	Assigned Importance
1	ES	692.84	0.000	2.84	Yes	High
2	AADTT	331.31	0.000	2.52	Yes	High
3	HAC	286.07	0.000	2.46	Yes	High
4	VCD	83.63	0.000	1.92	Yes	High
5	CLIMATE	35.73	0.000	1.55	Yes	High
6	ACBIND	16.90	0.000	1.23	Yes	High
7	HBASE	0.13	0.879	-0.89	No	Very Low
8	EB	0.13	0.876	-0.89	No	Very Low

Summary of Sensitivity for New AC Pavement Design

The overall sensitivity rankings in Figures 3.1 through 3.3 are assigned based on the average logF values computed as follows:

Overall cracking sensitivity:
mean logF (Cracking)= average [logF (long. crack.), logF (allig. crack.), logF (trans. crack.)]

Overall rutting sensitivity:
mean logF (Rutting)= average [logF (AC layer rut.), logF (tot. rut.)]
Overall IRI sensitivity: as computed from Table 3.11

From Figure 3.1, one can surmise that as far as cracking in new AC pavements is concerned, AC thickness, traffic, and subgrade stiffness inputs should be obtained on as high a level of detail as possible. In addition, some differences in performance of pavements with the same design parameters located in different climatic zones throughout Connecticut should be anticipated. With respect to rutting and IRI predictions, all inputs except base layer thickness and stiffness should be considered highly important for new AC pavement designs (see Figures 3.2 and 3.3).

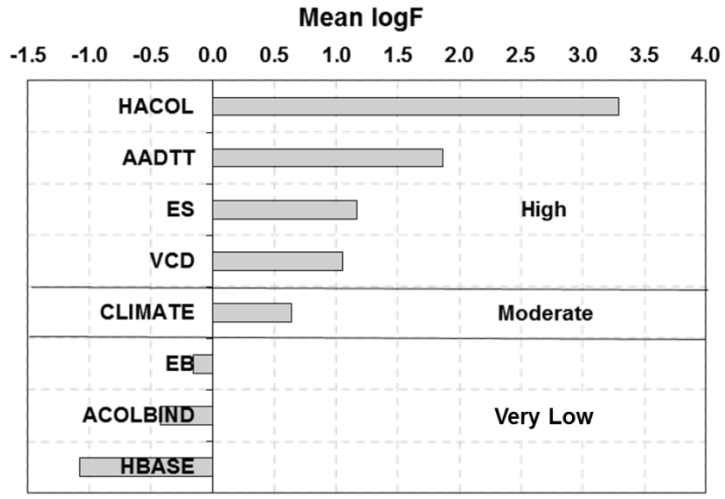

Figure 3.1 Cracking sensitivity to the AC design inputs

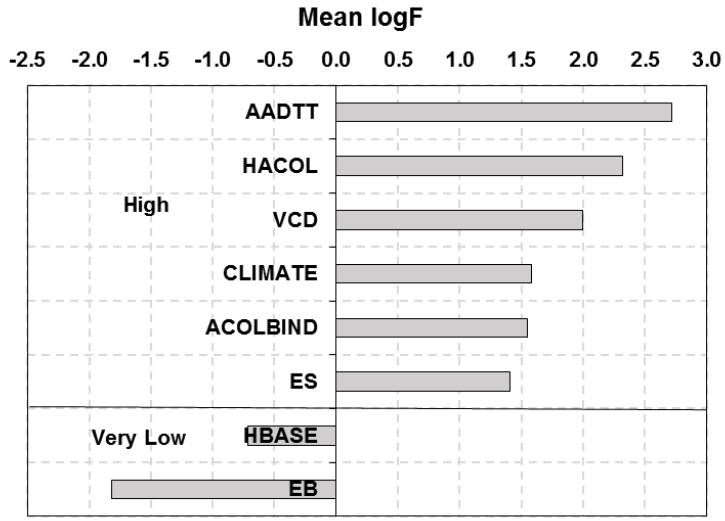

Figure 3.2 Rutting sensitivity to the AC design inputs

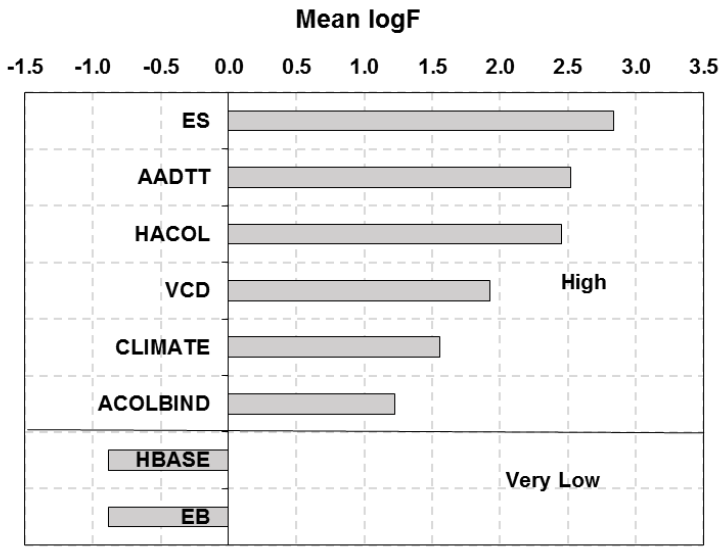

Figure 3.3 IRI sensitivity to the AC design inputs

AC-Overlaid AC-on-PCC Pavement

Tables 3.13 through 3.18 present importance rankings of the following inputs for AC-overlaid AC on PCC pavement:

- Average annual daily truck traffic (AADTT)
- Performance grade of AC overlay binder (ACOLBIND)
- Geographic location (CLIMATE)
- Resilient modulus of subbase (ESB)
- Resilient modulus of subgrade (ES)
- Thickness of AC overlay layer (HACOL)
- Milled-off thickness of existing AC layer (HMILL)
- Thickness of PCC slab (HPCC)
- Thickness of subbase (HSB)
- Performance rating of existing AC-on-PCC pavement (PR)
- Total rutting in existing AC-on-PCC pavement (TOTRUTEXIST)
- Vehicle class distribution (VCD)

Upon observing the importance ranking of the above inputs with respect to different distress indicators, one can conclude the following:

- The geographic location (CLIMATE) of a pavement has a highly significant effect on all of the distresses in discussion, especially on longitudinal and transverse cracking.
- Truck traffic volume (AADTT) shows to be the most critical input for predicting alligator cracking, rutting, and IRI, and being as important as geographic location (CLIMATE) for the longitudinal cracking model. The vehicle class distribution (VCD) has an effect similar to AADTT with the only difference being low significance for longitudinal cracking.

- The AC overlay thickness (HACOL) has only a moderate effect on longitudinal and transverse cracking, while remaining highly important for adequately predicting rutting. The AC overlay's binder performance (ACOLBIND) is most critical for thermal (transverse) cracking and AC layer rutting models. It also shows a somewhat significant effect on alligator cracking predictions.
- Knowing subgrade stiffness (ES) is highly important to adequately predict longitudinal and transverse cracking as well as IRI. On the other hand, rutting (AC layer and total) predictions (Figures 3.15 and 3.16) are shown to be less affected by subgrade characteristics, most likely due to the presence of a very stiff PCC slab under the AC layer.
- Among the rehabilitation inputs, performance rating (PR) is only shown to affect alligator cracking predictions. The milled-off thickness(HMILL) shows as being a highly significant factor in rutting prediction, while only moderately affecting load-related (longitudinal and alligator) cracking output.
- Neither thickness nor stiffness of subbase exhibited any significant effect on distresses for the given input range in this Phase of the project.

Table 3.13. ANOVA of inputs for the longitudinal cracking model in AC-Overlaid AC-on-PCC design

Order No.	Predictor Index	F	p-value	logF	Statistical Significance	Assigned Importance
1	CLIMATE	27.50	0.000	1.44	Yes	High
2	AADTT	26.22	0.000	1.42	Yes	High
3	HPCC	24.06	0.000	1.38	Yes	High
4	ES	22.01	0.000	1.34	Yes	High
5	HACOL	3.64	0.032	0.56	Yes	Moderate
6	HMILL	3.60	0.033	0.56	Yes	Moderate
7	PR	1.44	0.244	0.16	No	Low
8	ACOLBIND	1.21	0.275	0.08	No	Low
9	VCD	1.14	0.326	0.06	No	Low
10	HSB	0.04	0.963	-1.40	No	Very Low
11	ESB	0.03	0.972	-1.52	No	Very Low
12	TOTRUEXIST	0.02	0.978	-1.70	No	Very Low

Table 3.14. ANOVA of inputs for the alligator cracking model in AC-Overlaid AC-on-PCC design

Order No.	Predictor Index	F	p-value	logF	Statistical Significance	Assigned Importance
1	AADTT	184.46	0.000	2.27	Yes	High
2	PR	131.82	0.000	2.12	Yes	High
3	CLIMATE	43.72	0.000	1.64	Yes	High
4	VCD	32.42	0.000	1.51	Yes	High
5	ES	13.09	0.000	1.12	Yes	High
6	HACOL	8.23	0.001	0.92	Yes	Moderate
7	HMILL	7.80	0.001	0.89	Yes	Moderate
8	HPCC	6.72	0.002	0.83	Yes	Moderate
9	ACOLBIND	5.94	0.018	0.77	Yes	Moderate
10	HSB	0.17	0.846	-0.77	No	Very Low
11	TOTRUEXIST	0.08	0.927	-1.10	No	Very Low
12	ESB	0.08	0.927	-1.10	No	Very Low

Table 3.15. ANOVA of inputs for the transverse cracking model in AC-Overlaid AC-on-PCC design

Order No.	Predictor Index	F	p-value	logF	Statistical Significance	Assigned Importance
1	CLIMATE	904.85	0.000	2.96	Yes	High
2	ACOLBIND	20.04	0.000	1.30	Yes	High
3	HMILL	0.86	0.429	-0.07	No	Very Low
4	HACOL	0.83	0.440	-0.08	No	Very Low
5	HPCC	0.15	0.862	-0.82	No	Very Low
6	ES	0.14	0.867	-0.85	No	Very Low
7	AADTT	0.00	1.000	n/a	No	None
8	PR	0.00	1.000	n/a	No	None
9	TOTRUEXIST	0.00	1.000	n/a	No	None
10	HSB	0.00	1.000	n/a	No	None
11	ESB	0.00	1.000	n/a	No	None
12	VCD	0.00	1.000	n/a	No	None

Table 3.16. ANOVA of inputs for the AC layer rutting model in AC-Overlaid AC-on-PCC design

Order No.	Predictor Index	F	p-value	logF	Statistical Significance	Assigned Importance
1	AADTT	1460.35	0.000	3.16	Yes	Critical
2	CLIMATE	243.81	0.000	2.39	Yes	High
3	VCD	180.94	0.000	2.26	Yes	High
4	ACOLBIND	107.66	0.000	2.03	Yes	High
5	HACOL	10.79	0.000	1.03	Yes	High
6	HMILL	9.89	0.000	1.00	Yes	High
7	HPCC	4.57	0.014	0.66	Yes	Moderate
8	ES	1.47	0.238	0.17	No	Low
9	TOTRUEXIST	0.96	0.388	-0.02	No	Very Low
10	PR	0.73	0.485	-0.14	No	Very Low
11	HSB	0.29	0.750	-0.54	No	Very Low
12	ESB	0.26	0.772	-0.59	No	Very Low

Table 3.17. ANOVA of inputs for the total rutting model in AC-Overlaid AC-on-PCC design

Order No.	Predictor Index	F	p-value	logF	Statistical Significance	Assigned Importance
1	AADTT	1379.03	0.000	3.14	Yes	Critical
2	TOTRUEXIST	338.07	0.000	2.53	Yes	High
3	CLIMATE	226.97	0.000	2.36	Yes	High
4	VCD	171.35	0.000	2.23	Yes	High
5	ACOLBIND	101.51	0.000	2.01	Yes	High
6	HACOL	10.19	0.000	1.01	Yes	High
7	HMILL	9.31	0.000	0.97	Yes	Moderate
8	HPCC	4.32	0.017	0.64	Yes	Moderate
9	ES	1.30	0.280	0.11	No	Low
10	PR	0.70	0.503	-0.15	No	Very Low
11	HSB	0.28	0.757	-0.55	No	Very Low
12	ESB	0.25	0.778	-0.60	No	Very Low

Table 3.18. ANOVA of inputs for the IRI model in AC-Overlaid AC-on-PCC design

Order No.	Predictor Index	F	p-value	logF	Statistical Significance	Assigned Importance
1	AADTT	1391.58	0.000	3.14	Yes	Critical
2	ES	1225.13	0.000	3.09	Yes	Critical
3	TOTRUEXIST	339.16	0.000	2.53	Yes	High
4	CLIMATE	271.09	0.000	2.43	Yes	High
5	VCD	172.89	0.000	2.24	Yes	High
6	ACOLBIND	101.07	0.000	2.00	Yes	High
7	HACOL	10.00	0.000	1.00	Yes	High
8	HMILL	9.47	0.000	0.98	Yes	Moderate
9	HPCC	4.51	0.015	0.65	Yes	Moderate
10	PR	0.71	0.497	-0.15	No	Very Low
11	HSB	0.30	0.740	-0.52	No	Very Low
12	ESB	0.30	0.740	-0.52	No	Very Low

Summary of Sensitivity for AC-Overlaid AC-on-PCC Pavement Design

Figures 3.4 through 3.6 illustrate overall sensitivity rankings of each input category for cracking, rutting, and IRI, respectively. On average, all cracking prediction models in the M-EPDG version 1.1 package are highly sensitive to differences in climate and moderately sensitive to AC binder performance grade and subgrade stiffness. Based upon the statistical results, the M-EPDG rutting predictions are expected to be critically influenced by truck traffic volume, followed by geographic location, vehicle class distribution, AC binder performance grade, rutting in existing pavement, AC overlay thickness, and milled thickness. The PCC slab thickness effect on rutting and on IRI should not be neglected, as it indicates a moderate influence. Lastly, the subbase characteristics (thickness and stiffness) are not expected to significantly affect distress predictions for the AC-overlaid AC-on-PCC pavement design in Connecticut. It should be noted that the Pavement-ME software yielded no reflective cracking for this scenario.

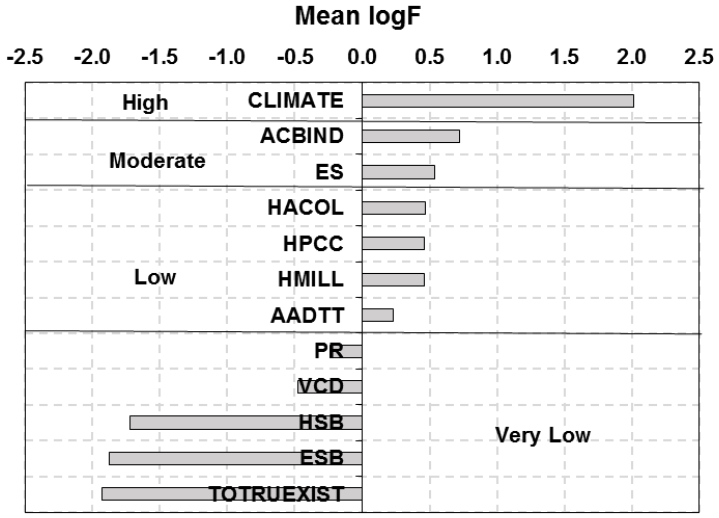

Figure 3.4 Cracking sensitivity to the AC-Overlaid AC-on-PCC design inputs

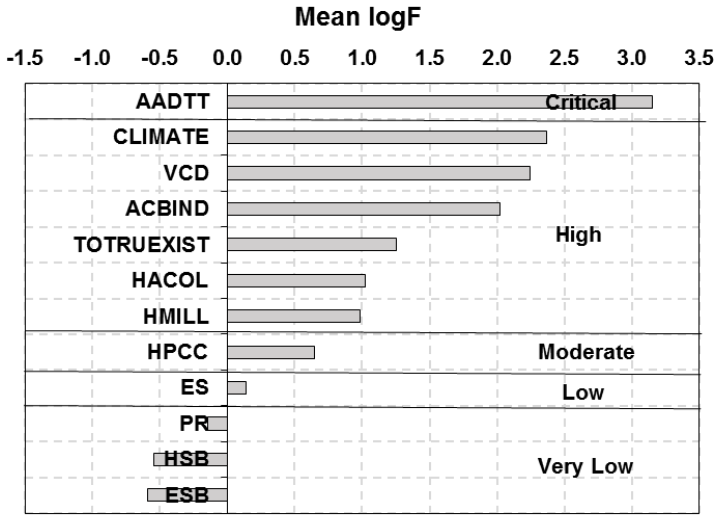

Figure 3.5 Rutting sensitivity to the AC-Overlaid AC-on-PCC design inputs

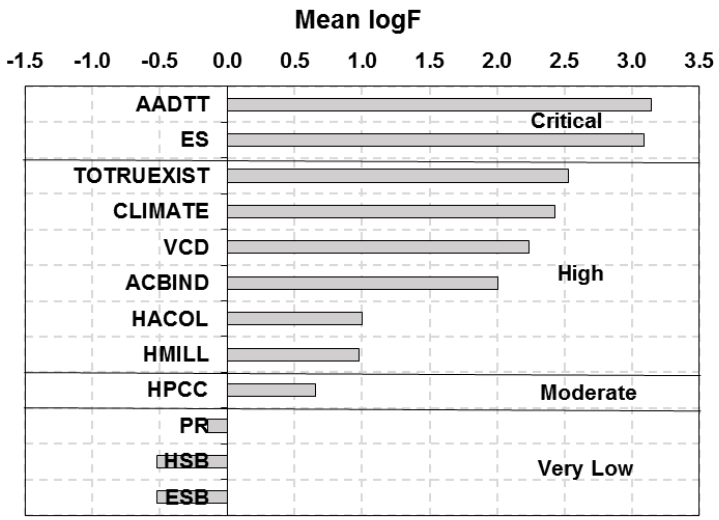

Figure 3.6 IRI sensitivity to the AC-Overlaid AC-on-PCC design inputs

AC-Overlaid Repaired PCC Pavement Design

The sensitivity analysis for this pavement design includes the following:

- Average annual daily truck traffic (AADTT)
- Performance grade of AC overlay binder (ACOLBIND)
- Geographic location (CLIMATE)
- Resilient modulus of subgrade (ES)
- Thickness of AC overlay layer (HACOL)
- Thickness of PCC slab (HPCC)
- Thickness of subbase (HSB)
- Resilient Modulus of subbase (ESB)
- Vehicle class distribution (VCD)
- Combined percent slabs cracked and repaired before restoration (PSB)
- Total percent slabs cracked after restoration (PSA)

In addition, the analysis includes two so-called rehabilitation inputs for combined percent slabs cracked and repaired before restoration (PSB) and for total percent slabs repaired after restoration (PSA). Note that difference between PSB and PSA yields percent slabs remaining cracked after restoration. Lastly, a new cracking performance indicator – reflective cracking – is introduced due to the probability of propagation upward through the AC overlay of the joints and transverse cracks contained in the PCC slabs.

Tables 3.19 through 3.23 rank the above input categories in descending order of statistical significance and, hence, the level of their contribution to the overall variability in predicted distress outputs. The following observations are worth noting:

- Significant differences in longitudinal and transverse cracking predictions were found between the three climatic zones in CT, as well between the three types of subgrades.
- Traffic inputs and layer thicknesses (HACOL, AADTT, VCD, and HPCC) yield high to moderate level (in that order) of the effect on longitudinal cracking. Note that among those inputs, only AC overlay thickness is expected to affect the transverse cracking prediction.
- Percentage of repaired and cracked slabs before and after restoration PSB and PSA is critical for adequate prediction of the reflective cracking, whereas PCC slab thickness is also highly important.
- With respect to AC layer rutting: traffic, climate, and AC layer inputs showed a highly significant effect on this distress prediction. Note that, in AC-overlaid repaired PCC pavements, only the AC layer is modeled to contribute to total rutting due to high PCC stiffness that results in a high level of protection from the underlying unbound layers.
- Interestingly, the IRI predictions show only moderate sensitivity to AC and PCC thickness yet high sensitivity to subbase stiffness with no effect of subgrade stiffness or subbase thickness. The rest of the inputs, namely, traffic, climate, AC binder type, and percentage of repaired and cracked slabs before and after restoration yield a high level of importance for reliably predicting IRI.

Table 3.19. ANOVA of inputs for the longitudinal cracking model in AC-Overlaid Repaired PCC design

Order No.	Predictor Index	F	p-value	logF	Statistical Significance	Assigned Importance
1	CLIMATE	18.71	0.000	1.27	Yes	High
2	ES	18.38	0.000	1.26	Yes	High
3	HACOL	15.43	0.000	1.19	Yes	High
4	AADTT	15.33	0.000	1.19	Yes	High
5	VCD	5.13	0.009	0.71	Yes	Moderate
6	HPCC	3.30	0.044	0.52	Yes	Moderate
7	ACOLBIND	0.66	0.420	-0.18	No	Very Low
8	PSA	0.23	0.792	-0.64	No	Very Low
9	PSB	0.05	0.952	-1.30	No	Very Low
10	HSB	0.05	0.952	-1.30	No	Very Low
11	ESB	0.05	0.952	-1.30	No	Very Low

Table 3.20. ANOVA of inputs for the reflective cracking model in AC-Overlaid Repaired PCC design

Order No.	Predictor Index	F	p-value	logF	Statistical Significance	Assigned Importance
1	PSB	16307.54	0.000	4.21	Yes	Critical
2	PSA	16274.97	0.000	4.21	Yes	Critical
3	HPCC	90.80	0.000	1.96	Yes	High
4	CLIMATE	2.53	0.088	0.40	No	Low
5	HACOL	0.07	0.937	-1.15	No	Very Low
6	VCD	0.05	0.955	-1.30	No	Very Low
7	ES	0.04	0.963	-1.40	No	Very Low
8	HSB	0.02	0.983	-1.70	No	Very Low
9	ACOLBIND	0.01	0.928	-2.00	No	Very Low
10	ESB	0.01	0.990	-2.00	No	Very Low
11	AADTT	0.00	0.996	n/a	No	None

Table 3.21. ANOVA of inputs for the transverse cracking model in AC-Overlaid Repaired PCC design

Order No.	Predictor Index	F	p-value	logF	Statistical Significance	Assigned Importance
1	ES	9.04	0.000	0.96	Yes	Moderate
2	CLIMATE	5.17	0.008	0.71	Yes	Moderate
3	HACOL	3.43	0.039	0.54	Yes	Moderate
4	AADTT	0.00	1.000	n/a	No	None
5	VCD	0.00	1.000	n/a	No	None
6	ACOLBIND	0.00	1.000	n/a	No	None
7	HPCC	0.00	1.000	n/a	No	None
8	PSA	0.00	1.000	n/a	No	None
9	PSB	0.00	1.000	n/a	No	None
10	HSB	0.00	1.000	n/a	No	None
11	ESB	0.00	1.000	n/a	No	None

Table 3.22. ANOVA of inputs for the AC layer rutting model in AC-Overlaid Repaired PCC design

Order No.	Predictor Index	F	p-value	logF	Statistical Significance	Assigned Importance
1	AADTT	721.00	0.000	2.86	Yes	High
2	VCD	213.48	0.000	2.33	Yes	High
3	CLIMATE	125.25	0.000	2.10	Yes	High
4	ACOLBIND	62.90	0.000	1.80	Yes	High
5	HACOL	9.87	0.000	0.99	Yes	Moderate
6	PSA	1.25	0.293	0.10	No	Low
7	HPCC	0.98	0.381	-0.01	No	Very Low
8	ES	0.13	0.875	-0.89	No	Very Low
9	HSB	0.01	0.987	-2.00	No	Very Low
10	ESB	0.01	0.989	-2.00	No	Very Low
11	PSB	0.00	0.998	n/a	No	None

Table 3.23. ANOVA of inputs for the IRI model in AC-Overlaid Repaired PCC design

Order No.	Predictor Index	F	p-value	logF	Statistical Significance	Assigned Importance
1	AADTT	636.73	0.000	2.80	Yes	High
2	PSB	378.09	0.000	2.58	Yes	High
3	PSA	317.06	0.000	2.50	Yes	High
4	VCD	187.36	0.000	2.27	Yes	High
5	CLIMATE	137.41	0.000	2.14	Yes	High
6	ACOLBIND	55.31	0.000	1.74	Yes	High
7	ESB	49.22	0.000	1.69	Yes	High
8	HACOL	8.08	0.001	0.91	Yes	Moderate
9	HPCC	3.74	0.029	0.57	Yes	Moderate
10	ES	0.13	0.874	-0.89	No	Very Low
11	HSB	0.01	0.992	-2.00	No	Very Low

Summary of Sensitivity for AC-Overlaid Repaired PCC Pavement Design

Figures 3.8 through 3.10 illustrate an average sensitivity of cracking, rutting, and IRI models to the variability in design inputs for AC-overlaid repaired PCC pavement design. According to the reported mean logF values, a given range of inputs yielded only moderate differences in combined longitudinal/reflective/transverse cracking between the three climatic zones in Connecticut. The Pavement-ME predictions yielded zero alligator cracking for this situation. The subgrade stiffness, asphalt thickness, and percentage of repaired PCC slabs should not be neglected by a designer, even though a low contribution to the overall variability in cracking was indicated. As expected, the traffic, climate, and asphalt-related inputs will be of highest importance to development of rutting. Due to built-in high dependence of IRI predictions on transverse cracking, the PCC rehabilitation inputs and subgrade support are expected to be the most influencing factors of pavement roughness.

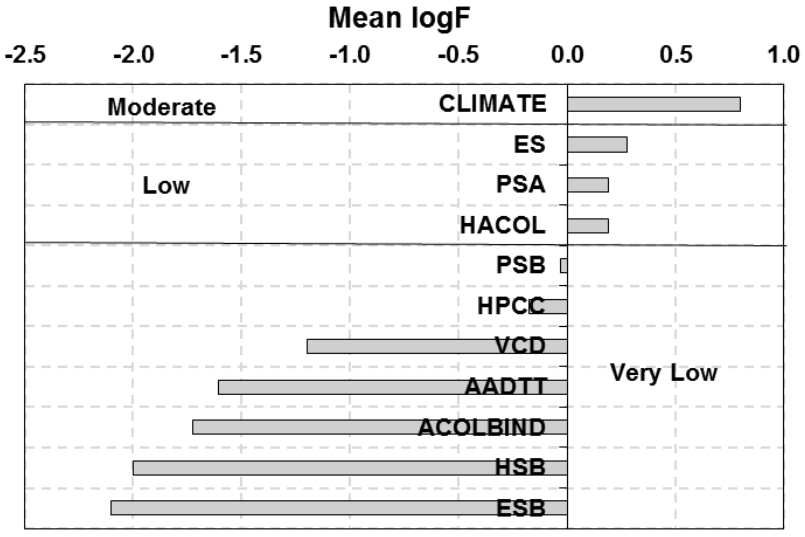

Figure 3.7 Cracking sensitivity to the AC-Overlaid AC-on-PCC design inputs

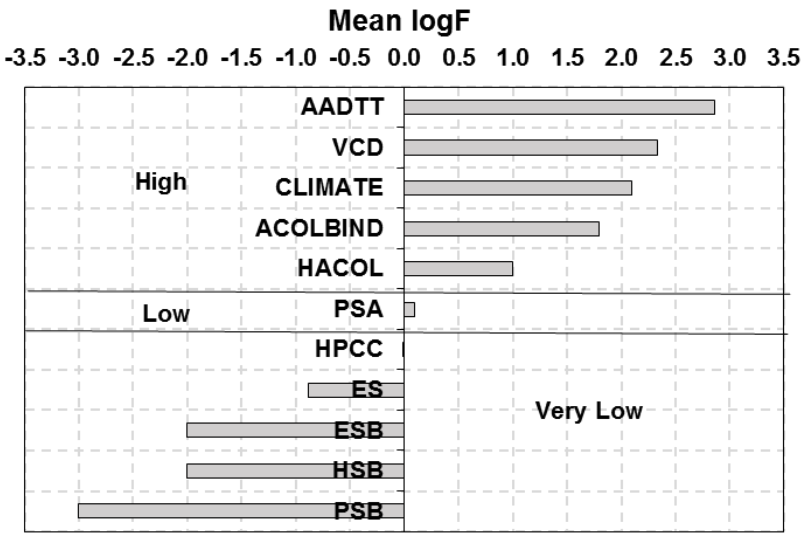

Figure 3.8 Rutting sensitivity to the AC-Overlaid AC-on-PCC design inputs

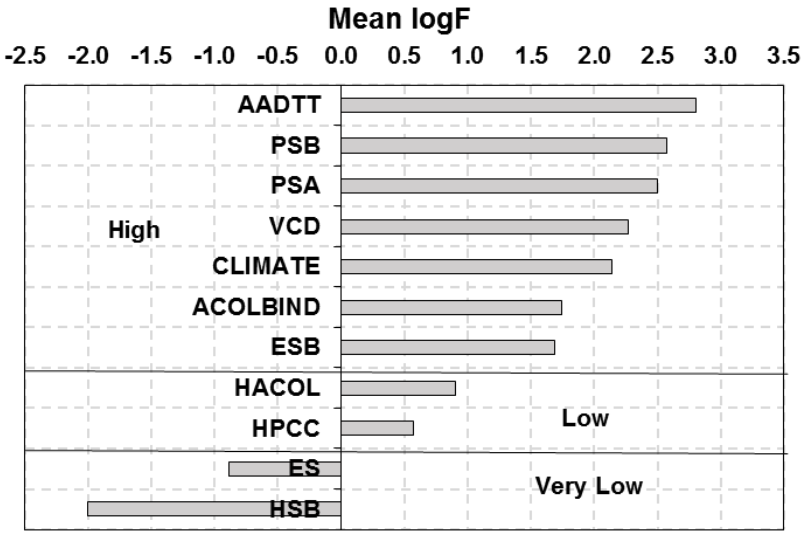

Figure 3.9 IRI sensitivity to the AC-Overlaid AC-on-PCC design inputs

CHAPTER 4 Sensitivity Analysis of Pavement-ME Version 2.1 Software

Introduction and Major Findings

This chapter summarizes major findings on a comparison between M-EPDG version 1.1 and Pavement-ME software in terms of the sensitivity of the predicted distress indicator outputs to design inputs. As noted in chapter 3, once the Pavement-ME software was acquired and installed on UConn's computer, the sensitivity analysis was rerun to evaluate any changes in importance ranking of input factors because of the change in software.

The major findings from the repeated sensitivity analysis indicate that:

1. The new Pavement-ME software allows for a faster run of simulation projects, although providing a more complicated structure of the reports.
2. The Pavement-ME sensitivity runs yielded similar but slightly different rankings in some cases of design input importance compared to sensitivity runs from the M-EPDG software.

Acquisition of Pavement ME 2.1 and Transition from M-EPDG 1.1

The AASHTO Pavement-ME Version 2.1 software has been installed and successfully run since July 2015. At variance with M-EPDG, the Pavement-ME runs much faster with a typical analysis completed within 3 to 4 minutes as opposed to 15 to 17 minutes by the M-EPDG 1.1. The new software is written in XML format, which allows for the use of design input databases in SQL and Oracle format for direct export of inputs into the new software. One notable difference with the M-EPDG is the increase in amount of information in the output files, which can be created in both PDF and Excel formats. The most important feature is that climatic data can be corrected or changed directly through the user interface. Lastly, the XML format allows for easier import or export of climate, traffic, and materials data.

The Pavement-ME software allows the importation of previously run simulations from M-EPDG 1.1 to the Pavement-ME environment. It was noticed, however, that some input values either were changed to default or were not successfully transferred. Below are a few examples:

- The 2-percent linear traffic growth rate changed into 4-percent compound growth in the Pavement ME.
- The subgrade resilient moduli were lost during transition.
- The Pavement-ME software appeared to be very sensitive to the lack of climatic data or unusual values. These were represented by the absence of hourly temperature, wind, and moisture values as well as drastic changes in an hour (e.g., greater than 30-degree in temperature).
- The aforementioned phenomena required manual change of project inputs to correct the values.

Reevaluation of Sensitivity Analysis

Although the original sensitivity analysis was completed before the Pavement ME software arrived (See Chapter 3), it was necessary to re-run the sensitivity analysis in order to evaluate the differences in the outputs between Pavement-ME 2.1 and M-EPDG 1.1. Accordingly, the set of 280 runs has been completed for the New AC, AC-overlaid composite (ACACPCC), and AC-overlaid repaired PCC (ACPCC) pavements in the three climatic zones. In this chapter, the effect

of design reliability on the sensitivity results is evaluated by analyzing the output distributions and the changes in importance ranking of outputs.

Comparison between M-EPDG and Pavement ME Results for New AC Pavements

Evaluation of Normal Distribution (Histograms)

The original sensitivity analysis was performed in the M-EPDG 1.1 environment with a deterministic approach using outputs at 50-percent reliability. In the new Pavement-ME analyses, the emphasis is made on designed reliability outputs with a default of 90 percent. To evaluate the effect of reliability on the sensitivity results, the distributions of distress indicator values (output value histograms) are plotted in Figures 4.1 through 4.3 for AC layer rutting, alligator cracking, and longitudinal cracking, in that order, for new AC pavements. With no sensitivity to a particular factor, a distribution is anticipated to have a bell shape, centered on the mean value. In statistics, if more than one peak shows in the histogram, it indicates a split of the "population" due to "treatment." In the current analysis, the "populations" consist of the predicted distress values, whereas the "treatments" are design input factors, such as AADTT, Climate, AC thickness, and others.

The observation of histogram shapes in Figure 4.1 indicates similarity of the M-EPDG and Pavement-ME predictions for AC layer rutting at 50% reliability. Furthermore, with an increase in design reliability from 50% to 90% the shape of the histogram for Pavement-ME predictions does not change much. Similarly, the histograms for alligator cracking predictions by M-EPDG and Pavement-ME at 50% reliability (Figure 4.2) appear to be identical. Their histograms also show very small mean values (less than 0.5-percent alligator cracking area) as compared with those at 90% reliability (around 2-percent area). A second, although very low, peak can be observed for all three histograms. To summarize, the observations from Figures 4.1 and 4.2 indicate no significant changes in predicted AC layer rutting and alligator cracking when migrating from M-EPDG to Pavement-ME software.

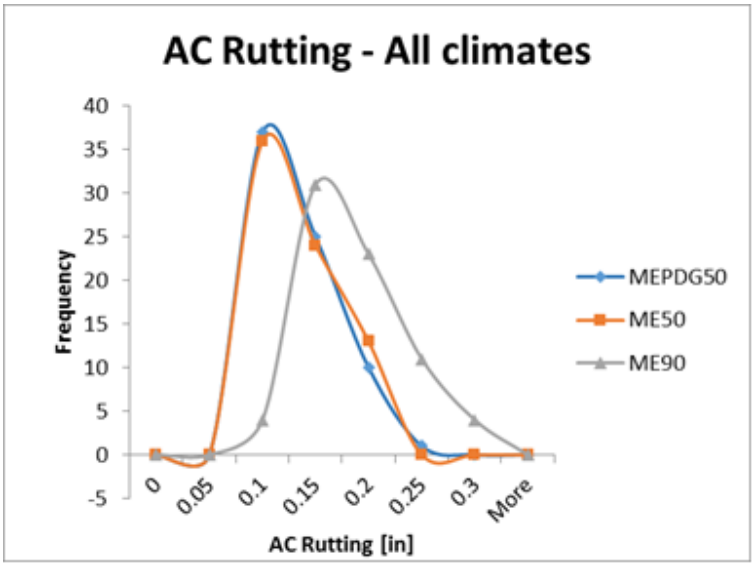

Figure 4.1 Histograms for AC rutting from M-EPDG and Pavement-ME runs at 50 and 90 percent reliability for new AC pavements

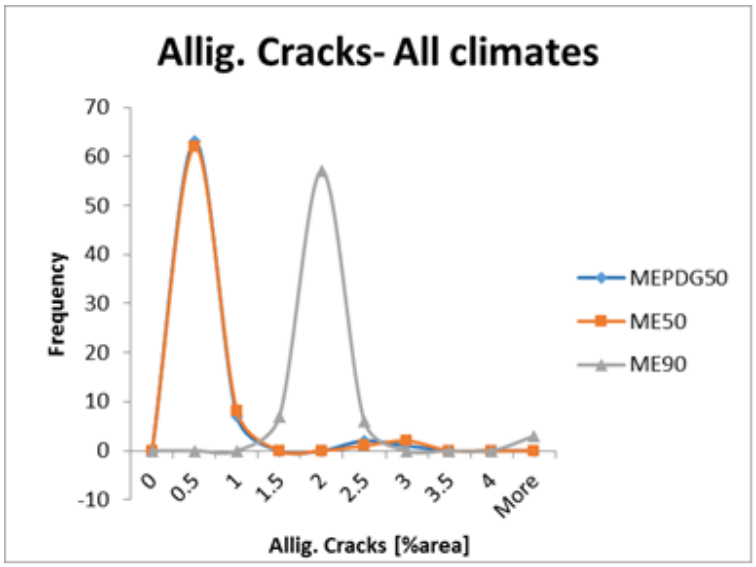

Figure 4.2 Histograms for alligator cracking from M-EPDG and Pavement-ME runs at 50 and 90 percent reliability for new AC pavements

At contrast with the above, much larger differences in predictions between the M-EPDG and Pavement-ME models occur when longitudinal cracking is a response. It can be easily observed in Figure 4.3 that at 50% reliability, Pavement-ME predicts less longitudinal cracking on average as compared with M-EPDG, with a greater variation between the three peaks. Interestingly, the new Pavement-ME software at 50% reliability predicts a higher frequency of small longitudinal crack values as compared with M-EPDG at the same reliability level. The 90%-reliability prediction is at least two orders of magnitude higher than those at 50% reliability are, as its histogram is spread over a larger range of values. This phenomenon can be explained by a very high degree of uncertainty for the prediction model.

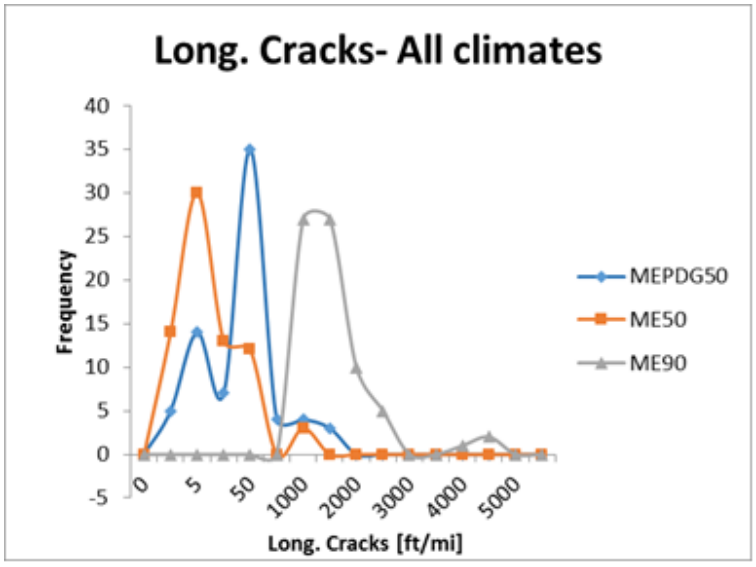

Figure 4.3 Histograms for longitudinal cracking from M-EPDG and Pavement-ME runs at 50 and 90 percent reliability for new AC pavements

The histograms of the IRI predictions in Figure 4.4 indicate no difference in 50%-reliability trends between M-EPDG and Pavement-ME models. However, the distribution of the IRI predictions at 90% reliability is characterized by two extra peaks, which indicate that the IRI model at this level is more sensitive to specific factors as investigated by the regression analysis presented and discussed in the next section.

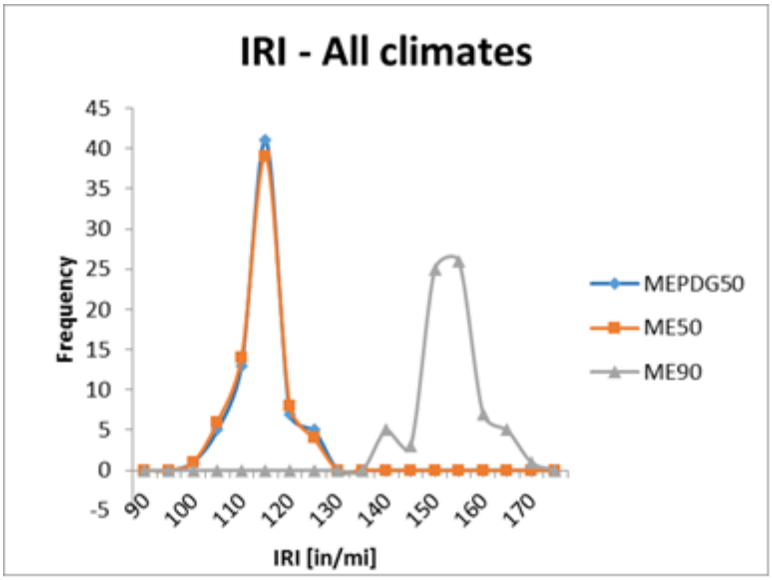

Figure 4.4 Histograms for IRI from M-EPDG and Pavement-ME runs at 50 and 90 percent reliability for new AC pavements

In summary, the analysis of predicted value distributions indicated some changes in the sensitivity of the Pavement-ME models for new AC pavements, especially with respect to longitudinal cracking and IRI. This warranted a re-evaluation of both the sensitivity and input importance ranking for this pavement type, as reported next.

Re-evaluation of Sensitivity and Importance Rankings for New AC Pavements

As stated in the proposal, this study characterizes the sensitivity of distress models to the change in a particular design input through analysis of its F-statistic parameter. The F-value describes the contribution of the variation in the input into the total variance in the distress. The higher the F-value the higher is the importance of the input for the distress prediction model. The statistical significance of F-values is evaluated at the 5% level of confidence, meaning if a p-value for a particular F-value is less than 0.05, the F-value is statistically significant. The importance of inputs is characterized by the logarithm of F-values, as shown in Tables 4.1 through 4.3 for overall cracking, rutting, and IRI sensitivity, in that order.

Table 4.1 compares overall cracking sensitivity of M-EPDG and Pavement-ME models with longitudinal, alligator, and transverse cracking combined. No difference in assigned ranking is shown for critical, high or moderately important inputs, with AC thickness (HAC) being critically important, truck traffic volume (AADTT) and vehicle class distribution (VCD) as well as subgrade modulus (ES) being highly important, and location (CLIMATE) being moderately important. Notably, the binder performance grade (ACBIND) is shown to be more influential (moderate at 90% reliability), with granular base thickness (HBASE) and base modulus (EB) remaining least important.

Table 4.1. Summary of Cracking Sensitivity for New AC Pavements

M-EPDG at 50% reliability			Pavement-ME at 50% Reliability			Pavement ME at 90% Reliability		
Predictor	logF	Assigned importance	Predictor	logF	Assigned importance	Predictor	logF	Assigned importance
HAC	3.29	Critical	HAC	3.10	Critical	HAC	3.89	Critical
AADTT	1.87	High	AADTT	1.89	High	AADTT	2.25	High
ES	1.17	High	ES	1.23	High	ES	1.57	High
VCD	1.06	High	VCD	1.09	High	VCD	1.53	High
CLIMATE	0.64	Moderate	CLIMATE	0.54	Moderate	CLIMATE	0.99	Moderate
EB	-0.16	Very Low	ACBIND	-0.15	Very low	ACBIND	0.94	Moderate
ACBIND	-0.42	Very Low	EB	-0.24	Very low	EB	0.19	Low
HBASE	-1.08	Very Low	HBASE	-0.80	Very low	HBASE	-0.51	Very low

With respect to overall rutting sensitivity (combined AC layer and total rutting), Table 4.2 does not show differences in input rankings. Notably, the logF values are higher for Pavement ME as compared with M-EPDG, which indicates somewhat better correlation between inputs and outputs in the new prediction models. The best correlation is indicated at 90% reliability with the highest logF values out of the three compared modes of prediction.

Table 4.2. Summary of Rutting Sensitivity for new AC Pavements

M-EPDG at 50% reliability			Pavement-ME at 50% Reliability			Pavement ME at 90% Reliability		
Predictor	logF	Assigned importance	Predictor	logF	Assigned importance	Predictor	logF	Assigned importance
AADTT	2.72	High	AADTT	3.03	Critical	AADTT	3.12	Critical
HAC	2.32	High	HAC	2.65	High	HAC	2.72	High
VCD	1.99	High	VCD	2.29	High	VCD	2.38	High
CLIMATE	1.58	High	ACBIND	1.93	High	ACBIND	2.00	High
ACBIND	1.55	High	ES	1.84	High	ES	1.96	High
ES	1.41	High	CLIMATE	1.62	High	CLIMATE	1.72	High
HBASE	-0.71	Very Low	HBASE	0.00	Low	HBASE	-1.62	Very Low
EB	-1.82	Very Low	EB	-0.40	Very Low	EB	-1.86	Very Low

Table 4.3 compares the importance rankings for IRI inputs. The Pavement-ME results at 50 and 90 percent reliability show an increase in importance from high to critical for subgrade (ES), truck traffic (AADTT), and AC thickness (HAC). In addition, the granular base thickness (HBASE) shows a slightly higher ranking in Pavement-ME predictions as compared with M-EPDG predictions. Similar to the cracking and rutting predictions, the IRI results are characterized by overall higher logF values, which suggest an average increase in significance of correlations for all Pavement-ME models.

Table 4.3. Summary of IRI Sensitivity for new AC Pavements

M-EPDG at 50% reliability			Pavement-ME at 50% Reliability			Pavement ME at 90% Reliability		
Predictor	logF	Assigned importance	Predictor	logF	Assigned importance	Predictor	logF	Assigned importance
ES	2.84	High	ES	3.55	Critical	ES	3.61	Critical
AADTT	2.52	High	AADTT	3.20	Critical	AADTT	3.24	Critical
HAC	2.46	High	HAC	3.12	Critical	HAC	3.19	Critical
VCD	1.92	High	VCD	2.46	High	CLIMATE	2.51	High
CLIMATE	1.55	High	CLIMATE	2.46	High	VCD	2.51	High
ACBIND	1.23	High	ACBIND	1.97	High	ACBIND	2.02	High
HBASE	-0.89	Very Low	HBASE	0.00	Low	HBASE	0.00	Low
EB	-0.89	Very Low	EB	-0.31	Very Low	EB	-0.23	Very Low

Comparison between M-EPDG and Pavement ME results for AC-overlaid Composite Pavements(ACACPCC)

Evaluation of Normal Distribution (Histograms)

The histograms of the AC layer rutting predictions for M-EPDG at 50 percent reliability and Pavement-ME at 50 and 90 percent reliability are compared in Figure 4.5. One can see similarity in these histogram shapes. Interestingly, at 90 percent reliability, three distinctive peaks can be observed on the histogram as opposed to only two peaks at 50% reliability for Pavement-ME. The histogram for longitudinal cracking predictions for Pavement-ME at 50% reliability (Figure

4.6) shows very low values (less than 5 ft/mi) for all simulation runs. However, at 90% reliability, longitudinal cracking as high as 500 ft/mi is predicted. Those results are a vast contrast with M-EPDG at 50% reliability, which yields wider distribution, and is positively skewed toward larger values (10 to 50 ft/mi). At variance with cracking and rutting histograms, the IRI predictions shown in Figure 4.7 are distributed in almost perfect normal shape, except for a visible second peak for Pavement-ME at 90% reliability.

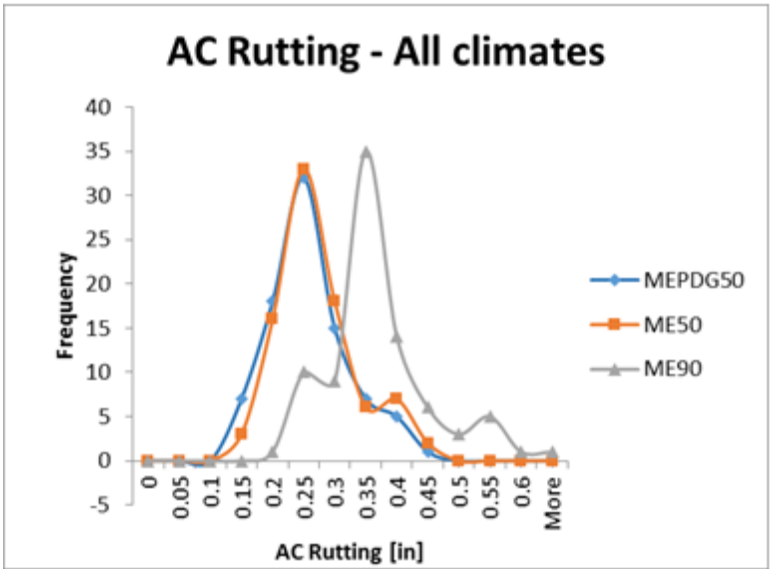

Figure 4.5 Histograms for AC Rutting from M-EPDG and Pavement-ME runs at 50 and 90 percent reliability for ACACPCC pavements

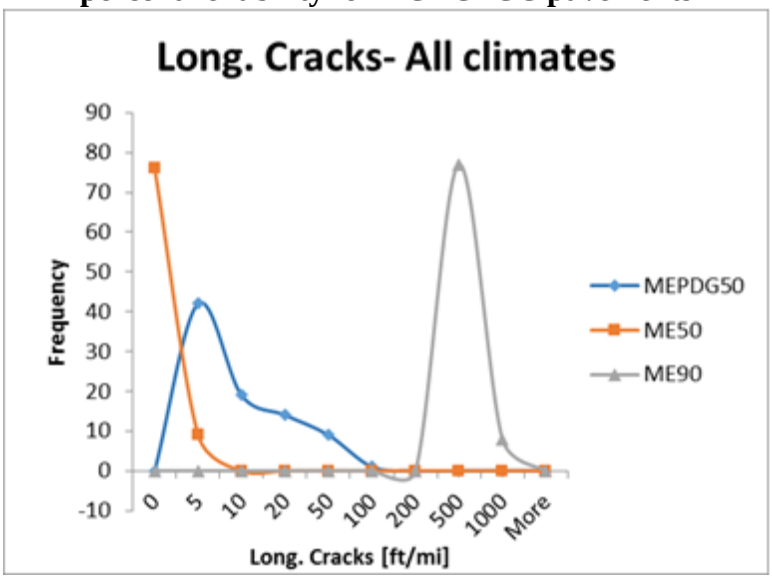

Figure 4.6 Histograms for Longitudinal Cracking from M-EPDG and Pavement-ME runs at 50 and 90 percent reliability for ACACPCC pavements

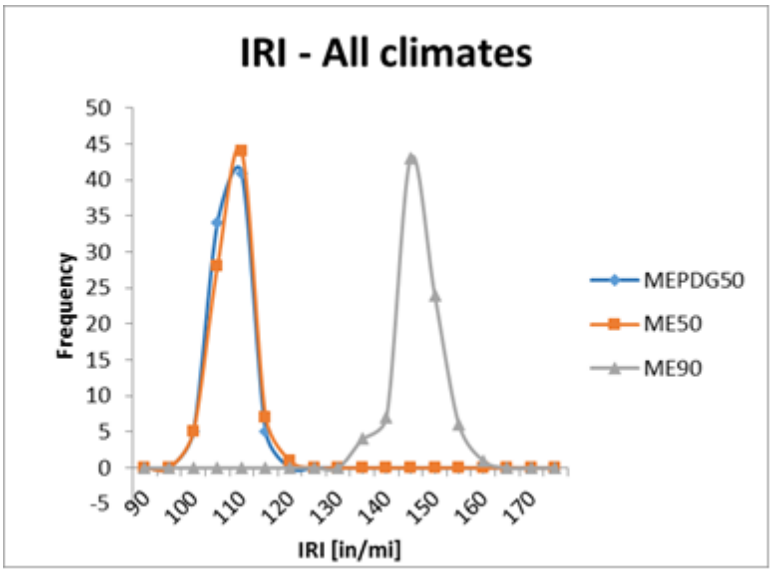

Figure 4.7 Histograms for IRI from M-EPDG and Pavement-ME runs at 50 and 90 percent reliability for ACACPCC pavements

Re-evaluation of Sensitivity and Importance Rankings for ACACPCC Pavements

Table 4.4 compares input importance rankings for cracking in ACACPCC between M-EPDG at 50% reliability and Pavement-ME at 50 and 90% reliability, respectively. Notably, geographic location (CLIMATE) remains the most important input as indicated by the descending order of sensitivity in the Table. It can be seen, however, that Pavement-ME analysis yielded, on average, much lower sensitivity of cracking predictions to all input as compared with M-EPDG.

Table 4.4. Summary of Cracking Sensitivity for ACACPCC Pavements

M-EPDG at 50% reliability			Pavement-ME at 50% Reliability			Pavement ME at 90% Reliability		
Predictor	logF	Assigned importance	Predictor	logF	Assigned importance	Predictor	logF	Assigned importance
CLIMATE	2.01	High	CLIMATE	0.92	Moderate	CLIMATE	0.06	Low
ACBIND	0.72	Moderate	ES	0.84	Moderate	EB	-0.50	Very Low
ES	0.54	Moderate	AADTT	0.02	Low	HBASE	-1.25	Very Low
HAC	0.47	Low	ACBIND	-0.29	Very Low	ACBIND	-1.72	Very Low
HPCC	0.46	Low	PR	-0.29	Very Low	HPCC	-1.94	Very Low
HMILL	0.46	Low	HPCC	-0.46	Very Low	ES	-2.14	Very Low
AADTT	0.23	Low	HMILL	-0.61	Very Low	HAC	-2.23	Very Low
PR	-0.24	Very Low	EB	-0.70	Very Low	HMILL	-2.67	Very Low
VCD	-0.48	Very Low	HAC	-0.80	Very Low	AADTT	-3.00	Very Low
HBASE	-1.72	Very Low	VCD	-1.55	Very Low	PR	-3.00	Very Low
EB	-1.87	Very Low	HBASE	-1.59	Very Low	VCD	-3.00	Very Low

The overall rutting sensitivity results for the aforementioned three modes are shown in Table 4.5. With truck traffic (AADTT), vehicle class distribution (VCD), and asphalt layer inputs

(ACBIND and HAC) being the most important. The three modes of analysis show the same order of sensitivity for all highly important inputs. It is worth noting that Pavement-ME analysis yielded a larger effect (as measured by logF values) of subgrade as compared with M-EPDG. In addition, the pre-overlay performance rating of the existing surface (PR) is assigned low importance at 90 percent reliability.

Table 4.5. Summary of Rutting Sensitivity for ACACPCC Pavements

M-EPDG at 50% reliability			Pavement-ME at 50% Reliability			Pavement ME at 90% Reliability		
Predictor	logF	Assigned importance	Predictor	logF	Assigned importance	Predictor	logF	Assigned importance
AADTT	3.15	Critical	AADTT	3.27	Critical	AADTT	3.29	Critical
CLIMATE	2.37	High	VCD	2.37	High	VCD	2.41	High
VCD	2.25	High	CLIMATE	2.22	High	CLIMATE	2.26	High
ACBIND	2.02	High	ACBIND	2.09	High	ACBIND	2.12	High
HAC	1.02	High	HAC	1.27	High	HAC	1.35	High
HMILL	0.98	Moderate	HMILL	1.20	High	HMILL	1.28	High
HPCC	0.65	Moderate	ES	0.89	Moderate	ES	0.88	Moderate
ES	0.14	Low	HPCC	0.83	Moderate	HPCC	0.79	Moderate
PR	-0.15	Very Low	PR	-0.05	Very Low	PR	0.10	Low
HBASE	-0.55	Very Low	EB	-0.52	Very Low	EB	-0.39	Very Low
EB	-0.59	Very Low	HBASE	-1.61	Very Low	HBASE	-2.00	Very Low

Table 4.6 compares the input sensitivity rankings for the IRI prediction models. The three modes of analysis do not differ in the order of importance of the design inputs. In addition, the logF values for critical and highly important parameters are very similar. In knowing that the IRI predictions are highly dependent on rutting and transverse cracking values as well as subgrade and climatic variables, the rankings in Table 4.6 appear to be reasonable.

Table 4.6. Summary of IRI Sensitivity for ACACPCC Pavements

M-EPDG at 50% reliability			Pavement-ME at 50% Reliability			Pavement ME at 90% Reliability		
Predictor	logF	Assigned importance	Predictor	logF	Assigned importance	Predictor	logF	Assigned importance
AADTT	3.14	Critical	AADTT	3.28	Critical	AADTT	3.27	Critical
ES	3.09	Critical	ES	3.12	Critical	ES	3.12	Critical
CLIMATE	2.43	High	CLIMATE	2.78	High	CLIMATE	2.78	High
VCD	2.24	High	VCD	2.38	High	VCD	2.37	High
ACBIND	2.00	High	ACBIND	2.11	High	ACBIND	2.10	High
HAC	1.00	High	HAC	1.29	High	HAC	1.27	High
HMILL	0.98	Moderate	HMILL	1.23	High	HMILL	1.20	High
HPCC	0.65	Moderate	HPCC	0.85	Moderate	HPCC	0.85	Moderate
PR	-0.15	Very Low	PR	0.00	Low	PR	-0.03	Very Low
HBASE	-0.52	Very Low	EB	-0.43	Very Low	EB	-0.52	Very Low
EB	-0.52	Very Low	HBASE	-2.00	Very Low	HBASE	-1.52	Very Low

Comparison between M-EPDG and Pavement ME results for AC-overlaid Repaired PCC Pavements (ACPCC)

The simulation runs of the Pavement-ME software for AC-overlaid Repaired PCC (ACPCC) pavement projects revealed the AC layer rutting, PCC slab cracking, and IRI as the only distress indicators of concern. Therefore, the comparison of the M-EPDG and Pavement-ME predictions is discussed with respect to these three distresses.

Evaluation of Normal Distribution (Histograms)

Figure 4.8 presents the distributions of AC layer rutting predictions for M-EPDG at 50% reliability and Pavement-ME at 50% and 90% reliability. Obviously, all three distribution shapes indicate normality. One can surmise that Pavement-ME predicts slightly higher AC layer rutting on average than M-EPDG does. The histogram shapes of the percentages of PCC slabs cracked as predicted by the M-EPDG at 50% and Pavement-ME at 50% and 90% reliability are very similar (Figure 4.9). It can be seen, however, that Pavement-ME predicts a higher PCC slab cracking level than does M-EPDG. For reasons unknown at the moment, Pavement-ME predicts much lower IRI at 50% reliability as compared with M-EPDG (Figure 4.10).

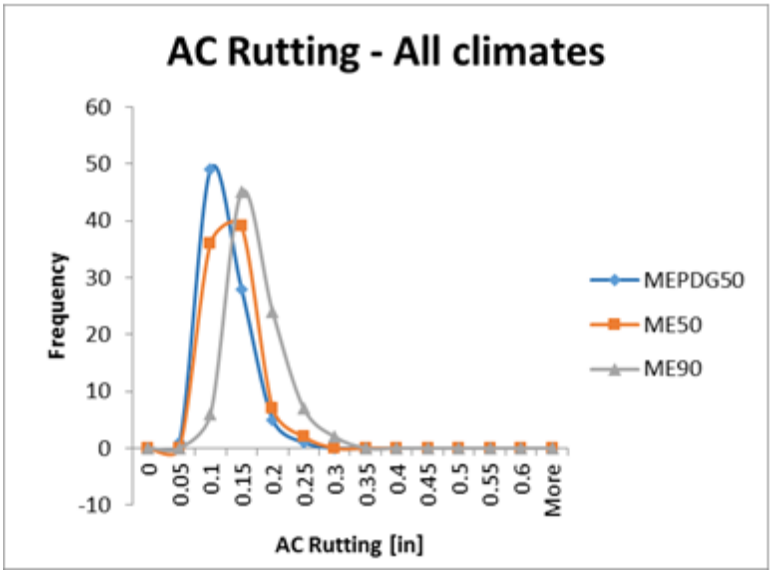

Figure 4.8 Histograms for AC Rutting from M-EPDG and Pavement-ME runs at 50 and 90 percent reliability for ACPCC pavements

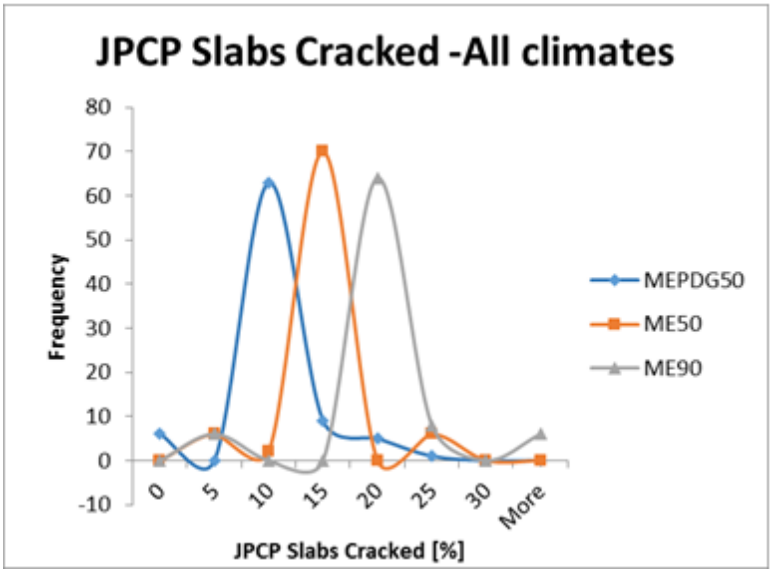

Figure 4.9 Histograms for PCC slab cracking from M-EPDG and Pavement-ME runs at 50 and 90 percent reliability for ACPCC pavements

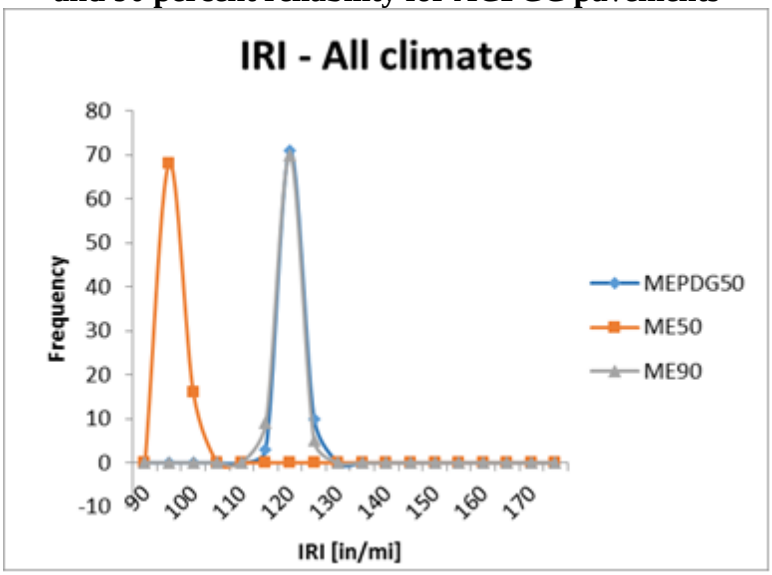

Figure 4.10 Histograms for IRI from M-EPDG and Pavement-ME runs at 50 and 90 percent reliability for ACPCC pavements

Re-evaluation of Sensitivity and Importance Rankings for AC-Overlaid Repaired PCC (ACPCC) Pavements

Similar to the two previously discussed pavement designs, the ACPCC distress outputs were analyzed by regression method to establish ranking of the contributing design input factors. The logarithms of individual F-statistics served as a measure of the contribution of the corresponding input into the variability of the resultant output. The significance of such a contribution was evaluated by the p-values at the level α=0.05 (95% reliability). Tables 4.7 through 4.9 compare assigned importance rankings for cracking, rutting, and IRI, respectively.

A noticeable difference in cracking sensitivity rankings between the three design cases is evident from Table 4.7. Interestingly, asphalt and PCC layer thicknesses (HAC and HPCC, respectively) yield overall low cracking sensitivity in the M-EPDG prediction models, high sensitivity of the Pavement-ME at 50% reliability, yet highly insignificant (very low) sensitivity of the Pavement-ME model at 90% reliability. The two main reasons for that phenomenon include zero sensitivity of transverse (thermal) cracking and an enormously high (up to 2300%) variation in longitudinal cracking predictions. Nevertheless, the CLIMATE variables stay near or at the top of the sensitivity-ranking list in all three cases (see Table 4.7).

Table 4.7. Summary of Cracking Sensitivity for ACPCC Pavements

M-EPDG at 50% reliability			Pavement-ME at 50% Reliability			Pavement ME at 90% Reliability		
Predictor	logF	Assigned importance	Predictor	logF	Assigned importance	Predictor	logF	Assigned importance
CLIMATE	0.80	Moderate	HAC	1.10	High	CLIMATE	0.45	Low
ES	0.27	Low	HPCC	0.87	Moderate	PSB	-0.41	Very Low
PSA	0.19	Low	CLIMATE	0.79	Moderate	PSA	-0.41	Very Low
HAC	0.19	Low	ES	-0.04	Very Low	HBASE	-0.50	Very Low
PSB	-0.03	Very Low	PSB	-0.42	Very Low	HPCC	-0.77	Very Low
HPCC	-0.17	Very Low	PSA	-0.42	Very Low	HAC	-1.10	Very Low
VCD	-1.20	Very Low	AADTT	-0.53	Very Low	ACBIND	-1.31	Very Low
AADTT	-1.60	Very Low	VCD	-0.89	Very Low	EB	-1.43	Very Low
ACBIND	-1.73	Very Low	ACBIND	-1.31	Very Low	ES	-1.63	Very Low
HBASE	-2.00	Very Low	EB	-1.41	Very Low	VCD	-1.66	Very Low
EB	-2.10	Very Low	HBASE	-1.47	Very Low	AADTT	-2.00	Very Low

The sensitivity of all three rutting models for ACPCC pavements, as compared in Table 4.8, is only governed by AC layer rutting. Since no changes have been reported for the AC rutting model in transition from the M-EPDG to Pavement-ME, the inputs related to traffic (AADTT and VCD), geographic location (CLIMATE), and performance grade of binder (ACBIND) remain highly significant and in the same order of rankings for the three cases. Table 4.9 shows very similar input ranking for IRI sensitivity, with the addition of granular base modulus (EB) as being highly significant, and ACBIND being high.

Table 4.8. Summary of Rutting Sensitivity for ACPCC Pavements

M-EPDG at 50% reliability			Pavement-ME at 50% Reliability			Pavement ME at 90% Reliability		
Predictor	logF	Assigned importance	Predictor	logF	Assigned importance	Predictor	logF	Assigned importance
AADTT	2.86	High	AADTT	3.00	High	AADTT	3.00	High
VCD	2.33	High	VCD	2.47	High	VCD	2.49	High
CLIMATE	2.10	High	CLIMATE	1.96	High	CLIMATE	1.98	High
ACBIND	1.80	High	ACBIND	1.81	High	ACBIND	1.80	High
HAC	0.99	Moderate	HAC	1.13	High	HAC	1.03	High
PSA	0.10	Low	ES	0.34	Low	ES	0.48	Low
HPCC	-0.01	Very Low	HPCC	0.13	Low	HPCC	-0.06	Very Low
ES	-0.89	Very Low	EB	-0.66	Very Low	HBASE	-0.40	Very Low
EB	-2.00	Very Low	HBASE	-1.70	Very Low	EB	-2.00	Very Low
HBASE	-2.00	Very Low	PSB	-2.00	Very Low	PSB	-2.00	Very Low
PSB	-3.00	Very Low	PSA	-2.00	Very Low	PSA	-2.00	Very Low

Table 4.9. Summary of IRI Sensitivity for ACPCC Pavements

M-EPDG at 50% reliability			Pavement-ME at 50% Reliability			Pavement ME at 90% Reliability		
Predictor	logF	Assigned importance	Predictor	logF	Assigned importance	Predictor	logF	Assigned importance
AADTT	2.80	High	AADTT	2.98	High	AADTT	3.00	High
PSB	2.58	High	CLIMATE	2.54	High	CLIMATE	2.57	High
PSA	2.50	High	VCD	2.46	High	VCD	2.47	High
VCD	2.27	High	EB	2.20	High	EB	2.24	High
CLIMATE	2.14	High	ACBIND	1.80	High	ACBIND	1.81	High
ACBIND	1.74	High	HAC	1.09	High	HAC	1.12	High
EB	1.69	High	ES	0.32	Low	ES	0.34	Low
HAC	0.91	Moderate	HPCC	0.08	Low	HPCC	0.13	Low
HPCC	0.57	Moderate	HBASE	-1.52	Very Low	HBASE	-1.70	Very Low
ES	-0.89	Very Low	PSB	-2.00	Very Low	PSB	-2.00	Very Low
HSB	-2.00	Very Low	PSA	-2.00	Very Low	PSA	-2.00	Very Low

CHAPTER 5 Evaluation of Connecticut PMIS Data

Introduction

An important task of this Project was aimed at obtaining agency-specific inputs to populate the pavement design input database to be used for validation of the Pavement-ME predictive models. This input data was provided to the research team by CTDOT. The traffic levels, layer thicknesses, and material data were retrieved for a validation set of 48 representative pavement sections provided by the CTDOT. The performance data for those sections in terms of cracking, rutting, and IRI was extracted from the CTDOT Wisecrax^{TM} database. Next, in order to rank the importance effect of the input on performance outcomes a formal statistical analysis of the relationships between performance indicators and PMIS inputs was conducted. Then, in order to validate the applicability of PMIS data for use with the Pavement-ME design, the PMIS ranking was compared with Pavement-ME rankings determined earlier (see Chapter 4 for details).

Transfer of PMIS data for the period of 2008-2014

During a visit with CTDOT staff in May 2015, a pavement condition database was transferred to the CTI computer. This database included a wide range of pavement information collected during ARAN surveys between 2008 and 2014, and averaged for each 0.1 lane-mile. For each year, an Excel workbook was created with 41750 rows (corresponding to a total of 41750 miles) and a variable number of columns (115 columns in 2008 and 90 columns for years 2009-2014). Since the primary goal of this project is to validate the Pavement-ME prediction of distresses against the measured values reported by CTDOT's PMIS, the initial evaluation of PMIS data targeted the pavement sections to be included in the validation phase of the project. For that purpose, the entire PMIS dataset was reduced to 48 pavement sections with a total of 17.7 lane-mile lengths (177 rows of data). In addition, only data columns relevant to the analysis were extracted from the PMIS database. A formal statistical analysis is aimed at determining the importance ranking of designated inputs on distress outputs, as reported in the PMIS. The PMIS ranking is then compared with sensitivity rankings outputted via Pavement-ME. Such a comparison is helpful in understanding how the PMIS data trends are aligned with Pavement-ME sensitivity trends.

Selection of Candidate Sections

The list of pavement sections to be included in the validation phase of the project was provided by the CTDOT in accordance with research team recommendations. A total of 48 sections with 177 0.1-mile long units were chosen to represent a typical range of pavement structures for specified traffic levels, and in specified climatic zones. Table 5.1 summarizes the most important characteristics for those sections, whereas the detailed information on their pavement characteristics can be found in Appendix B.

Table 5.1. Characteristics of the Validation Pavement Dataset

Climate	Traffic	Structure	Surface Age (Years)	Number of Observations
Climate I - Shore	Level 2 (AADTT=400)	AC on PCC Thick AC (>4.5 in.) Thin AC (<4.5 in.)	0 to 9 2 to17 13 to 17	9 11 4
	Level 3 (AADTT=1000)	AC on AC on PCC AC on PCC Thick AC (>4.5 in.)	12 to 13 17 3 to 23	10 3 14
	Level 4 (AADTT=25000)	AC on AC on PCC	2 to 9	10
Climate II - Inland	Level 1 (Not used in the final analysis)	Thin AC (<4.5 in.)	16	2
	Level 2 (AADTT=400)	AC on PCC Thick AC (>4.5 in.) Thin AC (<4.5 in.)	2 to 13 10 to 17 17	9 17 3
	Level 3 (AADTT=1000)	Thick AC (>4.5 in.) Thick AC on PCC Thin AC (<4.5 in.)	9 9 to 11 14	3 11 2
	Level 4 (AADTT=2500)	AC on AC on PCC	0 to 6	12
Climate III - Hills	Level 2 (AADTT=400	AC on PCC Thick AC (>4.5 in.) Thin AC (<4.5 in.)	4 to 16 3 to 8 16 to 17	15 12 5
	Level 3 (AADTT=1000	AC on AC on PCC Thick AC (>4.5 in.)	3 5	3 8
	Level 4 (AADTT=2500)	AC on AC on PCC	5 to 13	14

Evaluation of Normal Distributions

Before a linear regression analysis is performed, it is necessary to evaluate normality of the distribution of values for participating variables. This is done with an evaluation of histogram shapes. To illustrate this approach, Figures 5.1 and 5.2 show the histograms of cracking values and surface age for the validation pavement sections. Those variables are chosen in knowing that age of pavement surface, which is correlated with cumulative traffic load, is a primary factor of cracking distress in all types of pavement.

Figure 5.1 (left) shows a histogram of longitudinal cracking with separate plots for non-wheelpath (NWP) and wheelpath (WP) cracking locations. When observing the longitudinal cracking histogram, one can first notice that both NWP and WP distributions are skewed toward the same value of 25 ft/10 m-lane. In addition, the WP longitudinal cracking occurs more frequently than NWP cracking. Another important difference between the NWP and WP histograms is the presence of two additional peaks around 75 ft/10 m-lane and 125 ft/10 m-lane for the WP cracking, whereas NWP cracking is distributed in a smoother manner. The significant distance between peaks on the longitudinal WP histogram can indicate the presence of some subsets of data with different means, due to influence of such factors as pavement type, which

warrant a multivariate analysis of variance. The transverse cracking distributions shown in Figure 5.1 (right) indicate virtually no difference between NWP and WP trends. This trend aligns with a premise that transverse cracking could depend more on climatic conditions rather than traffic load, for instance. In summary, nevertheless, all histograms in Figure 5.1 have primarily a normal distribution shape, which justifies the use of a linear regression approach.

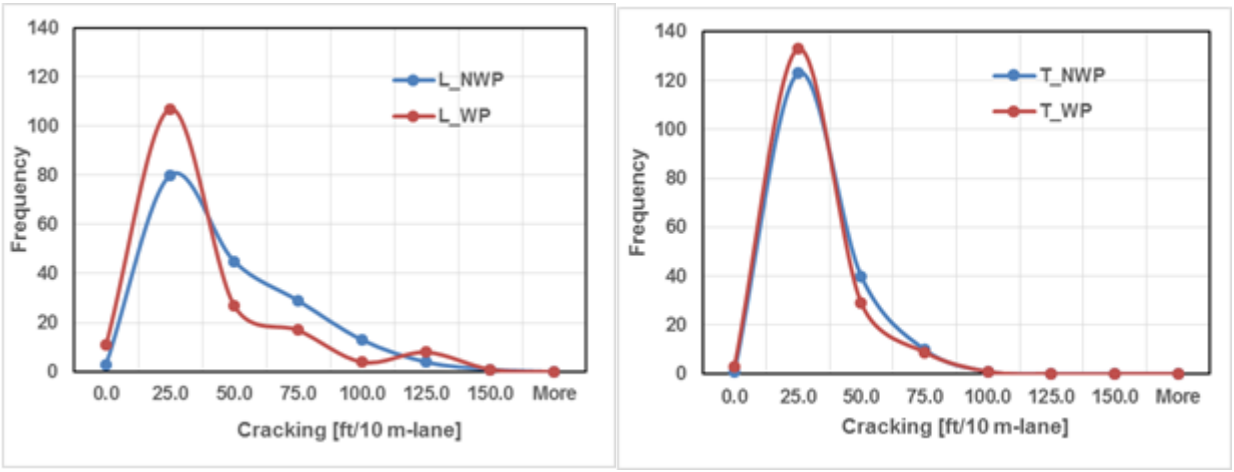

Figure 5.1 Longitudinal cracking histogram (left) and transverse cracking histogram (right) for non-wheelpath (NWP) and wheelpath (WP) locations

Figure 5.2 superimposes distributions of surface age for 1) all pavement types 2) flexible and 3) composite pavements in the validation dataset. Evidently, two surface age groups of composite pavements are present with an average age of 7 and 15 years, which should be accounted for in the statistical analysis. The flexible pavement ages, on the other hand, are distributed more uniformly, however, with one distinctive group of 17 to 22 year old sections. This phenomenon may be a reason for the 125-ft/10 m-lane peak in Figure 5.1 (left). Once again, the distribution of surface ages indicates the possibility of a confounding effect of pavement type and surface age on the outcomes of statistical analysis. It should be noted that the statistical inferences discussed in this report only apply to the given dataset of sections provided by the CTDOT for this project. Therefore, they cannot be used to make any conclusions on the entire Connecticut road network.

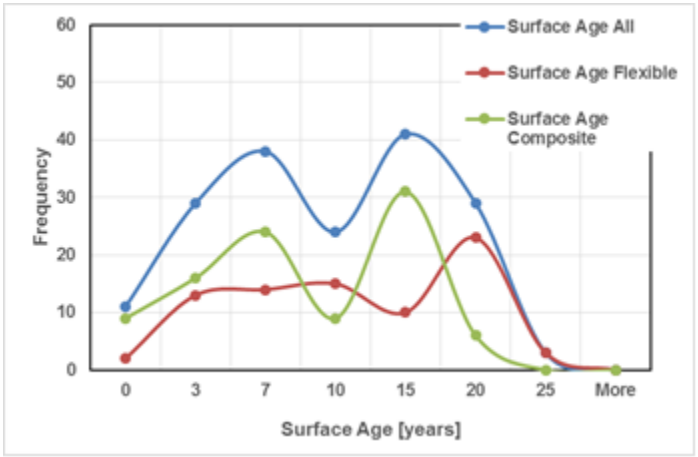

Figure 5.2 Surface age histogram of the validation pavement sections

General Trends

The validation set of pavement sections was compiled based on recommendations to represent typical climate, traffic, and pavement structure inputs in the CTDOT PMIS. As such, it is a designed experiment with fixed "treatments", or factors. This section starts with an evaluation of general linear trends for different responses (type of cracking). Next, the results of a Student's t-test for significance of the difference in mean response is reported for climate, designed traffic level as designated by CTDOT, and pavement type. Lastly, some collinearity issues are reported.

Evaluation of Linear Trends

Figures 5.3 and 5.4 depict total WP and NWP cracking trends with respect to surface age in years 2008 and 2014, respectively. The 2008 cracking trends are characterized by virtually no association between amount of cracking and age with low average values (about 5 ft/10m-lane) for both NWP and WP cracking. At variance with 2008, Figure 5.4 presents a stronger correlation of cracking with surface age, with an overall slightly higher amount of non-wheelpath cracking. One possible reason for such a significant change in trends could be an upgrade in ARAN technology, which in 2014 allows for detecting more cracking at a higher resolution. This phenomenon may provide a distorted perspective on the existing pavement condition as see in Figures 5.3 and 5.4. It worth noting that the average surface age in 2008 was 8±4 years whereas, in 2014, it was 9±6 years. In addition, 110 pavement segments were left untreated, while the remaining 67 were overlaid during the analysis period of 6 years (between 2008 and 2014). The 62% sections left untreated may explain the increased deterioration rate in 2014.

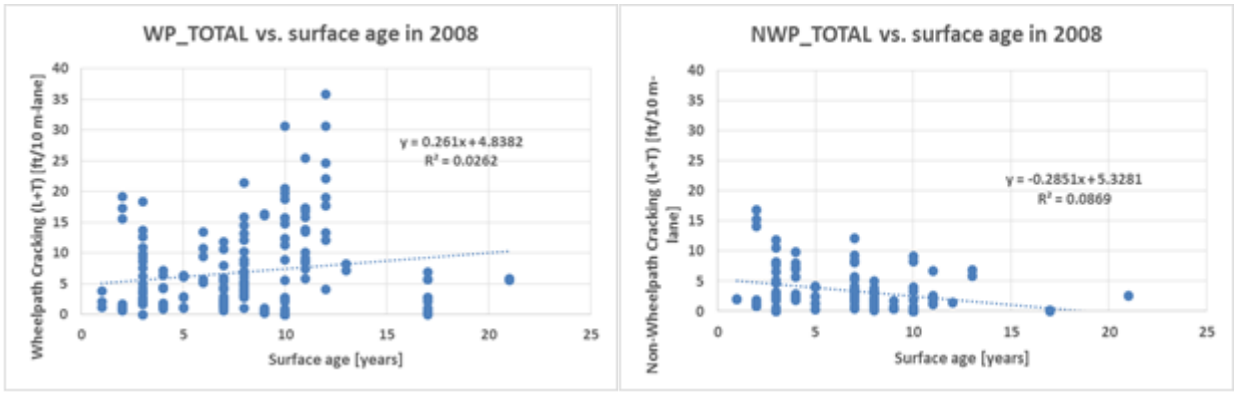

Figure 5.3 Total wheelpath and non-wheelpath cracking as a function of surface age in 2008

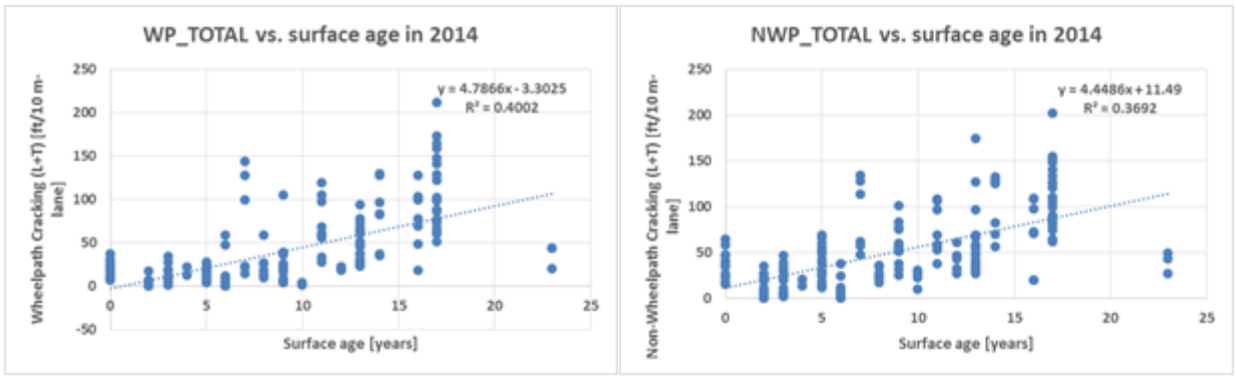

Figure 5.4 Total wheelpath and non-wheelpath cracking as a function of surface age in 2014

Significance Tests for Difference of Means

The Student's t-test for significance of the differences in sample means is a valuable method for testing a no-difference hypothesis. The significance of the reported t-statistic is evaluated by its p-value at a given level of confidence α. If the p-value is less than α, the probability of a no-difference hypothesis being true is small, which suggests that the difference between two sample means is statistically significant. For this project a confidence level α=0.05 is chosen due to the relatively small sample size. The total set of observations is divided into groups with respect to climate, traffic, and pavement type, and the group means are subjected to Student's t-test. The t-test results are presented in a matrix form (Tables 5.2 through 5.9) in which diagonal values show mean±standard deviation for each variable category. The matrix cells above the diagonal report p-value of a t-test for significance of the difference in mean between two categories, whereas the corresponding conclusion on significance of the test is noted in the cells below the diagonal.

Tables 5.2 through 5.5 summarize the t-test results for differences in cracking between the three climatic zones, i.e. Hills, Inland, and Shore. No statistical difference in any type of cracking between Hills and Inland climates is reported, whereas the Shore climate shows lesser longitudinal NWP cracking and greater transverse cracking (both NWP and WP) as compared with Hills locations.

Table 5.2. Summary of t-test for difference in Longitudinal WP cracking between climatic zones in 2014

Climate	Hills	Inland	Shore
Hills	14.7±15.5	0.388	0.047
Inland	Not significant	13.8±14.8	0.023
Shore	Significant	Significant	19.8±17.6

Table 5.3. Summary of t-test for difference in Longitudinal NWP cracking between climatic zones in 2014

Climate	Hills	Inland	Shore
Hills	16.3±16.3	0.406	0.040
Inland	Not significant	15.5±16.3	0.023
Shore	Significant	Significant	22.0±18.7

Table 5.4. Summary of t-test for difference in Transverse WP cracking between climatic zones in 2014

Climate	Hills	Inland	Shore
Hills	14.7±15.5	0.388	0.047
Inland	Not significant	13.8±14.8	0.023
Shore	Significant	Significant	19.8±17.6

Table 5.5. Summary of t-test for difference in Transverse NWP cracking between climatic zones in 2014

Climate	Hills	Inland	Shore
Hills	16.3±16.3	0.406	0.040
Inland	Not significant	15.5±16.3	0.023
Shore	Significant	Significant	22.0±18.7

Tables 5.6 through 5.9 show the results of t-tests for difference in cracking between pavements with designed traffic levels 2, 3, and 4. Note that since only 2 out 177 observations are available for traffic Level 1, they are excluded from the analysis. Another important notion here is that the higher the designed traffic level the stronger (and most of the time thicker) the pavement structure is and, hence, no difference in load-related (WP) cracking would be expected at the same surface age. The evaluation of t-statistic significances in Tables 5.6 and 5.7 leads to a conclusion of a significant decrease in both WP and NWP longitudinal cracking. On the other hand, the mean NWP transverse cracking level shows similarity between Levels 3 and 4, these being significantly lower than at Level 2. Those counterintuitive trends warranted an evaluation of collinearity of designed traffic levels, pavement types and surface age, as presented and discussed in the next subsection.

Table 5.6. Summary of t-test for difference in Longitudinal WP cracking between designed Traffic Levels in 2014

Traffic	Level 2	Level 3	Level 4
Level 2	34.1±34.6	0.009	0.000
Level 3	Significant	22.0±25.0	0.000
Level 4	Significant	Significant	0.8±2.9

Table 5.7. Summary of t-test for difference in Longitudinal NWP cracking between designed Traffic Levels in 2014

Traffic	Level 2	Level 3	Level 4
Level 2	42.3±32.4	0.130	0.000
Level 3	Not significant	36.9±23.4	0.000
Level 4	Significant	Significant	8.7±12.9

Table 5.8. Summary of t-test for difference in Transverse WP cracking between designed Traffic Levels in 2014

Traffic	Level 2	Level 3	Level 4
Level 2	21.3±19.5	0.001	0.000
Level 3	Significant	12.8±11.2	0.133
Level 4	Significant	Not significant	10.3±9.7

Table 5.9. Summary of t-test for difference in Transverse NWP cracking between designed Traffic Levels in 2014

Traffic	Level 2	Level 3	Level 4
Level 2	23.0±20.6	0.002	0.001
Level 3	Significant	14.5±12.3	0.253
Level 4	Significant	Not significant	12.8±12.3

Collinearity Issues

Collinearity of predictors is evaluated by the coefficient of correlation between them. If found significant; such collinearity calls for removing a variable from the regression analysis. Therefore, the mean cracking values were calculated for traffic and pavement type groups as shown in Tables 5.10 and 5.11, respectively.

Table 5.10 indicates a high positive association of both types of cracking with pavement surface age, while showing a sharp decrease in mean cracking associated with an increase in traffic level. On the other hand, Table 5.11 shows a clear increase in mean surface age associated with a decrease in thickness. Likely, it means that thicker pavements were overlaid (or constructed) more recently. Concurrently, the increase in age in Table 5.11 is highly associated with an increase in cracking, which is expected. Thus, it can be safely concluded that neither pavement type nor designed traffic level are independent of surface age, because they are pairwise collinear. However, each traffic level includes all pavement types. Therefore, at this moment, traffic level is excluded from the analysis whereas the effect of surface age, which is obviously correlated with cumulative traffic load (i.e., the older the surface the greater the accumulated traffic), is evaluated separately from the effect of pavement type. The results of a multivariate analysis of variance, shown next, support such an approach.

Table 5.10. Summary of means for collinearity grouped by traffic level

Designed Traffic	Number of Observations	Mean Surface Age [years]	Mean Longitudinal WP cracking [ft/10 m-lane]	Mean Longitudinal NWP cracking [ft/10 m-lane]
Level 2	85	10.0	34.1	42.3
Level 3	54	9.0	22.0	36.9
Level 4	36	6.1	0.8	8.7

Table 5.11. Summary of means for collinearity grouped by pavement type

Pavement Type	Number of Observations	Mean Surface Age [years]	Mean Longitudinal WP cracking [ft/10 m-lane]	Mean Longitudinal NWP cracking [ft/10 m-lane]
AC on AC on PCC	52	6.9	3.8	13.07
AC on PCC	38	8.4	29.0	41.42
Thick AC	63	9.1	28.4	40.25
Thick AC on PCC	6	11.0	42.9	38.39
Thin AC	16	15.9	48.1	52.01

Multivariate Analysis of Variance

Dataset for Linear Regression

The first step of the formal statistical analysis is to compile a dataset, while carefully choosing type of predictor between numerical (continuous values) and categorical (discrete values) variables. For instance, the surface age can be used as a numerical variable. However, pavement type and traffic level cannot be expressed numerically. Therefore, they are included in the prediction model as categorical predictors, or factors. With regard to pavement layer thicknesses, the validation dataset has many repetitions for a particular AC, PCC, and granular base thickness. Hence, it is preferred to use those most common thickness values observed in the dataset as factors in a prediction model. One additional factor included in the analysis is CTDOT ARAN vehicle number. This is done because of differences in Strobe and 2-D Scan systems that are installed in CTDOT vans No. 7 and No. 8, respectively. Table 5.12 summarizes the variables and range values included in the regression analysis.

Table 5.12. Dataset Used for Multivariate Analysis of Variance

Input Group	Input Description	Input Index	Response/ Predictor	Numerical/ Categorical	Values
Distress Indicators	Longitudinal NWP cracking	L_NWP	Response	Numerical	0 - 131
	Longitudinal WP cracking	L_WP	Response	Numerical	0 - 141
	Transverse NWP cracking	T_NWP	Response	Numerical	0 – 82
	Transverse WP cracking	T_WP	Response	Numerical	0 - 83
Site Factors	Surface Age	AGE	Predictor	Numerical	0 - 23
	Climatic Zone	CLIMATE	Predictor	Categorical	Hills, Inland, Shore
	Measurement System	VAN	Predictor	Categorical	7 (Strobe); 8 (2-D Scan)
Pavement Design Features	Pavement Type	P_TYPE	Predictor	Categorical	AC on AC on PCC AC on PCC Thick AC Thick AC on PCC Thin AC
	Top AC layer thickness	HAC1	Predictor	Numerical	0 – 6.25
	Bottom AC layer thickness	HAC2	Predictor	Categorical	0, 0.75, 1, 2, 2.25, 2.4, 2.75, 4, 6, unknown
	PCC thickness	HPCC	Predictor	Categorical	0, 8.25, 8.5, 9, 9.5, 10, 10.5, unknown
	Granular base/subbase thickness	HBASE	Predictor		6, 6.5, 7, 7.5, 8.25, 10, 10.4, 12, 13.5, 16, unknown

Evaluation of Best-Fit Regression Models

Three types of linear regression models are considered in this analysis. The first type includes only site factors, i.e. AGE, CLIMATE, and VAN, as predictors. The second type of regression model only accounts for pavement design features (P_TYPE, HAC1, HAC2, HPCC, and HBASE). The last type includes a combination of all variables and factors from Table 5.12. Note that separate models are considered for each of the four responses, longitudinal cracking non-wheelpath and wheelpath, and transverse cracking non-wheelpath and wheelpath (L_NWP, L_WP, T_NWP, and T_WP). When all factors are included in a model, the interactions between climate, traffic (as represented by surface age), and subgrade (as represented by HBASE) are considered. The R-squared and overall F-statistic are considered as criteria to compare the goodness of fit of the twelve models. Such a comparison helps to illustrate the contribution of various group factors into development of pavement distresses for the given validation dataset.

Table 5.13 compares best-fit models for site factors. The R-squared value shows how much of the data is explained by a model, whereas F-statistic serves as an indicator of explained variance in the model. If the p-value for F-test is less than 0.01, the model is accepted as statistically significant at 99% reliability. The results in Table 5.13 show that not much difference between models can be noted with 42 to 46 percent of data explained by site factors. While the significance of these models cannot be neglected, the results in Table 5.13 indicate that the majority of cracking data is associated with factors other than surface age, location, and differences in ARAN technology.

Table 5.13. Summary of Type I regression models (SITE FACTORS)

Predictors Included	Response	Model R-Squared	Model F-statistics	p-value
AGE (Numerical) CLIMATE (Factor) VAN (Factor) CLIMATE*AGE (Interaction)	L_NWP	0.415	20.7	0.0000
	L_WP	0.447	22.60	0.0000
	T_NWP	0.460	23.81	0.0000
	T_WP	0.459	23.78	0.0000

The goodness of fit for predicting longitudinal and transverse cracking from pavement features (as represented by layer thickness) differs significantly, as shown in Table 5.14. For example, while at least 56 percent of longitudinal cracking data is associated with the regression model (see R-Sq. values), only about 38 percent of transverse cracking is explained by the same predictors. This trend is supported by much lower F-values for transverse cracking models. These phenomena are expected, since transverse cracking in asphalt surfaces is mostly caused by variations in ambient temperature and the propagation of cracks as a reflection of transverse joints.

Table 5.14. Summary of Type II regression models (PAVEMENT FEATURES)

Predictors Included	Response	Model R-Squared	Model F-statistics	p-value
HAC1 (Numerical) HAC2 (Factor) HPCC HBASE HPCC	L_NWP	0.559	7.92	0.0000
	L_WP	0.570	8.29	0.0000
	T_NWP	0.368	3.64	0.0000
	T_WP	0.387	3.95	0.0000

Where all variables and factors are considered, the goodness of fit drastically increases to 75-80 percent of cracking data being explained by the predictors, as shown in Table 5.15. As expected, the difference between R-squared values is not very large, which indicates that the variables and factors extracted from the PMIS data can equally explain all types of measured cracking values. The next step is to differentiate between inputs in terms of their individual influence on the cracking values predicted by the model, which is discussed in the next subsection.

Table 5.15. Summary of Type III regression models (ALL VARIABLES AND FACTORS)

Predictors Included	Response	Model R-Squared	Model F-statistics	p-value
AGE (Numerical) CLIMATE (Factor) VAN (Factor) HAC1 HAC2 (Factor) HPCC (Factor) HBASE (Factor) HPCC (Factor) CLIMATE *AGE (Interaction) CLIMATE*HBASE (Interaction)	L_NWP	0.745	10.09	0.0000
	L_WP	0.804	14.17	0.0000
	T_NWP	0.764	11.21	0.0000
	T_WP	0.773	11.76	0.0000

Importance Ranking of PMIS Inputs

The approach used for influence ranking of the PMIS inputs is similar to the approach used in the task 2 sensitivity analysis. This approach utilizes multiple analyses of variance through evaluating the significance of F-values associated with each input. The F-value measures the contribution of a variability of a particular input, i.e. predictor, into overall variability of output, i.e. response of a model. The higher the individual F-statistic values of the predictor the higher its importance for a prediction model. Tables 5.16 and 5.17 present the importance rankings in descending order of the individual input F-values for longitudinal and transverse cracking, respectively. The F-values are considered statistically insignificant at p-value greater than 0.05 and as such their corresponding inputs are of low importance. The F-values with $0.01 \leq$ p-value ≤ 0.05 are considered of moderate significance whereas p-value equal or less than 0.01 indicates high significance of the corresponding F-value.

The importance rankings shown in Table 5.16 indicate that differences in longitudinal cracking in Connecticut pavements are mostly governed by their age, cumulative traffic load (correlated with age), and presence of supporting AC or PCC layer. It is also important to acknowledge the significance of interactions between CLIMATE and AGE variables, which suggest a difference in deterioration rates of pavements in Hills, Shore, and Inland climatic zones. High influence of CLIMATE and HBASE interaction on wheelpath cracking indicates a difference in the influence of unbound base thickness in different climatic zones. The insignificant F-values for the top AC layer (HAC1) can be explained by its masked interaction with PCC presence and binder course (HAC2). Notably, the difference in longitudinal cracking measured with different ARAN technologies (VAN factor) appears to be highly significant.

Table 5.16. Summary of importance ranking of PMIS inputs for longitudinal cracking

Longitudinal Non-wheelpath cracking			Longitudinal Wheelpath cracking		
Predictor	F	Assigned importance	Predictor	F	Assigned importance
AGE	n/a*	Critical	AGE:	n/a*	Critical
CLIMATE	n/a*	Critical	CLIMATE:	n/a*	Critical
VAN	9.52	High	CLIMATE*AGE	6.08	High
HAC2	4.51	High	CLIMATE*HBASE	5.42	High
CLIMATE* AGE	4.32	High	HAC2	5.29	High
CLIMATE*HBASE	3.57	High	VAN	3.76	High
HPCC	3.27	High	HPCC	3.73	High
HBASE*AGE	2.41	Moderate	HBASE*AGE	0.85	Very Low
HAC1	2.35	Low	HBASE	0.41	Very Low
HBASE	1.16	Low	HAC1	0.36	Very Low

*Mean is overparametrized, hence, the input is a dominating variable.

The importance ranking of the PMIS inputs for transverse cracking are summarized in Table 5. 17. The order of importance for the site factors is similar to that for longitudinal cracking, including the effect of the interaction between site factors on wheelpath cracking. Interestingly, the top layer thickness appears to be important for transverse wheelpath cracking, which may indicate the presence of alligator cracking in the wheelpath. The non-importance of asphalt thickness (HAC1 and HAC2) for transverse non-wheel cracking is expected due to the environmental nature of this distress.

Table 5.17. Summary of importance ranking of PMIS inputs for transverse cracking

Transverse Non-wheelpath cracking			Transverse Wheelpath cracking		
Predictor	F	Assigned importance	Predictor	F	Assigned importance
AGE	n/a*	Critical	AGE:	n/a*	Critical
CLIMATE	n/a*	Critical	CLIMATE:	n/a*	Critical
VAN	14.82	High	VAN	15.57	High
CLIMATE*HBASE	10.53	High	CLIMATE*HBASE	13.23	High
HBASE*AGE	6.31	High	HBASE*AGE	7.65	High
HBASE	3.78	High	HBASE	5.56	High
HPCC	3.14	High	HAC1	4.75	High
CLIMATE*AGE	2.87	Moderate	HPCC	3.47	High
HAC1	2.78	Low	CLIMATE*AGE	2.82	Low
HAC2	1.27	Low	HAC2	1.04	Very Low

*Mean is overparametrized, hence, the input is a dominating variable

In summary, as far as overall cracking sensitivity is considered, AC thickness, traffic volume, and climatic zone appear to have high importance in both PMIS and Pavement-ME ranking. This suggests that the set of pavement sections chosen for validation phase is relatively balanced and suitable for use.

CHAPTER 6. Validation of PMIS Performance Data

Introduction

Seven-year performance data (2008 – 2014) was obtained from the CTDOT pavement management unit. The ID data field included Road name and beginning/end milepost for each 0.1-mile pavement section selected under Task 3. The following performance indicators were retrieved from the pavement condition database as reported by the WiseCrax^{TM} software for year 2014 (see Table C.1 in Appendix C):

- Wheelpath and non-wheelpath longitudinal and transverse cracking
- Average IRI
- Average Rut depth

Out of 177 0.1-mi segments, 20 were excluded from further analysis due to discrepancies or a lack of available information on their pavement structure. In addition, those 20 sections exhibited virtually no correlation with surface age (R-squared of 0.00 to 0.01) as compared with the rest of the dataset (R-squared of 0.45 to 0.56). Table C.1 (Appendix C) lists them as "outlier" sections.

Visual Evaluation of Photolog

A visual evaluation of Photolog images collected in 2012 (last year available through Digital Highway) was performed on roughly 40 percent of the pavement sections (61 out of 150 selected for the final analysis). Almost 2000 Photolog pavement images were evaluated. Due to time constraints and the variable visual quality of pavement images, crack lengths of all severities and locations (wheelpath and non-wheelpath) were summed up in the longitudinal and transverse directions, respectively. In addition, the alligator cracking was estimated by visual evaluation. The alligator cracking areas were further used to establish their correlation with linear cracking reported by Wisecrax^{TM}.

Units Conversion

The pavement condition database provided by CTDOT reported cracking lengths for each 0.1 miles in average feet per 10-meter lane-length. However, the visual assessment was done by determining total crack lengths as m per 0.1 mile. Therefore, a two-way conversion was done to make comparison between automatically and visually assessed cracking datasets possible. First, the *visually assessed crack lengths were converted to WiseCrax^{TM} units* for each 0.1-mi section, which produced 61 data points for each type of cracking (longitudinal and transverse) as shown in Table C.2 (Appendix C).

An *alternative conversion employed transforming both visual and Wisecrax units to total ft/mi f*or each route. This dataset produced 16 data points for each type of cracking as shown in Table C.3 (Appendix C).

Multiple Correlation analysis

Once conversions were done, the visual and Wisecrax datasets were analyzed for cross-correlation. The Pearson's coefficient of correlation *r* was used as a measure of association between corresponding crack types and their progression with surface age. The significance of each correlation coefficient was evaluated by Student's t-test as in the following equation:

$$t = r/\mathrm{sqrt}([1-r^2]/[N-2]) \qquad (6.1)$$

where N is a sample size. Three levels of significance were assigned based on the p-value of t-statistics as follows:

- High significance ($p<0.01$, $r>0.623$)
- Moderate significance ($0.01\leq p<0.05$, $0.498\leq r\leq 0.623$)
- Low significance ($p\geq 0.05$, $r<0.498$)

Table 6.1 summarizes correlation coefficients and their respective levels of significance. It can be inferred that:

1. Both visual and automated evaluations produced similar results with respect to corresponding distresses as supported by a high correlation of 0.94 for longitudinal and total cracking, with a lesser degree of association for transverse cracking (r=0.84).
2. Alligator cracking is highly correlated with both visually and automatically generated longitudinal and total cracking (r=0.8), while having lesser degree of association with transverse cracking (r=0.6).

Once a high degree of correlation between visual and automated distress datasets is established, a closer look at the magnitude of the relationship between them can be taken. The influencing factors of this relationship can be established, as discussed next.

Table 6.1. Summary of multiple correlation analysis of Photolog vs. WiseCrax™ cracking datasets

Pearson's *r* / Significance		Visual from Photolog				Automated from WiseCrax™		
		Longitudinal [ft/10m]	Transverse [ft/10m]	L+T [ft/10m]	Alligator [%Area]	Longitudinal [ft/10m]	Transverse [ft/10m]	L+T [ft/10m]
Visual from Photolog	Longitudinal [ft/10m]	1.00	0.67	0.98	0.79	0.94	0.57	0.90
	Transverse [ft/10m]	High	1.00	0.79	0.61	0.65	0.84	0.82
	L+T [ft/10m]	High	High	1.00	0.80	0.93	0.67	0.94
	Alligator [%Area]	High	Moderate	High	1.00	0.74	0.56	0.76
Automated from WiseCrax™	Longitudinal [ft/10m]	High	Moderate	High	High	1.00	0.54	0.93
	Transverse [ft/10m]	Moderate	High	High	Moderate	Moderate	1.00	0.81
	L+T [ft/10m]	High	High	High	High	High	High	1.00

Relationship between Visual and WiseCrax™ Distress Data

To evaluate the magnitude of the relationships between automatically and visually assessed cracking lengths, three bivariate plots were constructed as shown in Figure 6.1. The linear trend equations shown on the plots clearly indicate that WiseCrax™ software overestimates both longitudinal and transverse cracking by factors of 1.755 and 3.114, respectively, with very high probability. This results in reporting twice as much total crack length as compared with visual evaluation of the Photolog images. While identifying the reason for such a trend is beyond the scope of this project, two possible explanations are offered:

1. **Longitudinal Cracking**: The visual evaluation does not include secondary cracks associated with medium severity. However, WiseCrax™ may count even closely located (spaced) longitudinal cracks as independent, thus, increasing the reported crack length. In addition, the WiseCrax™ algorithm may be set so that edges of the traffic paint line are included in the count, thus increasing the overestimation.
2. **Transverse cracking**: Each Photolog image of pavement surface travelled by the CTDOT ARAN Van 7 is constructed from four snapshots collected by the Strobe system. As a result, such an image has three or four horizontal lines where the Strobe snapshots are joined. Those lines may be read by the WiseCrax™ algorithm as transverse cracks. The newer laser scan cameras installed on ARAN Van 8 are expected to produce data that are free of the "phantom joints." However, as discussed later, Van 8 also was found to overestimate transverse crack lengths.

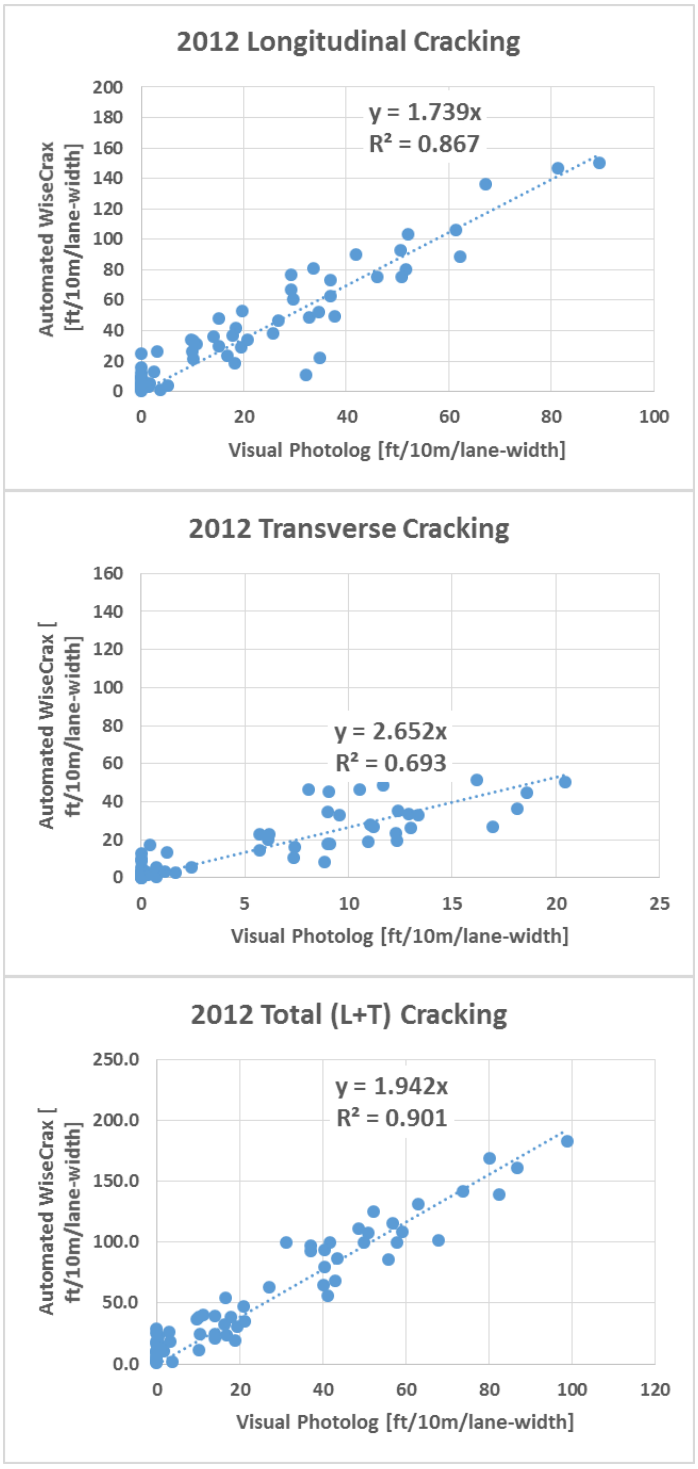

Figure 6.1 Bivariate plots of automated versus visual assessment of longitudinal (top), transverse (center), and total (bottom) linear cracking

Using Correlation Analysis to Estimate Alligator cracking from Linear Cracking

Useful information was obtained while comparing the extent of alligator cracking with linear cracking estimated by either visual or automated methods. Figure 6.2 shows the linear trend equations and fairly high degree of association of alligator cracking both with visually evaluated total cracking length (R-sq. =0.628) and with automatically evaluated total wheelpath cracking (R-sq. =0.592). Those trends indicate that total amounts of linear wheelpath cracking in feet can be used to estimate alligator cracking in percent area, which is an important distress indicator in the Pavement-ME analysis.

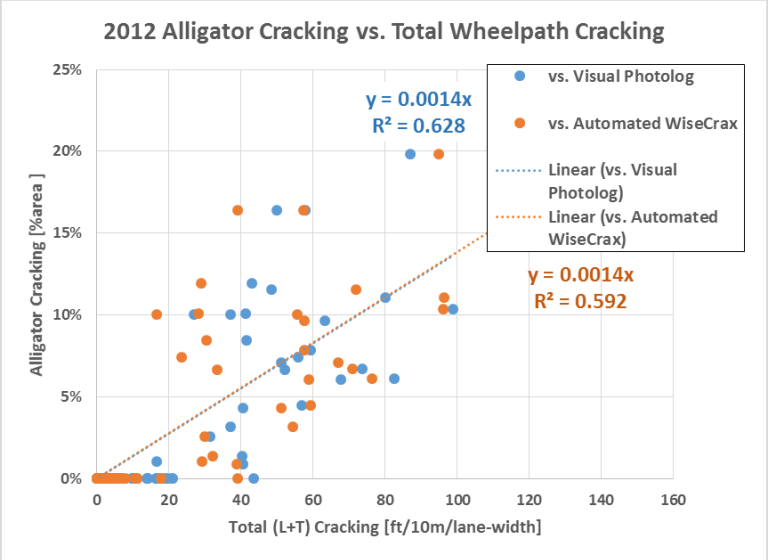

Figure 6.2 Bivariate plot of visually estimated alligator cracking vs. total linear (wheelpath) cracking

Effect of Van on Estimating Distresses

As stated before, the two ARAN vans used for collecting pavement data for the analyzed period (2008-2014) are equipped with different camera technologies. Van 7 employs Strobe photo cameras capturing sequential images of approximately 1.25-m long and half-lane wide pavement surface. Van 8 has been equipped with 2-D laser cameras continuously scanning the full lane-width pavement surface. Since the WiseCrax^{TM} employs the same algorithm for processing both vans' data, differences in amount of reported cracking between the two ARAN vans are expected. The CTDOT has been employing correction factors to harmonize the cracking data reported by the two different pavement data collection systems.

Figure 6.3 compares bivariate trends of automated versus visual cracking data between the two ARAN vans (Van7 and Van 8). As shown in the top chart, both vans tend to overestimate the extent of longitudinal cracking with a similar order of magnitude; Van 8 and Van 7 factors being around 1.8 and 1.5, respectively. It can also be noticed that the Van 7 trendline has a higher variance as compared with Van 8, hence, lower R-squared of 0.74. For transverse cracking, there is a greater difference between the ARAN vans in overestimating the cracking (Van 7 factor of

4.31 vs. Van 8 factor of 2.36) yet a similar degree of association, as shown in Figure 6.3 (center graph). This results, as shown in the bottom graph of Figure 6.3, in an overall higher overestimation of total (L+T) cracking by Van 7 (Strobe system) as compared with Van 8 (laser scan system).

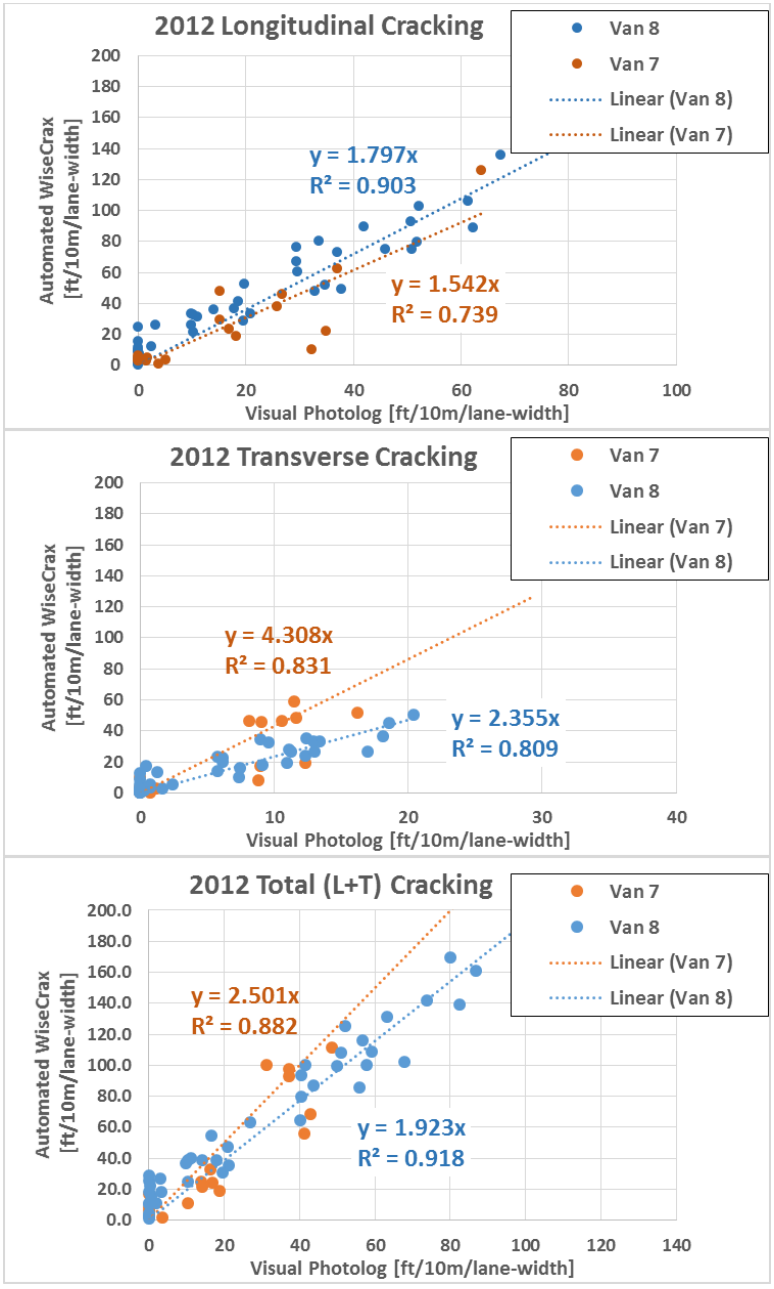

Figure 6.3 Bivariate plots of automated vs. visual evaluation of longitudinal (top), transverse (center), and total cracking (bottom) lengths for two ARAN vans

Effect of Surface Age on Estimating Distresses

The age of pavement surfaces analyzed under this task ranged between zero and 15 years. The age, which is normally correlated with accumulated traffic loads, is the major factor for the deterioration of pavement condition. Therefore, it was of some interest to compare annual cracking trends estimated by visual and automated methods. In particular, the degree of correlation between cracking extent and pavement surface age is looked at. The longitudinal, transverse, and total cracking trends for visual Photolog and Wisecrax datasets are shown in Figure 6.4. The slopes of linear trends are steeper for WiseCrax™-estimated R-squared values on all plots, which is the result of apparent overestimation of cracking extent by the WiseCrax™ system. The degree of correlation as measured by the R-squared parameter is always higher for visually estimated cracking, which suggests it being closer to the actual amount of cracking.

Summary

- For the analysis, pavement performance data generated by the WiseCrax™ software was complemented by the visual evaluation of distresses directly from the Photolog surface images.
- The 2012 PMIS data analysis indicated that WiseCrax™ software overestimated the extent of linear cracking in all directions, possibly, because of built-in settings of the processing algorithms. In particular, the factor of overestimation was slightly larger for Van 8 with respect to longitudinal cracking, whereas the Strobe system on Van 7 highly overestimated transverse cracking.
- While alligator cracking has never been reported by the WiseCrax™ system, it deems feasible and desirable to develop a transfer function to estimate alligator cracking in percent area from the total linear cracking length, as this is an input for the Pavement-ME software.
- The analysis of annual deterioration trends indicates visual assessment being closer to the actual extent of cracking than the automated method.

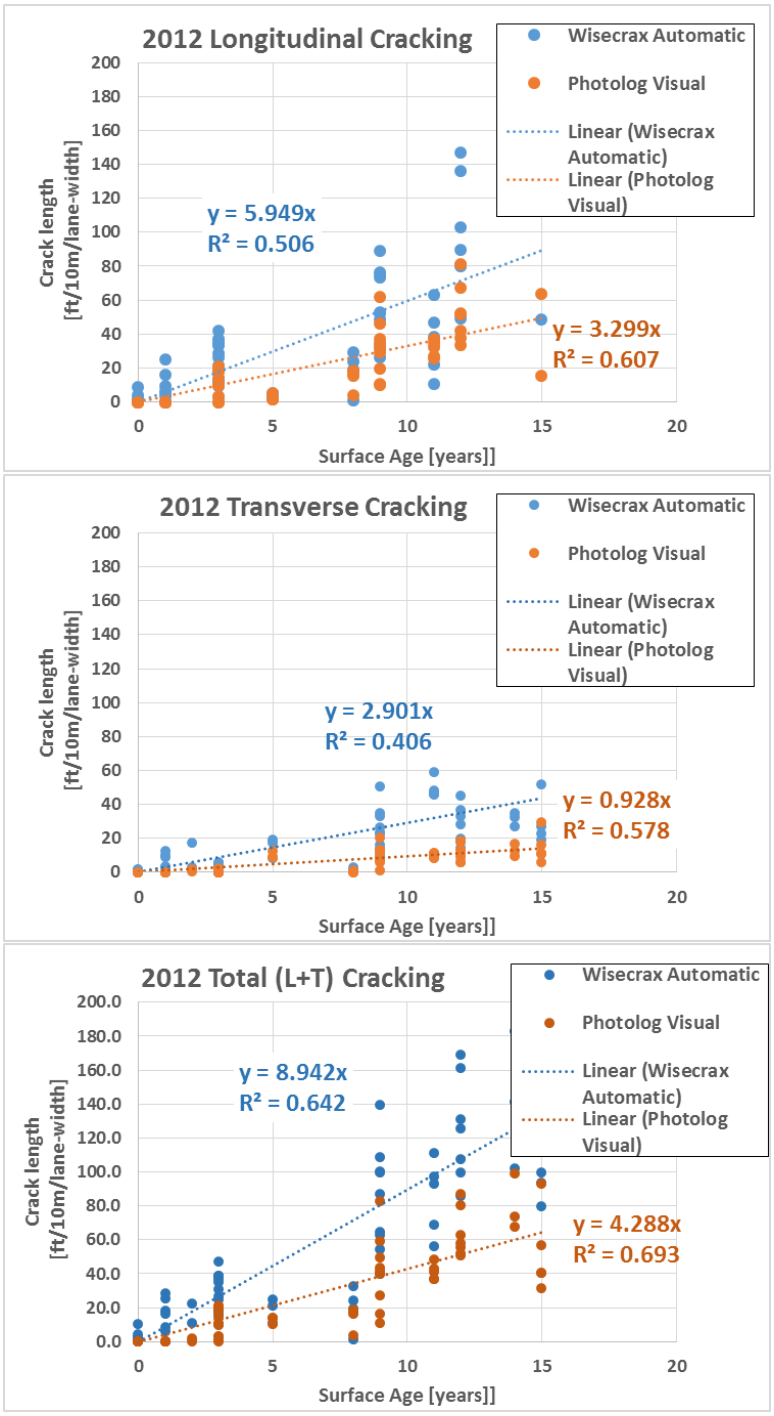

Figure 6.4 Comparison of annual deterioration trends for longitudinal (top), transverse (center), and total (bottom) cracking lengths measured by visual and automated methods

CHAPTER 7 Validation of Accuracy of the Pavement-ME Distress Predictions

Introduction

The main goal of project task 7 is to determine the accuracy of Pavement-ME prediction models with respect to surface distress indicators based on inputs obtained from the validation dataset of 48 pavement sections. The information on pavement structure, location, date of most recent maintenance, and traffic design level was provided by the CTDOT. Following the evaluation of data completeness under Task 3, 37 pavement sections were chosen for validation analysis. The inputs from those sections were used to create Pavement-ME design project files. Next, simulation Pavement-ME runs were performed to obtain deterioration trends for longitudinal, transverse, and alligator cracking as well as for AC-layer rutting, total rutting and roughness via IRI. Lastly, multiple correlation analysis was conducted to establish the degree of association between Pavement-ME-predicted and PMIS-reported distresses. In addition, multiple factor analysis was conducted to establish the effect of site factors, such as climate, pavement type, and traffic level on the accuracy of Pavement-ME predictions.

Description of Inputs for Validation Pavement-ME Design Projects

The design project files for validation purposes were generated through Pavement-ME templates, while changing default input values to those available through PMIS and other sources. Where no information was available, the default values were retained. Table 7.1 summarizes ranges of values for variable inputs, whereas the detailed input information for Pavement-ME simulations can be found in Tables D-1 through D-3 in Appendix D.

The pavement surface age obtained from the PMIS database served as input for the design life of the pavement sections included in the Pavement-ME simulations. Climatic inputs were generated based on the location of pavement sections, with use of the relevant weather stations previously determined during the sensitivity analysis. The traffic growth patterns and vehicle class distributions for validation were created based on the PMIS-reported three traffic design levels (expressed as AADTT in Table D-1 of 400, 1000 or 2500). The subgrade information for each pavement section was obtained from the NCHRP Web-only document 153, which includes a subgrade soil database to use with the M-EPDG. The range of subgrade resilient modulus (M_r) values for each AASHTO soil type was analyzed and the lower 95-percent reliability threshold for the mean M_r value was used as input for the M-EPDG simulation runs.

The pavement layer thicknesses were obtained from the PMIS data provided by the CTDOT. In some cases, granular base thickness was not reported, and, therefore, a 6-in thickness of base was assumed. The AC binder performance grade (PG) was inferred based on the date of construction reported by PMIS and the appropriate CTDOT specifications (Form 815 & 816) corresponding with the years of construction. Those specifications changed over the years, prescribing AC-20 grade before 1997, PG 64-28 between 1997 and 2008, and PG 64-22 after year 2009.

Table 7.1. Inputs for Validation Design Projects

Input Category	Input Name	Input Index	Range of Values	Source of Information
Site Factors	Location by weather station	CLIMATE	Bridgeport, CT (Shore) Willimantic, CT (Inland), Westfield/ Springfield, MA (Hills)	PMIS
	Traffic Design Level	AADTT	400 (Level2), 1000 (Level3), 2500 (Level4)	PMIS
	Subgrade AASHTO soil type by Resilient Modulus [psi]	MR_SG	21000(A-2-4), 17020 (A-2), 15740 (A-4), 10870 (A-2)	NCHRP Web-Only Document 153
	Pavement type	PTYPE	Composite, Flexible	PMIS
	Construction type	CONSTRUCTION	New, None, Rehab	PMIS
Layer Structure	Structure Type	ACACPCC ACPCC Thick AC (>4.5 in.) Thin AC (4.5 in.)	Overlaid AC on PCC New or AC-Overlaid PCC New or AC-Overlaid AC Milled and Overlaid AC	PMIS
	Top AC layer thickness [in]	HAC1	min=1.75, max=6.25, median=3.50	PMIS
	Bottom AC layer thickness [in]	HAC2	min=0.75, max=6.00, median=2.25	PMIS
	PCC slab thickness [in]	HPCC	min=8.25, max=10.50, median=9.25	PMIS
	Granular Base/Subbase thickness [in]	HBASE	min=6.0, max=16.5, median=6.5	PMIS
AC Material Properties	Top AC binder PG	ACBIND1	AC-20 (Built before 1997) PG 64-28 (Built 1997-2009) PG 64-22 (Built after 2009)	PMIS and CTDOT Form 815 & 816
	Bottom AC Binder PG	ACBIND2	AC-20 (Built before 1997) PG 64-22 (Built after 2009)	PMIS and CTDOT Form 815 & 816

Description of Dataset for Distress Validation Analysis

Datasets for a statistical analysis of correlation between predicted and measured values were created for 37 pavement sections included in the final validation dataset (Appendix D). Table D4 shows distress indicators as predicted by the Pavement-ME software, at the end of design life, at 90 percent reliability. Those indicators include IRI in in/mi, AC layer rutting and total rutting in

inches, total and alligator (bottom-up fatigue) cracking in percent area, longitudinal (top-down fatigue) and transverse (low-temperature) cracking in ft/mi, and PCC slab cracking in percent slabs cracked for the appropriate pavement structure types. Table D5 shows linear wheelpath and non-wheelpath cracking (longitudinal, transverse, and total) in ft/mi, IRI in in/mi, and rutting in inches as reported by WiseCrax™ in year 2014. Tables 7.2 and 7.3 summarize basic statistics formulated from data in Tables D4 and D5 (Appendix D) for Pavement-ME and WiseCrax™ datasets, respectively, in terms of minimum, maximum, median, and mean. For the reasons explained below, not all the distress indicators can be directly compared with each other.

For validation purposes, one should compare "apples" with "apples," which in this case is a cumbersome task as far as cracking is concerned. For instance, the Pavement-ME prediction models predict bottom-up fatigue cracking due to traffic load as alligator cracking in percent area, whereas top-down fatigue cracking is reported as longitudinal cracking in linear units (ft/mi). In addition, Pavement-ME reports total cracking in percent area for rehabilitated pavements where reflective cracking takes place. The PMIS cracking data generated from WiseCrax™ reports only linear cracking in the longitudinal and transverse directions, separately for inside and outside wheelpaths. The percent of cracked slabs (jpcpcrack) appears to be reported by Pavement-ME for overlaid PCC pavements for information only as it does not contribute to the total cracking value, or to the transverse cracking due to low-temperature stresses.

Tables 7.2 and 7.3 summarize basic statistical parameters for the distribution of distress values predicted by the Pavement-ME and reported by WiseCrax™, in that order. The difference between mean and median indicates the *skewness* of a distribution, whereas coefficient of variation (C.O.V.) measures its *spread*. Using those two criteria, one can notice that in terms of cracking the distribution of the longitudinal cracking predictions by Pavement-ME have parameters comparable to those reported by WiseCrax™, at least in terms of order of magnitude. Both predicted and measured cracking distributions have a C.O.V. greater than 100 percent and very large differences between the mean and median. The only other two comparable pairs of distributions appear to be IRI and AC layer rutting. Note that mean predicted and measured IRI values are very close, although measured IRI contains a larger variation. On the other hand, AC layer rutting values predicted by Pavement-ME appear to be spread around the same mean (0.16 in) as actual rutting from WiseCrax™, with very similar standard deviations of about 0.06 to 0.08 in.

Table 7.2. Summary of basic statistics for Pavement-ME predicted distress indicators

Distress Indicator	Unit Measure	Acronym	min	max	median	mean	Std	C.O.V.
Longitudinal (top-down fatigue) cracking	[ft/mi]	longcrack	257	7140	456	1881	2138	114%
Transverse (thermal) Cracking	[ft/mi]	transcrack	26	218	41	120	95	79%
PCC slab cracking	[%slabs)	jpcpcrack	20	24	20	21	2	7%
Alligator (bottom-up fatigue) cracking	[%area]	alligcrack	1.5	12.2	1.5	1.9	1.8	95%
Total cracking	[%area]	totcrack	1.5	33.2	7.3	12.4	9.4	76%
IRI	[in/mi]	IRI	102	162	116	122	18	15%
AC layer rutting	[in]	acrut	0.04	0.34	0.13	0.16	0.08	52%
Total rutting	[in]	totrut	0.04	0.94	0.35	0.37	0.29	80%

Table 7.3. Summary of basic statistics for WiseCrax™ validation dataset

Distress Indicator	Unit Measure	Acronym	min	max	median	mean	std	C.O.V.
Total Longitudinal cracking	[ft/mi]	L_TOT	112	30085	8969	10488	7994	76%
Total Transverse cracking	[ft/mi]	T_TOT	83	20918	5237	6107	5298	87%
Longitudinal wheelpath cracking	[ft/mi]	L_WP	9	17130	2924	4347	4389	101%
Longitudinal non-wheelpath cracking	[ft/mi]	L_NWP	103	13495	5794	6080	4167	69%
Transverse wheelpath cracking	[ft/mi]	T_WP	19	10392	2734	2979	2579	87%
Transverse non-wheelpath cracking	[ft/mi]	T_NWP	64	10526	2873	3303	2707	82%
Total cracking	[ft/mi]	TOTCRACK	579	45773	12878	16595	12091	73%
IRI	[in/mi]	IRI_AVG	50	270	122	129	49	38%
Rutting	[in]	RUT_AVG	0.06	0.31	0.15	0.16	0.06	39%

Kolmogorov-Smirnov test for normality of distributions and goodness of fit

One way to look at the accuracy of Pavement-ME predictions is to perform a formal test using a null hypothesis that the predicted and measured values belong to the same population. The Kolmogorov-Smirnov (KS) test, for example, evaluates normality of individual distributions by comparing its actual cumulative frequency distribution (CDF) with an assumed theoretical one. The test statistics, *D*, represent maximum vertical distance between two CDF curves, whereas the significance of *D* is evaluated by comparing its p-value with a specified level α. Similarly, the KS test can be used for evaluating the significance of difference between two distributions. Figure 7.1 illustrates the concept of the KS test, while showing actual (empirical) and theoretical

(normal) cumulative frequency functions and maximum distance (D_{max}) between them. The theoretical frequency values are computed based on the mean and standard deviation of the sample, which, in this case, comprises 37 total transverse cracking values. The D_{max} value is compared with critical D at level α=0.05. Since D_{max}=0.179 is greater than $D_{crit.}$=0.174, the null hypothesis of T_TOT distribution being normal is rejected.

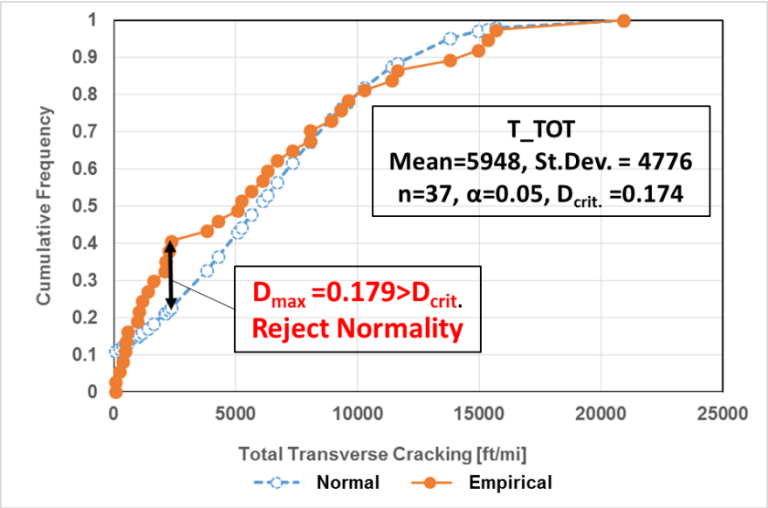

Figure 7.1 Concept of Kolmogorov-Smirnov test

Table 7.4 summarizes the analysis of normality of individual distributions for predicted and measured distress values as well as their pairwise KS parameters. With respect to WiseCrax-reported distresses, the D_{max} values and their corresponding p-values suggest that only T_TOT and L_WP deviate from normality, while the rest of the distresses follow normal distributions. As far as Pavement-ME predictions are concerned, none of the distress indicators appears to follow a normal distribution. Such a result is not surprising because (1) WiseCrax data is collected from different types of pavements that experience various traffic volumes and (2) Pavement-ME prediction models are heavily influenced by pavement type and/or thickness and traffic volume.

Table 7.4. Summary of KS test for normality of predicted and measured values with critical D=0.174 at level α=0.05

WiseCrax				Pavement-ME			
Reported Distress Indicator	Max D	p-value of KS test	Normality (accept/ reject)	Predicted Distress Indicator	Max D	p-value of KS test	Normality (accept/ reject)
L_TOT	0.119	0.19	accept	IRI	0.179	0.00	reject
T_TOT	0.179	0.04	reject	totrut	0.300	0.00	reject
L_WP	0.175	0.01	reject	totcrack	0.353	0.00	reject
L_NWP	0.085	0.62	accept	transcrack	0.251	0.00	reject
T_WP	0.164	0.08	accept	alligcrack	0.557	0.00	reject
T_NWP	0.153	0.11	accept	longcrack	0.292	0.00	reject
TOTCRACK	0.138	0.11	accept	acrut	0.210	0.00	reject
IRI_AVG	0.124	0.07	accept				
RUT_AVG	0.107	0.12	accept				

As a first step to evaluate accuracy of Pavement-ME predictions, a KS test was utilized to evaluate goodness of fit between predicted and reported distress values. A total of 63 pairs of distresses (9 types of reported x 7 types of predicted = 63) were tested for significance of D_{max} at the level α=0.05. Table 7.5 summarizes p-values for pairwise D_{max} values. The null hypothesis of a pair of samples belonging to the same continuous distribution is accepted if the p-value is greater than 0.05. Accordingly, only IRI and AC layer rutting predictions are found to be closely related to those reported by WiseCrax. However, if the level of confidence is lowered to 0.01, the longitudinal cracking predictions can be considered to be related to reported longitudinal wheelpath (L_WP) and transverse (T_WP and T_NWP) cracking.

Table 7.5. Summary of two-sample KS test for predicted and reported distress values

Predicted / Reported	longcrack	transcrack	alligcrack	totcrack	IRI	acrut	totrut
L_TOT[ft/mi]	0.000	0.000	0.000	0.000	0.000	0.000	0.000
T_TOT[ft/mi]	0.001	0.000	0.000	0.000	0.000	0.000	0.000
L_WP	0.031	0.000	0.000	0.000	0.000	0.000	0.000
L_NWP	0.000	0.000	0.000	0.000	0.000	0.000	0.000
T_WP	0.015	0.000	0.000	0.000	0.000	0.000	0.000
T_NWP	0.015	0.000	0.000	0.000	0.000	0.000	0.000
TOTCRACK	0.000	0.000	0.000	0.000	0.000	0.000	0.000
IRI_AVG[in/mi]	0.000	0.000	0.000	0.000	0.061	0.000	0.000
RUT_AVG [in]	0.000	0.000	0.000	0.000	0.000	0.111	0.000

Cross-Correlations between PMIS and Pavement-ME Distresses

Another way of looking at the accuracy of Pavement-ME predictions is to evaluate significance of Pearson's correlation coefficient r. Naturally, the expectation of real-life causation between two analyzed types of distress should be kept in mind. For example, it is unlikely that reported longitudinal wheelpath cracking would be correlated with transverse cracking, while some degree of correlation between IRI and rutting is expected due to the predictive model. Another critical aspect of the analysis is to establish level of significance of *r*-value, which depends on the sample size. Thus, low r-value for a large sample can be more significant than a very high r-value of a very small sample. The p-value of the t-statistics computed as in Equation 6.3 (Chapter 6) serve as a threshold of significance. In this analysis, the following levels of significance were assigned for the sample size of 37:

- Very high significance ($p<0.001$, $r>0.52$)
- High significance e ($0.001\leq p\leq 0.01$, $0.42\leq r\leq 0.52$)
- Moderate significance ($0.01<p\leq 0.05$, $0.32<r<0.42$)
- Low significance ($p>0.05$, $r\leq 0.32$)

Table 7.6 summarizes *r*-values for each of the 63 pairs of analyzed sample sets of predicted and reported distress indicators. Design life (life) and accumulated traffic load (million ESAL) are added to predicted values' pool to evaluate correlation of the reported distresses with the most important inputs into the Pavement-ME models. The following set of observations is worth noting:

- A very high correlation of all reported distresses with design life is countered by no correlation with predicted traffic load and any predicted distresses except rutting. In knowing that design life is directly correlated with cumulative traffic load, the most logical explanations for the lack of correlation with ESALs are (1) a strong prevalent effect of oxidative aging on the extent of cracking and (2) lack of data for actual vehicle class distribution into Pavement-ME.
- A lack of correlation between any of the predicted cracking types with transverse cracking is not entirely unexpected due to deficiencies in the transverse (thermal) cracking model within Pavement-ME. On the other hand, as it is discussed in Chapter 6, the extent of transverse cracking is very much overestimated in the WiseCrax reports.
- A moderate level of correlation between predicted and reported longitudinal cracking should not be ignored, especially with regard to wheelpath cracking (L_WP and T_WP with r=0.39) where most of the pavement fatigue is expected to occur. The lack of correlation between predicted longitudinal cracking and reported L_NWP cracking r=0.23) supports this notion.
- A highly significant correlation of predicted IRI with all cracking length reported by WiseCrax is not very surprising. The Pavement-ME algorithm models IRI as a function of rutting, age, fatigue and transverse cracking and climatic site factors with rutting and age being most significant contributors to the IRI model.
- Surprisingly, lower than expected albeit relatively significant correlation of about 0.50 is observed between predicted and measured IRI as well as between predicted and measured rutting.

Based on the above observations, with the exception of longitudinal cracking, it is concluded that the accuracy of cracking prediction is low to very low. A moderate level of accuracy can be surmised for IRI and rutting predictions. Obviously, these conclusions are only valid for the given dataset of 37 pavement sections for the information obtained from the PMIS. Ultimately, the longitudinal cracking, IRI, and AC layer rutting models appear to be the candidate models for calibration in the next phase of the Pavement-ME implementation process.

Table 7.6. Summary of multiple correlation analysis of Pavement-ME-predicted versus WiseCrax-reported distress indicators

Predicted / Reported	life	mln ESAL	tot crack	trans crack	allig crack	long crack	IRI	acrut	totrut
L_TOT	0.74	0.08	0.22	-0.24	-0.11	0.33	0.60	0.44	0.38
T_TOT	0.77	0.24	0.26	-0.14	-0.16	0.38	0.67	0.46	0.38
L_WP	0.58	0.16	0.22	-0.21	-0.12	0.39	0.58	0.45	0.38
L_NWP	0.53	0.15	0.18	-0.26	-0.08	0.23	0.48	0.42	0.35
T_WP	0.69	0.26	0.24	-0.14	-0.16	0.39	0.65	0.46	0.38
T_NWP	0.69	0.32	0.23	-0.09	-0.17	0.33	0.62	0.43	0.33
TOTCRACK	0.83	0.16	0.25	-0.22	-0.14	0.38	0.69	0.49	0.42
IRI_AVG	0.55	0.03	0.23	-0.44	0.08	0.37	0.50	0.42	0.44
RUT_AVG	0.70	0.55	0.43	-0.20	0.01	0.34	0.59	0.52	0.38

Cross-Correlation between Visual (Manual), Automated, and Pavement-ME Predicted Distresses

As reported in Chapter 6, a significant discrepancy was found between cracking length as reported by WiseCrax and visually estimated from the Photolog pavement surface images. Ultimately, it is important to understand the accuracy of automated pavement data collection systems and its effect on Pavement-ME validation and calibration efforts. Therefore, a smaller dataset of visually estimated (further, measured) distress values from 16 pavements (see Table C3 in appendix C) was added to the analysis. Total cracking length in the longitudinal and transverse directions served as distress indicators and correlations of both visually estimated from Photolog and Wisecrax-reported distress indicators with corresponding Pavement-ME predictions were computed and analyzed for significance. Visually estimated alligator cracking in percent area was added. Three levels of significance were assigned based on the p-value of t-statistics as follows:

- High significance ($p<0.01$, $r>0.623$)
- Moderate significance ($0.01\leq p\leq 0.05$, $0.498\leq r\leq 0.623$)
- Low significance ($p>0.05$, $r<0.498$)

Table 7.7 compares Photolog-estimated and WiseCrax-reported distresses in terms of their correlation with Pavement-ME predictions. Most of the correlation values for a given type of cracking (Longitudinal, transverse, and total) do not differ between Photolog and WiseCrax. One can notice, however, that Photolog-estimated distresses are somewhat better correlated with

surface age (life) and much better correlated with cumulative traffic load (mln ESAL) than WiseCrax reported data is, especially with regard to transverse cracking.

Table 7.7. Summary of multiple correlation analysis of Pavement-ME-predicted versus WiseCrax-reported and visually estimated distress indicators

Measured \ Predicted		life	mln ESAL	tot crack	trans crack	allig crack	long crack	IRI	acrut
Visually Estimated	L_PHOTOLOG2012	0.88	0.55	0.12	-0.11	-0.10	0.39	0.70	0.49
	T_PHOTOLOG2012	0.83	0.58	0.31	-0.06	-0.24	0.44	0.77	0.55
	L+T_PHOTOLOG2012	0.93	0.60	0.17	-0.10	-0.14	0.42	0.77	0.54
	ALLIG_PHOTOLOG2012	0.72	0.41	0.21	0.03	-0.23	0.37	0.61	0.42
Automatically Reported	L_WISECRAX2012	0.85	0.49	0.20	-0.18	-0.18	0.47	0.73	0.52
	T_WISECRAX2012	0.70	0.46	0.28	-0.14	-0.21	0.51	0.73	0.51
	L+T_WISECRAX2012	0.89	0.54	0.26	-0.18	-0.22	0.55	0.82	0.58

* The shaded values indicate low correlation

Effect of Site Factors on Validation Results

In order to better understand the underlying factors behind the relatively poor correlation found between PMIS distresses and Pavement-ME predictions, an analysis of influencing factors was conducted by introducing pavement type (PTYPE), construction type (CONSTRUCTION), geographic location (CLIMATE), and traffic design level (TRAFFIC) as factors into the regression model of predicted distress as a function of reported distress. Next, the individual contribution of each factor was evaluated via significance of their F-values. The importance of the factor was ranked based on log10 (F) as explained in Chapter 3.

Table 7.8 summarizes importance rankings of factors on the Pavement-ME validation results. It shows the pavement type (flexible vs. composite) and construction type (none vs. new vs. rehabilitated) to be major contributors to the predicted outcome where longitudinal cracking and rutting is concerned. On the other hand, construction type showed moderate to low effect on transverse cracking and IRI predictions. Lastly, neither traffic nor climate appear to be significant contributors to the variation in Pavement-ME predictions as far as the given dataset is concerned.

Table 7.8. Summary of the factor effect on Pavement-ME validation results

	Predicted by Pavement-ME at 90 % Reliability							
Factor	Longitudinal Cracking		Transverse Cracking		IRI		AC Rutting	
	logF	Assigned importance	logF	Assigned importance	logF	Assigned importance	logF	Assigned importance
PTYPE	1.76	High	4.39	Critical	1.12	High	1.71	High
CONSTRUCTION	1.43	High	0.03	Low	0.90	Moderate	1.18	High
TRAFFIC	0.31	Low	0.22	Low	-0.17	Very Low	-0.48	Very Low
CLIMATE	0.08	Low	0.19	Low	0.10	Low	0.08	Low

To illustrate the effect of pavement type on predicted distresses, Figure 7.2 shows plots of predicted versus reported distresses for longitudinal cracking, IRI, and AC layer rutting (top, center, and bottom, respectively.) Each plot displays two series, i.e. flexible and composite pavements. The trendline equations in Figure 7.2 indicate larger bias (intercept of the regression line) for cracking and IRI (but not for rutting) predictions for flexible pavements as compared with composite ones. They also indicate a higher degree of correlation with reported values for flexible cracking and rutting compared with composite pavements.

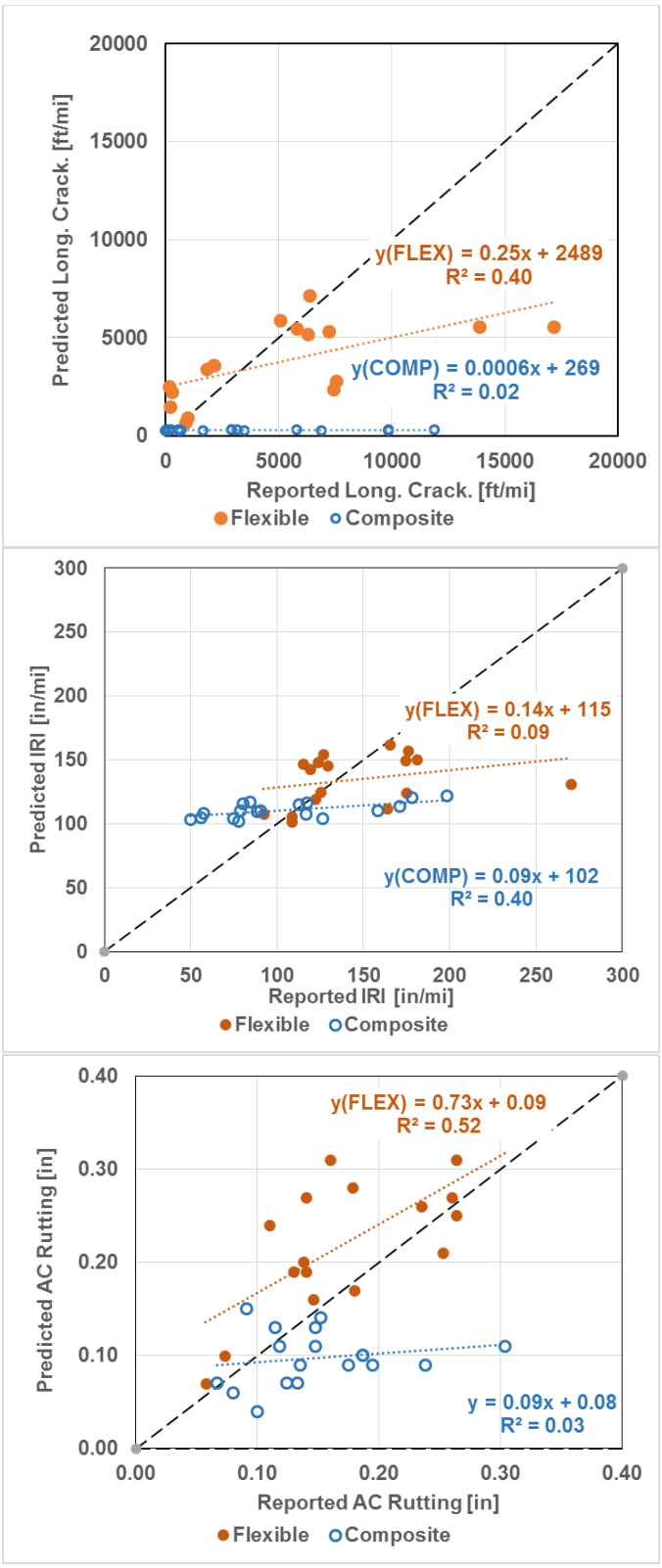

Figure 7.2 Effect of pavement type on Pavement-ME validation results for longitudinal cracking (top), IRI (center), and AC rutting (bottom)

Effect of Pavement-ME Hierarchy Level of Input on Validation Results

Similar to the first phase of this Project (SPR 2274), the validation runs of Pavement-ME models were performed at the lowest hierarchy level of input, at Level 3. At this level, default values of HMA material properties are used, which only indicate performance grade (PG) of AC binder. Obtaining properties at a higher level of hierarchy will require a significant testing effort in the next phase of the Pavement-ME implementation. However, a limited set of simulation runs was performed to gauge changes in distress predictions due to an increase in input detail. As an example, two types of pavement, Thick AC and AC on PCC are discussed below.

For each of the two sections (Route 7 milepost 12.7 to 13 [AC on PCC] and Route 10 milepost 26.9 to 27.4 [Thick AC]) utilized in this analysis, three Pavement-ME simulation runs were performed, while changing detail of input for the top HMA layer as shown in Table 7.9. Effectively, the first run used Level 3 default values for AC mix gradation, effective binder content, air voids and a known binder grade. The second run involved changing gradation, binder content, and air voids in order to predict dynamic modulus, E*, of the AC mix based on the value reported by the NETC06-3 study (Jackson et al., 2011). The final run utilized all the changes from the second run, plus the addition of AC master curve characteristics for the AC binder, as reported in the above-mentioned study.

Table 7.9. Summary of Top HMA Layer Material Inputs for Increasing Levels of Hierarchy

<table>
<tr><th>Parameter</th><th>Level 3 Default</th><th>Level 3 NETC06</th><th>Level 2 NETC06</th></tr>
<tr><td>AC Mix Gradation to predict E*</td><td>3/4" – 100%
3/8” – 77%
#4 – 60%
#200 – 6%</td><td>3/4" – 100%
3/8” – 78%
#4 – 58%
#200 – 4%</td><td>3/4" – 100%
3/8” – 78%
#4 – 58%
#200 – 4%</td></tr>
<tr><td>Effective AC Binder Content</td><td>11.6%</td><td>9.8%</td><td>9.8%</td></tr>
<tr><td>Air Voids</td><td>7%</td><td>7.4%</td><td>7.4%</td></tr>
<tr><td>AC Binder Type and Viscosity-Temperature Susceptibility</td><td>PG 64-28
A=10.312,
VTS = -3.44</td><td>PG 64-28
A=10.312,
VTS = -3.44</td><td>Master Curve Parameters
<table>
<tr><th>Temperature (ºF)</th><th>Binder Gstar (Pa)</th><th>Phase angle (deg)</th></tr>
<tr><td>72</td><td>870000</td><td>66.5</td></tr>
<tr><td>82</td><td>348000</td><td>69.3</td></tr>
<tr><td>93</td><td>92400</td><td>72.4</td></tr>
<tr><td>104</td><td>33500</td><td>75.1</td></tr>
<tr><td>115</td><td>14900</td><td>77.7</td></tr>
<tr><td>136</td><td>2760</td><td>82.9</td></tr>
<tr><td>147</td><td>1390</td><td>84.7</td></tr>
<tr><td>158</td><td>664</td><td>86.2</td></tr>
</table></td></tr>
</table>

Table 7.10 compares structure and site factors along with the distress predictions for increasing levels of hierarchy. It can be noticed that a change in gradation does not significantly change any

of outputs, except for longitudinal cracking. The change in this distress is especially large for AC on PCC pavements with almost a five-fold increase when the real master curve values are used for the AC binder at Level 2.

Table 7.10. Summary of the inputs and outputs for changing input levels of hierarchy

Section ID	Thick AC (Route 7 mile 12.7-13)			AC on PCC (Route 10 mile 26.9-27.4)		
Inputs						
Pavement Type	Thick AC			AC on PCC		
Construction Type	New			Rehabilitation		
Surface Age (Life)	11 years			11 years		
Layer 1	4-in HMA			5.75-in HMA		
Layer 2	2.4-in HMA			9.5-in PCC		
Layer 3	10.4-in Granular Base			6-in Granular Base		
Subgrade	A-4			A-4		
Climate	Inland			Hills		
Traffic Design Level	Level 3			Level 2		
Pavement-ME Outputs						
Distress Indicator at 90% reliability	Run 1 (Level 3 default)	Run 2 (Level 3 NETC06)	Run 3 (Level 2 NETC06)	Run 1 (Level 3 default)	Run 2 (Level 3 NETC06)	Run 3 (Level 2 NETC06)
Terminal IRI [in/mi]	131.3	131.9	133.8	113.4	114.7	116.1
Total Rutting [in]	0.63	0.64	0.68	0.10	0.13	0.17
Total Cracking [ft/mi]	3.5	3.7	4.9	7.6	7.5	7.5
AC Thermal Cracking [ft/mi]	27	27	27	217	217	217
Alligator cracking [%area]	3.5	3.7	4.9	1.5	1.5	1.5
Longitudinal Cracking [ft/mi]	2774	3516	3773	289	786	1340
AC rutting [in]	0.25	0.26	0.29	0.01	0.13	0.17

Figure 7.3 compares longitudinal cracking outputs at Levels 3 and 2 with values for longitudinal wheelpath cracking reported by WiseCrax. It is obvious that Level 2 of input hierarchy produces predictions closer to the reported values. Although the difference between Level 2 predictions and WiseCrax reported is still very large, one should keep in mind that WiseCrax tends to overestimate the amount of cracking. Once the correction factor is found, an increasing level of detail for asphalt material properties is expected to produce better accuracy. It is highly recommended that this matter be investigated in the next phase of the Pavement-ME implementation process.

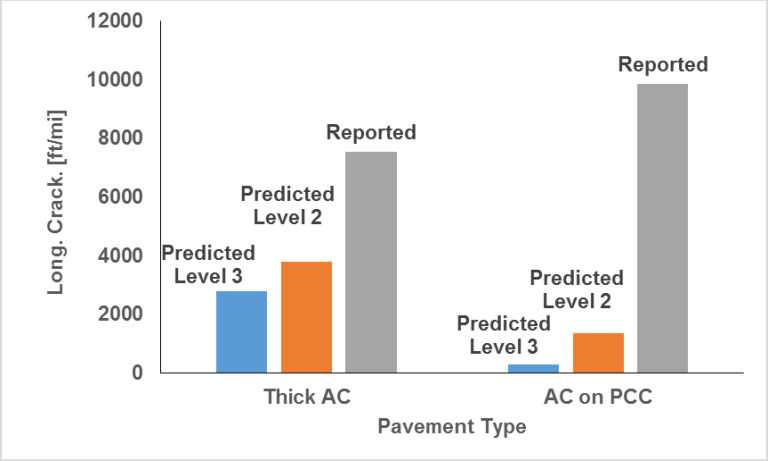

Figure 7.3 Comparison of Pavement-ME predictions with WiseCrax report for increasing input levels of hierarchy

Conclusions on Accuracy of Pavement-ME Distress Prediction

- Extensive analysis of distributions along with multiple correlation analysis of predicted and reported distress values indicated generally poor accuracy of Pavement-ME predictions in regards to cracking, except for longitudinal cracking, IRI and AC layer rutting.
- Analysis of the influencing factors on the accuracy of Pavement-ME predictions revealed pavement type to have the highest influence on bias in prediction of all distresses, followed by construction type.
- It has been confirmed that an increase in level of detail for asphalt material properties leads to an increase in accuracy of longitudinal cracking prediction.
- It is recommended to choose longitudinal cracking, IRI, and AC layer rutting models for calibration in the next phase of Pavement-ME implementation in Connecticut.
- Based on the comparison between PMIS-reported crack length and those visually evaluated from the Photolog images, it is recommended to establish correction factors to improve probability of success in calibration of the Pavement-ME prediction models for cracking.

CHAPTER 8 Summary, Conclusions and Recommendations

Summary of Research Approach

The second phase of the preparation for M-EPDG implementation in Connecticut involved expanded sensitivity analysis of the M-EPDG inputs and validation of M-EPDG distress predictive capability using State (CTDOT) PMIS data. The sensitivity analysis was conducted with both M-EPDG version 1.1 (previously available online) and the latest commercial version of Pavement-ME software (version 2.1). Altogether, 600 simulation runs of design software were performed, with inputs including weather station data, subgrade soil type, asphalt overlays, existing PCC (concrete) slab, granular base/subbase thickness, asphalt material properties, and pre-overlay pavement surface conditions. An importance ranking was assigned to each input based on its contribution to the variability in predicted distress outcome.

Since the original analysis of sensitivity was completed before the Pavement ME software arrived, it was necessary to re-run sensitivity analyses to evaluate the differences in the outputs between Pavement-ME 2.1 and M-EPDG 1.1. Accordingly, the set of runs has been completed for the new AC, AC-overlaid AC on PCC, and AC-overlaid PCC pavements in three Connecticut climatic zones. Consequently, the effect of design reliability and changes in software on the sensitivity results was evaluated by analyzing the output distributions and the changes in importance ranking of outputs.

The PMIS input data included information on 48 pavement sections representative of the Connecticut climates, traffic design levels, and pavement structures. The performance data for those sections included crack lengths and orientations, average IRI, and average rutting per 0.1-mile segment for a total of 177 segments. The relationship between PMIS inputs and the reported pavement performance was established using statistical analysis. Next, the sensitivity ranking of PMIS input categories was compared with that of Pavement-ME to confirm the suitability of the chosen PMIS dataset for use in the process of Pavement-ME validation. The PMIS performance data was also crosschecked for accuracy by visual estimation of crack lengths and their comparison with the PMIS-reported values.

The accuracy of Pavement-ME distress predictions was evaluated by the analysis of a correlation between predicted and reported distress values. This analysis included performing a two-sample Kolmogorov-Smirnov test for normality of distributions, followed by the analysis of the significance of Pearson's correlation between datasets of predicted and reported distress values.

Conclusions on Sensitivity Analysis of Pavement-ME Inputs

Overall, the new Pavement-ME software allows for faster runs of simulation projects, although having a more complicated structure of the reports. The Pavement-ME sensitivity runs mostly yielded similar rankings of design input importance compared with that of the M-EPDG runs, with the following observations worth noting:

- The Pavement-ME longitudinal cracking model for new AC pavements is much more sensitive to input changes as compared with the M-EPDG software.

- For thicker AC-overlaid AC on PCC pavements, the Pavement-ME analysis yielded on average much lower sensitivity of cracking predictions to all input as compared with M-EPDG software. In addition, for this pavement type, the Pavement-ME analysis yielded larger effects of subgrade and pre-overlay pavement surface condition on rutting and IRI as compared with M-EPDG software.
- For AC-overlaid PCC pavements, cracking sensitivity rankings were noticeably different between the Pavement-ME and M-EPDG prediction models. This included finding of zero sensitivity for the transverse (thermal) cracking model and an enormously high (up to 2300%) variation in longitudinal cracking predictions.

Evaluation of PMIS Input Data

The original dataset for validation included 48 pavement sections with the variables of pavement structure, traffic design level, and with performance in terms of linear cracking, rutting, and IRI, thus creating a total of 177 0.1-mile segments. However, only 37 pavement sections were found to have complete and reliable inputs in terms of pavement structure and performance. The data from only those 37 sections was used for the Pavement-ME validation. The actual traffic data was not available for this project, while, instead, the traffic volume predictions were simulated based on projected AADTT, which, in turn, were inferred from the traffic design levels provided by the CTDOT.

Accuracy of PMIS Performance Data

The analysis of pavement performance data generated by the WiseCrax™ software was complemented by the visual evaluation of distresses directly from the Photolog pavement surface images. The following are the most significant findings from the analysis:

- It appears that PMIS reports overestimate the extent of linear cracking in all directions, possibly, because of built-in settings of the processing algorithms. In particular, the factor of overestimation was slightly larger with respect to longitudinal cracking for data collected with laser cameras used on CTDOT van 8 whereas the strobe system (CTDOT van 7) significantly overestimated transverse cracking.
- The analysis of annual deterioration trends indicated that visual assessment of the images is likely to be closer than the automated method to "ground truth."
- Although alligator cracking has never been reported by the WiseCrax™ system, it is deemed feasible and advantageous to develop a transfer function to estimate the alligator cracking in percent area from the total linear cracking length. This is important because the alligator cracking is one of the major distress outputs in Pavement-ME analysis.

Validation of Accuracy of Pavement-ME Predictions

- Extensive analysis of distributions along with multiple correlation analysis of predicted and reported distress values generally indicated poor accuracy of Pavement-ME predictions regarding cracking, with the exceptions being longitudinal cracking, and also IRI and AC layer rutting.

- Analysis of the influencing factors on the accuracy of Pavement-ME predictions revealed pavement type having the highest influence on bias in prediction of all distresses, followed by construction type (new or rehabilitation).
- It has been confirmed that an increase in the level of detail for asphalt material properties can lead to an increase in accuracy for longitudinal cracking prediction.

Recommendations

The following studies and activities are proposed for the next phase (Phase III) of the implementation of M-EPDG in Connecticut:

1. Develop a database of vehicle class distributions based on the average daily traffic data for the set of pavements used in this project, and use this data in the calibration phase.
2. Determine master curves for typical AC binders historically used in Connecticut (PG 64-22, PG 64-28, and AC-20) and use this information in the calibration phase.
3. Calibrate AC layer rutting, Longitudinal Cracking, and IRI models on the set of pavements used in the validation analysis.
4. Use Level 2 data for traffic and asphalt material data in order to increase the accuracy of the Pavement-ME distress predictions.

REFERENCES

1. Connecticut Department of Transportation (CTDOT), 2004, Standard Specifications for Roads, Bridges and Incidental Construction, Form 816, CTDOT, Newington, CT
2. Mahoney J. et al., 2014, Comprehensive Forensic Evaluation of the Long Term Pavement Performance Specific Pavement Study SPS-9A Project in Connecticut, Draft Report.
3. Yut I. and Mahoney J., 2014, Preparation of the Implementation Plan of AASHTO Mechanistic-Empirical Pavement Design Guide (M-EPDG) in Connecticut, Report No. CT-2274-15, Connecticut Department of Transportation, Newington, CT.
4. National Cooperative Highway Research Program (NCHRP), 2004, Guide for Mechanistic-Empirical Design of New and Rehabilitated Pavement Structures, http://www.trb.org/mepdg/guide.htm, Transportation Research Board, Washington, DC.
5. American Association of State Highway and Transportation Officials (AASHTO), 2010, Guide for the Local Calibration of the Mechanistic-Empirical Pavement Design Guide, AASHTO, Washington, DC
6. Applied Research Associates, Inc., Survey Results & Analysis for AASHTOWare Pavement ME Design Customer Survey, 2013, http://www.me-design.com/MEDesign/data/AASHTOWare%20Pavement%20ME%20Design%20Customer%20Survey%20Results.pdf, Accessed on November 11, 2014.
7. Applied Research Associates, Inc., AASHTOWare Pavement ME Documentation, http://www.me-design.com/MEDesign/Documents.html, Accessed on November 11, 2014
8. Ceylan H., Kim S., Gopalakrishnan K., and Ma D., 2013, Iowa Calibration of MEPDG Performance Prediction Models, InTrans Project Report 11-40, Iowa department of Transportation, Ames, IA
9. Williams R. and Shaidur R., 2013, Mechanistic-Empirical Pavement Design Guide Calibration for Pavement Rehabilitation, Report No. FHWA-OR-RD-13-10, Oregon Department of Transportation, Salem, OR
10. Hall K., Xiao D., and Wang K., 2011, Calibration of the MEPDG for Flexible Pavement Design in Arkansas, Paper No. 11-3562, 90th Annual Transportation Research Board Meeting, Washington, DC
11. Federal Highway Administration (FHWA), 2011, Local Calibration of the MEPDG Using Pavement Management Systems, Report No. HIF-11-026, FHWA Office of Asset Management, Washington, DC
12. Kim Y., Jadoun F., and Hou T., 2011, Local Calibration of the MEPDG for Flexible Pavement Design, Report No. FHWA\NC\2007-07, North Carolina Department of Transportation, Raleigh, NC
13. Jannat G-E., Yuan X-X., and Shehata M., 2013, Local Calibration of MEPDG Distress Models for Flexible Pavements using Ontario's Long Term PMS Data, Presented at the 92nd Annual Meeting of Transportation Research Board, January 13-17, 2013, Washington, DC
14. Kasperick, Taylor; Ksaibati, Khaled. Calibration of the Mechanistic-Empirical Pavement Design Guide for Local Paved Roads in Wyoming. University of Wyoming, Laramie; Mountain-Plains Consortium; Research and Innovative Technology Administration, 2015
15. Tarefder R. and Rodriguez-Ruiz J., 2013, Local Calibration of MEPDG for Flexible Pavements in New Mexico, Journal of Transportation Engineering, 139(10), 981–991
16. Kaya, O.; Kim, S.; Ceylan, H.; Gopalakrishnan, K., Optimization of Local Calibration Coefficients of AASHTOWare Pavement ME Design Jointed Plain Concrete Pavement

Performance Models. Transportation Research Board 95th Annual Meeting, Transportation Research Board, 2016
17. Wu, Zhong; Xiao, Danny X. Development of DARWin-ME Design Guideline for Louisiana Pavement Design. Louisiana Transportation Research Center; Louisiana Department of Transportation and Development; Federal Highway Administration, 2016,
18. Mallela, J., Titus-Glover, L., Sadasivam, S., Bhattacharya, B., Darter, M., Von Quintus, H., 2013, Implementation of the AASHTO Mechanistic-Empirical Pavement Design Guide for Colorado, Report CDOT-2013-4, Colorado Department of Transportation, Denver, CO.
19. Mallela, J., Von Quintus, H., Darter, M., Bhattacharya, B., 2014, Road Map for Implementing The AASHTO Pavement ME Design Software for the Idaho Transportation Department, Report HWA/ID-14-211A, Idaho Transportation Department, Boise, ID.
20. Darter, M., Titus-Glover, L., Von Quintus, H., Bhattacharya, B., Mallela, J., 2014, Calibration and Implementation of the AASHTO Mechanistic-Empirical Pavement Design Guide in Arizona, Report FHWA-AZ-14-606, Arizona Department of Transportation, Phoenix, AZ.
21. Von Quintus, Harold L; Darter, Michael I; Bhattacharya, Biplab; Titus-Glover, Leslie. Implementation and Calibration of the MEPDG in Georgia. Applied Research Associates; Georgia Department of Transportation; Federal Highway Administration, 2016
22. Velasquez, R., Hoegh, K., Yut, I, Funk, N., Cochran, G., Marasteanu, M., Khazanovich, L., 2009, Implementation of the MEPDG for New and Rehabilitated Pavement Structures for Design of Concrete and Asphalt Pavements in Minnesota, Minnesota Department of Transportation, St. Paul, MN.
23. Guo, Xiaolong; Timm, David H. Local Calibration of MEPDG Using National Center for Asphalt Technology Test Track Data. Transportation Research Board 94th Annual Meeting, Transportation Research Board, 2015, 15p
24. Zapata C., 2010, A National Catalog of Subgrade Soil-Water Characteristic Curve (SWCC) Default Inputs and Selected Soil Properties for Use with the MEPDG, NCHRP 09-23A Final Report, Transportation Research Board, Washington, DC
25. Yut, I., Nener-Plante D., and Zofka A., 2010, Preservation of Flexible Pavement in Connecticut, Proceedings, First International Conference on Pavement Preservation, Newport Beach, California, April 12-16, 2010
26. Alavi S., LeCates J., and Tavares M., 2008, Falling Weight Deflectometer Usage: A Synthesis of Highway Practice, NCHRP Synthesis 381, Transportation Research Board, Washington, DC
27. Von Quintus, H.L., and A. L. Simpson. Back-Calculation of Layer Parameters for LTPP Test Sections, Volume II: Layered Elastic Analysis for Flexible and Rigid Pavements. Report FHWA-RD-01-113, Federal Highway Administration, McLean, VA, 2002.
28. Schmalzer, P.N. Long-Term Pavement Performance Program Manual for Falling Weight Deflectometer Measurements. Report FHWA-HRT-06-132, Federal Highway Administration, McLean, VA, 2006.
29. Pierce L., Smith K., Bruinsma J., and Sivaneswaran N., 2011, Case Studies Using Falling Weight Defelctometer Data with Mechanistic-Empirical Design and Analysis, Publication STP1555, American Society for Testing and Materials (ASTM), West Conshohocken, PA
30. Golapakrishnan K., Kim S., Ceylan H., and Kaya O., 2014, Development of Asphalt Dynamic Modulus Master Curve Using Falling Weight Deflectometer Measurements, IHRB Project TR-659 Report, Iowa Department of Transportation, Ames, IA

31. R.N. Stubstad, R.N., Y.J. Jiang, M.L. Clevenson, and E.O. Lukanen. Review of the Long-Term Pavement Performance Backcalculation Results—Final Report. Report FHWA-HRT-05-150, Federal Highway Administration, McLean, VA, 2006.
32. Chatti, K., N. Buch, S. W. Haider et al. LTPP Data Analysis: Influence of Design and Construction Features on the Response and Performance of New Flexible and Rigid Pavements. NCHRP Web-Only Document 74, Transportation Research Board for National Academies, Washington, D.C., 2005.
33. Drumm, E.C., and R. Meyer. LTPP Data Analysis: Daily and Seasonal Variations in Insitu Material Properties. NCHRP Web-Only Document 60, Transportation Research Board fof National Academies, Washington, D.C., 2003.

Appendix A. Expanded List of References with Abstracts

Alavi S., LeCates J., and Tavares M., 2008, Falling Weight Deflectometer Usage: A Synthesis of Highway Practice, NCHRP Synthesis 381, Transportation Research Board, Washington, D.C.

This synthesis reports on the state of the practice of falling weight Deflectometer (FWD) usage as it involves state departments of transportation (DOTs) using these devices to measure pavement deflections in response to a stationary dynamic load, similar to a passing wheel load. The data obtained are used to evaluate the structural capacity of pavements for research, design, rehabilitation, and pavement management practices. It is anticipated that this synthesis will provide useful information to support guidelines, advancing the state of the practice for state DOTs and other FWD users, as well as equipment manufacturers and other involved in pavement research, design, rehabilitation, and management. Based on a survey conducted for this report, 45 state highway agencies (SHAs) reported using 82 FWDs, produced by 3 different manufacturers. The importance of FWDs among SHAs appears to be reflected in the survey results, as it was noted that SHAs conduct FWD tests on up to 24 100 lane-km (15,000 lane-miles) annually. Survey information presented in this report is supplemented by an extensive literature search, as well as communication with FWD calibration centers and FWD manufacturers. Individual SHA websites were also searched. Although current practice was limited to the United States, research published internationally was considered for historical context and for potential future research topics. A series of case studies share lessons learned from utilizing FWDs.

American Association of State Highway and Transportation Officials (AASHTO), 2010, Guide for the Local Calibration of the Mechanistic-Empirical Pavement Design Guide, AASHTO, Washington, D.C.

This book provides guidance to calibrate the Mechanistic-Empirical Pavement Design Guide (MEPDG) software to local conditions, policies, and materials. It provides the highway community with a state-of-the-practice tool for the design of new and rehabilitated pavement structures, based on mechanistic-empirical (M-E) principles. The design procedure calculates pavement responses (stresses, strains, and deflections) and uses those responses to compute incremental damage over time. The procedure empirically relates the cumulative damage to observed pavement distresses.

Applied Research Associates, Inc., ERES Division, 2003, Guide for Mechanistic-Empirical Design of New and Rehabilitated Pavement Structures, Final Document, Appendix HH: Field Calibration of the Thermal Cracking Model, Transportation Research Board, Washington, D.C.

This Appendix covers the details of the field calibration of the thermal cracking model that was originally developed under the NCHRP 9-19 research project: Superpave Support and Performance Models Management. The main purpose of this study, developed by Witczak, Roque, Hiltunen, and Buttlar, was the modification and recalibration of the Superpave Thermal Cracking model (TCMODEL) developed under the SHRP A005 research contract. The details of the NCHRP 9-19 research results can be found in Annex A. The re-calibrated model was incorporated into the 2002 Design Guide software based on three different levels of analysis. A general overview of the parameters needed for each level of analysis is presented herein along with the calibration results obtained. Based on the calibration results of the TCMODEL incorporated into the 2002 Design Guide and given the poor performance of the model for the Level 3 analysis, the ASU research team decided to modify the correlations involved in the process at this level. The new correlations are also presented in the main body of this Appendix. In addition to a new approach for Level 3 analysis, the results from a study on different calibration factors to the Paris Law are shown in this Appendix. The details of the study can be found in Annex B. Lastly, a sensitivity analysis was carried out to evaluate the validity of the Level 3 Thermal Cracking model (TCModel) built into the 2002 Design Guide. Details of the analysis can be found in Annex C.

Applied Research Associates, Inc., AASHTOWare Pavement ME Documentation, http://www.me-design.com/MEDesign/Documents.html. Accessed on November 11, 2014.

This website provides the release notes of the updated versions of Pavement-ME software and the database resource documents.

Applied Research Associates, Inc., Survey Results & Analysis for AASHTOWare Pavement ME Design Customer Survey, 2013, http://www.me-design.com/MEDesign/data/AASHTOWare%20Pavement%20ME%20Design%20Customer%20Survey%20Results.pdf. Accessed on November 11, 2014.

This report contains a detailed statistical analysis of the results to the survey titled AASHTOWare Pavement ME Design Customer Survey. The results analysis includes answers from all respondents who took the survey in the 32-day period from Tuesday, July 16, 2013 to Friday, August 16, 2013. 53 completed responses were received to the survey during this time.

Baus R. and Stires N., 2010, Mechanistic-Empirical Pavement Design Guide Implementation, Report No. FHWA-SC-10-01, South Carolina Department of Transportation, Columbia, SC.

Currently, the South Carolina Department of Transportation (SCDOT) designs flexible and rigid pavement structures using AASHTO regression equation methodology (1972 and later with some modifications). Implementation of the MEPDG will require a substantial effort. This report summarizes an initial study undertaken to 1) gain an understanding of the new methodology, required inputs, and limitations, 2) conduct preliminary input sensitivity studies and review sensitivity studies performed by others, and 3) summarize implementation strategies undertaken or planned at other state highway agencies. Based on this investigation, general recommendations for SCDOT MEPDG implementation are proposed.

Cambridge Systematics, Inc., Washington State Transportation Center, Chaparral Systems Corporation, 2005, Traffic Data Collection, Analysis, and Forecasting for Mechanistic Pavement Design, NCHRP Report 538, Transportation Research Board, Washington, D.C.

This report includes guidelines for collecting traffic data to be used in pavement design and software for analyzing traffic data and producing traffic data inputs required for mechanistic pavement analysis and design. The software—designated TrafLoad—is available to users online (http://trb.org/news/blurb_detail.asp?id=4403). The report also describes the actions required at both the state and national level to promote successful implementation of the software. The report is a useful resource for state personnel and others involved in planning and designing highway pavements.

Cambridge Systematics, Inc., Washington State Transportation Center, Chaparral Systems Corporation, 2004, TrafLoad User's Manual, Cambridge Systematics, Inc., Chevy Chase, MD.

Abstract is not available.

Ceylan H., Kim S., Gopalakrishnan K., and Ma D., 2013, Iowa Calibration of MEPDG Performance Prediction Models, InTrans Project Report 11-40, Iowa department of Transportation, Ames, IA.

This study aims to improve the accuracy of AASHTO Mechanistic-Empirical Pavement Design Guide (MEPDG) pavement performance predictions for Iowa pavement systems through local calibration of MEPDG prediction models. A total of 130 representative pavement sites across Iowa were selected. The selected pavement sites represent flexible, rigid, and composite pavement systems throughout Iowa. The required MEPDG inputs and the historical performance data for the selected sites were extracted from a variety of sources. The accuracy of the nationally-calibrated MEPDG prediction models for Iowa conditions was evaluated. The local calibration factors of MEPDG performance prediction models were identified to improve the accuracy of model predictions. The identified local calibration coefficients are presented with other significant findings and recommendations for use in MEPDG/DARWinME for Iowa pavement systems.

Chatti, K., N. Buch, S. W. Haider et al., 2005, LTPP Data Analysis: Influence of Design and Construction Features on the Response and Performance of New Flexible and Rigid Pavements. NCHRP Web-Only Document 74, Transportation Research Board fof National Academies, Washington, D.C.

This report documents and presents the results of a study on the relative influence of design and construction features on the response and performance of new flexible and rigid pavements, included in SPS-1 and SPS-2 experiments. The SPS-1 experiment is designed to investigate the effects of HMA layer thickness, base type, base thickness, and drainage on flexible pavement performance, while the SPS-2 experiment is aimed at studying the effect of PCC slab thickness, base type, PCC flexural strength, drainage, and lane width on rigid pavement performance. The effects of environmental factors, in absence of heavy traffic, were also studied based on data from the SPS-8 experiment. Various statistical methods were employed for analyses of the LTPP NIMS data (Release 17 of DataPave) for the experiments. In summary, base type seems to be the most critical design factor in achieving various levels of pavement performance for both flexible and rigid pavements, especially when provided with in-pavement drainage. The other design factors are also important, though not at the same level as base type. Subgrade soil type and climate also have considerable effects on the influence of the design factors. Although, most of the findings from this study support the existing understanding of pavement performance, the methodology in this study provides a systematic outline of the interactions between design and site factors as well as new insights on various design options.

Connecticut Department of Transportation (CT DOT), 2004, Standard Specifications for Roads, Bridges and Incidental Construction, Form 816, CT DOT, Newington, CT.

This document describes State of Connecticut describes construction detail specifications for earthworks, surface courses (concrete and bituminous), and structures. Material selection specifications (Division III) include requirements for granular, bituminous, and portland cement concrete materials used in pavement construction.

Darter M., Titus-Glover L., and Von Quintus H., 2009, Implementation of the Mechanistic-Empirical Pavement Design Guide In Utah: Validation, Calibration, And Development of the UDOT MEPDG User's Guide, Report UT-09.11, Utah Department of Transportation, Salt Lake City, UT.

Highway agencies across the nation are moving towards implementation of the new AASHTO Mechanistic Empirical Pavement Design Guide (MEPDG) for pavement design. The objective of this project was to implement the MEPDG into the daily operations of the Utah Department of Transportation (UDOT). The implementation of the MEPDG as a UDOT standard required modifications in some UDOT pavement design protocols (i.e., lab testing procedures, equipment, and protocols, traffic data reporting, software issues, design output interpretation, and others). A key requirement is validation of the MEPDG's nationally calibrated pavement distress and smoothness prediction models when applied under Utah conditions and performing local calibration if needed. This was accomplished using data from Long Term Pavement Performance (LTPP) projects located in Utah and UDOT pavement management system (PMS) pavement sections. The nationally calibrated MEPDG models were evaluated. With the exception of the new hot-mix asphalt (HMA) pavement total rutting model, all other models were found to be reasonable. The rutting model was locally calibrated to increase goodness of fit and remove significant bias. Due to the nature of the data used in model validation, it is recommended that further MEPDG model validation be accomplished in the future using a database that contains HMA pavement and jointed plain concrete pavement (JPCP) exhibiting moderate to severe deterioration. This report represents Phase II of the UDOT MEPDG implementation study and builds on the Phase I study report completed in 2005 for UDOT. The Draft User's Guide for UDOT Mechanistic-Empirical Pavement Design (UDOT Research Report No. UT-09.11a, dated October 2009) incorporates the findings of this report as inputs and pavement design guidelines for Utah for use by UDOT's pavement design engineers during trial implementation of the MEPDG.

Darter M., Titus-Glover L., and Wolf D., 2013, Development of a Traffic Data Input System in Arizona for the MEPDG, Arizona Department of Transportation, Phoenix, AZ.

This research study addresses the collection, preparation, and use of traffic data required for pavement design by the Arizona Department of Transportation (ADOT), focusing on data required as inputs for the American Association of State Highway and Transportation Officials (AASHTO) Mechanistic-Empirical Pavement Design Guide (MEPDG) design procedures. ADOT's current traffic data collection and preparation processes are not adequate to meet the

needs of the MEPDG procedure, and improvements are needed. Use of the MEPDG in Arizona will require (1) an annual flow of updated key traffic data and (2) the ability to collect on-site (MEPDG Level 1) data in a timely manner for key projects. An action plan (Chapter 8) calls for the establishment of an Arizona Traffic Segment Database that includes all state highways (or the expansion of an existing traffic database). This database would include all traffic inputs required for the AASHTO MEPDG and AASHTO 1993 design procedures, as well as ADOT pavement management activities. Traffic segments would be identified by beginning and ending milepost numbers and global positioning system (GPS) coordinates along each highway. The researchers propose, and have partly developed, a system for traffic data collection for the MEPDG in Arizona. Level 1 data collection procedures are provided for selected traffic inputs. ADOT's traffic data collection group will need to develop a process for collecting Level 1 data in a timely manner for important projects requested from the pavement design group. This report also discusses recommended Level 2 and Level 3 inputs, which were prepared based on the best historical data available. These data represent a good initial set of inputs that can be used over the next few years. However, the inputs should be updated annually using improved data collection methods beginning as soon as possible.

Drumm, E.C., and R. Meyer, 2003, LTPP Data Analysis: Daily and Seasonal Variations in Insitu Material Properties. NCHRP Web-Only Document 60, Transportation Research Board fof National Academies, Washington, D.C.

A pavement's ability to withstand traffic loading depends on the stiffness of its component layers and the temperature and moisture conditions inside the pavement. These conditions change continuously due to daily and seasonal fluctuations in environmental factors such as air temperature, solar radiation, precipitation, and water table depth. The most pronounced environmental effects on a pavement's ability to withstand traffic loading occur in situations where ice accumulates beneath the pavement during the winter. As part of the Long Term Pavement Performance (LTPP) Seasonal Monitoring Program (SMP), pavement sites across North America were instrumented to periodically measure the temperature and moisture conditions inside the pavement and some of the environmental factors that affect those conditions. Coupled with periodic FWD tests to determine the stiffness of the pavement layers, this program has produced a data set that can be used to investigate daily and seasonal changes in pavement material properties and relate those changes to the changes in structural capacity that would necessitate load restrictions. From the flexible pavement sites in the LTPP SMP, site-specific models of asphalt modulus as a function of internal temperature, surface temperature, and air temperature were developed.

Federal Highway Administration (FHWA), 2011, Local Calibration of the MEPDG Using Pavement Management Systems, Report No. HIF-11-026, FHWA Office of Asset Management, Washington, D.C.

This project was initiated to assist state highway agencies with an important aspect of the MEPDG implementation by building on prior research activities and implementation efforts. In this regard, this project's objective was to develop a framework for using existing pavement management data to calibrate the MEPDG performance models. The feasibility of the framework was demonstrated using actual data from a SHAs pavement management system. One of the major challenges with calibration will be in correlating the pavement condition data collected as part of the LTPP program to that contained within each States pavement management system. There are a number of challenges in this process that include: LTPP sections are comprised of 500 ft (152.5 m) lengths and may not fully represent the project distress, the LTPP data definitions may not completely reflect the distress definitions of each SHA, and many highway agencies may have only limited pavement condition data; the latter is particularly critical because the calibration process requires numerous pavement sections with performance data that extends over the analysis period. The research team demonstrated how existing pavement data for flexible and rigid pavement sections from the NCDOT could be used to calibrate the pavement distress models contained within the MEPDG. For the HMA pavement sections, a MS Excel® solver was used to iterate the calibration coefficients to result in a minimum error, while an iterative process was used for the JCP pavement sections. In both cases, revisions to the calibration coefficients produced a better fit between predicted and measured distress; however, caution was also noted that additional pavement sections and performance data were needed prior to NCDOT consideration for adoption of the recommended calibration coefficients.

Golapakrishnan K., Kim S., Ceylan H., and Kaya O., 2014, Development of Asphalt Dynamic Modulus Master Curve Using Falling Weight Deflectometer Measurements, IHRB Project TR-659 Report, Iowa Department of Transportation, Ames, IA.

The objective of this feasibility study was to develop frameworks for predicting AC |E*| master curve from FWD deflection-time history data collected by the Iowa Department of Transportation (DOT). A neural networks (NN) methodology based on a synthetically generated viscoelastic forward solutions database was developed to predict AC relaxation modulus (E(t)) master curve coefficients from falling weight deflectometer (FWD) deflection time history data. Several case studies focusing on full-depth AC pavements were conducted to isolate potential backcalculation issues that are only related to the modulus master curve of the AC layer. For the proof-of-concept demonstration, a comprehensive full-depth hot-mix asphalt (HMA) analysis was carried out through 10,000 batch simulations using a viscoelastic (VE) forward analysis program. Anomalies were detected in the comprehensive raw synthetic database and were eliminated through imposition of certain constraints involving the sigmoid master-curve coefficients. The surrogate forward modeling results showed that NNs are able to predict deflection-time histories from E(t) master curve coefficients and other layer properties very well. The NN inverse modeling results demonstrated the potential of NNs to backcalculate the E(t) master curve coefficients from single-drop FWD deflection-time history data although the current prediction accuracies are not sufficient to recommend these models for practical implementation.

Guo, Xiaolong; Timm, David H. Local Calibration of MEPDG Using National Center for Asphalt Technology Test Track Data. Transportation Research Board 94th Annual Meeting, Transportation Research Board, 2015, 15p

As states consider implementing the new Mechanistic-Empirical Pavement Design Guide (MEPDG) adopted by the American Association of State Highway and Transportation Officials (AASHTO), there is a need to evaluate the nationally-calibrated transfer functions to assess their local applicability and conduct local calibration, if warranted. This investigation utilized a limited number of full-scale sections from the National Center for Asphalt Technology (NCAT) Pavement Test Track to conduct evaluation, local calibration and validation of rutting, fatigue cracking and ride quality transfer functions in the MEPDG, respectively. MEPDG input data were collected with the highest level of detail. Distress predictions by the nationally-calibrated models were compared against field measurements to evaluate the model prediction accuracy. Local calibration was then conducted to remove bias and improve model prediction accuracy. Finally, the local calibration was validated by an independent set of data to examine the prediction accuracy of the locally-calibrated models. The evaluation of the nationally-calibrated models showed the fatigue cracking predictions to be adequate while the rutting and International Roughness Index (IRI) models needed improvement. All three were locally calibrated based on the 2003 cycle data which resulted in no statistical differences between measured and predicted pavement distress. The validation of local calibration based on the 2006 cycle data showed the fatigue cracking and rutting predictions to be improved while the IRI predictions were negatively impacted by calibrating the rutting model. Only the locally-calibrated fatigue cracking model resulted in no statistical differences between measured and predicted values. It was recommended that nationally-calibrated models need to be evaluated and calibrated to local conditions before implementation.

Hall K., Xiao D., and Wang K., 2011, Calibration of the MEPDG for Flexible Pavement Design in Arkansas, Paper No. 11-3562, 90th Annual Transportation Research Board Meeting, Washington, D.C.

Arkansas has invested heavily in efforts to implement the MEPDG. The initial local calibration of flexible pavement models in the MEPDG for Arkansas is summarized. For the current MEPDG, predicted distresses did not accurately reflect measured distresses, particularly for longitudinal and transverse cracking. However, the pavement sections available for this study are generally in good condition. Due to the lack of measured transverse cracking, the transverse cracking model was not calibrated. The difference in defining transverse cracking between the MEPDG and LTPP may be critical in terms of data collection and identification. Thermal cracking should be specifically identified in a transverse cracking survey to calibrate the transverse cracking model in MEPDG. Calibration coefficients were optimized for the alligator cracking and longitudinal cracking models. In general, the alligator cracking and longitudinal cracking models are improved by calibration. However, a question remains regarding the suitability of the calibrated models for routine design. In addition, the smoothness model (IRI) was not calibrated, since the predicted IRI is a function of the other predicted distresses. A lack of data forced the use of many default values in the MEPDG. It is recommended that additional sites in Arkansas be established and a more robust data collection procedure be implemented for future calibration efforts. The procedure for local calibration of the MEPDG using LTPP and PMS data in Arkansas is established. Additional development of database software for data manipulation, pre-processing, and quality control – currently underway in Arkansas – will significantly streamline the calibration process.

Jackson E., Li J., Zofka A., Yut I., Mahoney J., 2011, Establishing Default Dynamic Modulus Values For New England, New England Transportation Consortium, Fall River, MA.

The primary objective of this research is to test commonly used Hot Mix Asphalt (HMA) mixtures throughout New England to determine their respective dynamic modulus master curves. Four mixes were requested from each of the New England states for modulus testing. Physical testing consisted of two replicates of each mix, outfitted with 3, linear variable differential transformers (LVDTs). AASHTO TP 62 was followed for the testing of these samples. Comparisons of plant produced mix vs. lab produced mix shows no significant difference between the two methods. Thus indicating lab produced samples are analogous to real-world pavements for dynamic modulus testing. Furthermore, the results of physical modulus testing were compared to predicted modulus values from three different theoretical modulus models. Comparisons of Predicted |E*| values from the Mechanistic-Empirical Pavement Design Guide (MEPDG) and physical testing indicates the predicted |E*| values may be off by as much as 100% for New England Mixes. Through this research, scaling factors were developed for all the mixes tested to allow state DOTs to forgo expensive and labor intensive physical testing. Furthermore, the minimal range and standard deviation of scaling factors for the Hirsh and Witczak models indicates there is potentially a constant scaling factor that could be applied to all New England mixes, regardless of aggregate source, and binder type. However, further testing may be required to determine if a uniform scaling factor for our region is truly valid.

Jannat G-E., Yuan X-X., and Shehata M., 2013, Local Calibration of MEPDG Distress Models for Flexible Pavements using Ontario's Long Term PMS Data, Presented at the 92nd Annual Meeting of Transportation Research Board, January 13-17, 2013, Washington, D.C.

Local calibration is an important step before a transportation agency adopts the AASHTO mechanistic-empirical pavement design guide (MEPDG). This paper presents the challenges and findings from the local calibration of flexible pavements in provincial highways under the jurisdiction of the Ministry of Transportation of Ontario (MTO). A calibration database was developed that involved a hierarchical framework of the input parameters required for DARWin-ME (the MEPDG software) and the historical field performance data based on the MTO's second-generation pavement management system (PMS-2). A calibration-clustering-validation approach was taken for the local calibration. The analysis suggested that whereas the MEPDG provided fairly unbiased prediction of the IRI value, it often over predicted the total rutting. A further clustering analysis based on functional class and geographical zone for the rutting and IRI, respectively, improved the precision of the locally calibrated models.

Kasperick, Taylor; Ksaibati, Khaled. Calibration of the Mechanistic-Empirical Pavement Design Guide for Local Paved Roads in Wyoming. University of Wyoming, Laramie; Mountain-Plains Consortium; Research and Innovative Technology Administration, 2015, 145p

Since release of the Mechanistic-Empirical Pavement Design Guide (MEPDG) in 2004, many national and state agencies have been working toward implementation of the new pavement design guide through calibration and validation. In order to aide Wyoming's Department of Transportation in its push toward total implementation, this study developed a set of traffic distributions and calibration coefficients for use within the MEPDG on designs of local paved roads that experience heavy truck traffic associated with the energy industry. A sensitivity analysis was also performed during this study to determine the effect of varying layer thicknesses on the prediction capabilities of the MEPDG. Findings of this report can be implemented on local paved roads that experience heavy truck traffic associated with the oil and gas industry.

Kaya, Orhan; Kim, Sunghwan; Ceylan, Halil; Gopalakrishnan, Kasthurirangan. Optimization of Local Calibration Coefficients of AASHTOWare Pavement ME Design Jointed Plain Concrete Pavement Performance Models. Transportation Research Board 95th Annual Meeting, Transportation Research Board, 2016, 12p

The Mechanistic Empirical Pavement Design Guide (MEPDG) was developed under the National Cooperative Highway Research Program (NCHRP) Project 1-37A as a novel pavement design methodology. The MEPDG evolved into DARWin-ME and, most recently, marketed as the AASHTOWare Pavement ME Design. Upon completion of national calibration of MEPDG and Pavement ME Design pavement performance prediction models, it was recommended that state highway agencies (SHAs) also conduct local calibration of the models to fully implement the software in their routine design practices. The accuracy of locally calibrated performance prediction

models is dependent upon efficient and scientifically sound calibration and validation processes. A number of previous studies have focused on the local calibration of MEPDG and Pavement ME design jointed plain concrete pavement (JPCP) performance models, but very few of them have presented their optimization procedure in detail on local calibration considerations. In this study, a detailed review of JPCP transverse cracking prediction model was conducted in consultation with the developers of Pavement ME design software to identify reliable optimization procedure for local calibration. Detailed steps involved in the optimization of local calibration coefficients of the model to match the actual Iowa JPCP transverse cracking measurements are presented. The accuracy of locally calibrated JPCP transverse cracking prediction model for Iowa JPCP systems are discussed along with the optimization approaches in light of future Pavement ME design software updates.

Kim Y., Jadoun F., and Hou T., 2011, Local Calibration of the MEPDG for Flexible Pavement Design, Report No. FHWA\NC\2007-07, North Carolina Department of Transportation, Raleigh, NC.

The work presented in this report focuses on four major topics: (1) the development of a GIS-based methodology to enable the extraction of local subgrade soils data from a national soils database; (2) the rutting and fatigue cracking performance characterization of twelve asphalt mixtures commonly used in North Carolina; (3) the characterization of local North Carolina traffic; and (4) calibration of the flexible pavement distress prediction models in the MEPDG to reflect local materials and conditions. The scope of this research is limited to rutting and fatigue cracking. The total number of sections available for this study is 46 sections: 22 long-term pavement performance (LTPP) sections (6 SPS and 16 GPS sites) and 24 non-LTPP sites. Because the LTPP sites have more complete distress and materials information available than the other sites, the research team used all the LTPP sites for calibration and used the 24 non-LTPP sites for validation. , the rut depth and fatigue cracking predictions are significantly different from the measured values. Two approaches were used to calibrate the rutting and fatigue cracking models for local conditions and materials. The first approach uses the generalized reduced gradient (GRG) method, whereas the second approach uses the genetic algorithm (GA) optimization technique. The GA-based approach is found to result in statistically better total rut depth and alligator cracking predictions than the GRG method. The calibration results demonstrate the importance of using material specific performance test results, having detailed and reliable distress data, and taking permanent deformation measurements from individual layers through forensic investigation. This study results in a set of local calibration factors for the permanent deformation and fatigue cracking performance prediction models in the MEPDG for the State of North Carolina and the North Carolina MEPDG User Reference Guide, along with a list of future research recommendations.

Kim, Sunghwan; Ceylan, Halil; Ma, Di; Gopalakrishnan, Kasthurirangan. Calibration of Pavement ME Design and Mechanistic-Empirical Pavement Design Guide Performance Prediction Models for Iowa Pavement Systems. Journal of Transportation Engineering, Volume 140, Issue 10, 2014, Content ID 04014052

The American Association of State Highway and Transportation Officials (AASHTO) mechanistic-empirical pavement design guide (MEPDG) pavement performance models and the associated AASHTOWare pavement ME design software are nationally calibrated using design inputs and distress data largely from the national long-term pavement performance (LTPP). Further calibration and validation studies are necessary for local highway agencies' implementation by taking into account local materials, traffic information, and environmental conditions. This study aims to improve the accuracy of MEPDG/pavement ME design pavement performance predictions for Iowa pavement systems through local calibration of MEPDG prediction models. A total of 70 sites from Iowa representing both jointed plain concrete pavements (JPCPs) and hot mix asphalt (HMA) pavements were selected. The accuracy of the nationally calibrated MEPDG prediction models for Iowa conditions was evaluated. The local calibration factors of MEPDG performance prediction models were identified using both linear and nonlinear optimization approaches. Local calibration of the MEPDG performance prediction models seems to have improved the accuracy of JPCP performance predictions and HMA rutting predictions. A comparison of MEPDG predictions was also performed between two software programs to assess if the local calibration coefficients determined from one software program is acceptable with the use of another software program, which has not been addressed before. Few differences are observed between one software program and MEPDG predictions with nationally and locally calibrated models for: (1) faulting and transverse cracking predictions for JPCP; and (2) rutting, alligator cracking, and smoothness predictions for HMA. With the use of locally calibrated JPCP smoothness (IRI) prediction model for Iowa conditions, the prediction differences between the two software programs are reduced. Finally, recommendations are presented on the use of identified local calibration coefficients with the two software programs for Iowa pavement systems.

Mahoney J. et al., 2014, Comprehensive Forensic Evaluation of the Long Term Pavement Performance Specific Pavement Study SPS-9A Project in Connecticut, Draft Report.

This project has two major objectives: (1) Obtain data required by the LTPP program for submittal to the LTPP database, and (2) Conduct comprehensive forensic study of six sections on the SPS-9A LTPP project on Route 9 in Connecticut. The LTPP testing protocol includes evaluation of pavement cores' thickness and volumetric properties. The asphalt binder recovered from the cores is tested to determine its terminal performance grade. The comprehensive forensic investigation targeted performance trends over the 12-year service period in terms of distresses, roughness, and oxidation in asphalt layers.

Mallela, J., Titus-Glover, L., Sadasivam, S., Bhattacharya, B., Darter, M., Von Quintus, H., 2013, Implementation of the AASHTO Mechanistic-Empirical Pavement Design Guide for Colorado, Report CDOT-2013-4, Colorado Department of Transportation, Denver, CO.

The objective of this project was to integrate the American Association of State Highway and Transportation Officials (AASHTO) Mechanistic-Empirical Pavement Design Guide, Interim Edition: A Manual of Practice and its accompanying software into the daily pavement design, evaluation, rehabilitation, management, and forensic analysis practices and operations of the Colorado Department of Transportation (CDOT). The Pavement ME Design software (formerly DARWin-ME) is a state-of-the-practice analysis tool for evaluating new, reconstructed, and rehabilitated flexible, rigid, and semi-rigid pavement structures based on mechanistic-empirical principles. Using project specific traffic, climate, and materials data, Pavement ME Design estimates and accumulates pavement damage and other forms of deterioration over a specified design/analysis period and then applied transfer functions to transform damage/deterioration into distress and smoothness. The pavement designer then determines the adequacy of a desired pavement section by evaluating predicted distress and smoothness at a given reliability level at the end of the design period. As a forensic analysis tool, Pavement ME Design can be used to model a pavement structure, simulate the combined effect of application of traffic load and climate cycles, and determine the performance (or lack of) for a specified time period.

The implementation of Pavement ME Design as a CDOT standard required modifications in some aspects of CDOT pavement design practices (materials testing, testing equipment, traffic data reporting, software/database integration, development of statewide defaults for key inputs, policy regarding design output interpretation, and others). Also, implementation required validation (and sometimes calibration) of the software's "global" pavement distress and smoothness prediction models for Colorado conditions. This was accomplished using data from Long Term pavement Performance (LTPP) projects located in Colorado and CDOT pavement management system sections. Default key data inputs were also developed, as was guidance for using the Pavement ME Design procedure for pavement design in Colorado.

Mallela J, Von Quintus H., Darter M., and Bhattacharya B, 2014a, Road Map for Implementing The AASHTO Pavement ME Design Software for the Idaho Transportation Department, Idaho Transportation Department, Boise, ID.

This report provides a Road Map for implementing the AASHTOWare Pavement ME Design software for the Idaho Transportation Department (ITD). The Road Map calls for a series of three stages: Stage 1 - Immediate, Stage 2 - Near Term, and Stage 3 - Future or Long Range. Within each stage are various specific steps to achieve the required objectives for implementation. The general implementation plan is to develop for ITD the Idaho AASHTOWare Pavement ME Design User's Guide, Version 1.1 under Stage 1 for use by designers and others for preliminary design and training purposes. Specific deficiencies in inputs and calibrations are identified in the draft guide for further improvement under the next stage. Stage 2 represents a major work effort over several years to fill the deficiencies for inputs, to conduct local Idaho calibration of distress and IRI models, and to provide training. Stage 3 represents future long-term work to improve various inputs and to maintain unbiased models.

Mallela J, Titus-Glover L., Bhattacharya B, Darter M., and Von Quintus H., 2014b, Idaho AASHTOWare Pavement ME Design User's Guide, Version 1.1, Idaho Transportation Department, Boise, ID.

Abstract is not available.

Mohammad L., Kim M., Raghavendra A., and Obulareddy S., 2014, Characterization of Louisiana Asphalt Mixtures Using Simple Performance Tests and MEPDG, Louisiana Transportation Research Center, Baton Rouge, LA.

The National Cooperative Highway Research Program (NCHRP) Project 9-19, Superpave Support and Performance Models Management, recommended three Simple Performance Tests (SPTs) to complement the Superpave volumetric mixture design method. These are the dynamic modulus, flow time, and flow number tests. In addition, the Mechanistic Empirical Pavement Design Guide (MEPDG) developed under NCHRP project 1-37A uses dynamic modulus to characterize Hot Mix Asphalt mixtures for pavement structural design. The objectives of this study were to (1) characterize common Louisiana asphalt mixtures using SPT protocols, (2) develop a catalog of dynamic modulus values for input into the MEPDG software, (3) evaluate the sensitivity of rut prediction of the MEPDG program, (4) assess the prediction of dynamic modulus values using Witczak and Hirsch models, and (5) compare dynamic modulus data obtained from axial and Indirect Tensile (IDT) modes of testing. Fourteen rehabilitation projects across Louisiana were selected to provide a total of 28 asphalt mixtures for this study. Laboratory mechanistic tests were performed to characterize the asphalt mixtures including the dynamic modulus in axial and IDT modes, flow time, flow number, and Hamburg type loaded wheel tracking tests. A catalog of dynamic modulus values was developed and grouped by design traffic level. Test results indicated that dynamic modulus was sensitive to the design traffic level, nominal maximum aggregate size, and the high temperature performance grade of the binder. Mixtures designed for higher traffic levels, with larger aggregate, and higher grade binder tended to have higher dynamic modulus values at high temperature. The MEPDG simulations carried out using the "nationally calibrated" default calibration factors overestimated the rut predictions by a significant amount. To address this problem, a local calibration of the MEPDG rut prediction model was performed and preliminary ranges of local calibration factors were developed. Both the Witczak and Hirsch models predicted dynamic modulus with reasonable accuracy. Dynamic modulus test results obtained from axial and IDT modes showed no statistical differences for the majority of the mixtures tested.

National Cooperative Highway Research Program (NCHRP), 2004, Guide for Mechanistic-Empirical Design of New and Rehabilitated Pavement Structures, http://www.trb.org/mepdg/guide.htm, Transportation Research Board, Washington, D.C.

This Guide provides a uniform and comprehensive set of procedures for the design of new and rehabilitated flexible and rigid pavements. The Guide employs common design parameters for traffic, subgrade, environment, and reliability for all pavement types. Recommendations are provided for the pavement structure (layer materials and thickness), including procedures to select pavement layer thickness, rehabilitation treatments, subsurface drainage, foundation improvement strategies, and other design features. The procedures can be used to develop alternative designs using a variety of materials and construction procedures.

Pierce L., Smith K., Bruinsma J., and Sivaneswaran N., 2011, Case Studies Using Falling Weight Deflectometer Data with Mechanistic-Empirical Design and Analysis, Publication STP1555, American Society for Testing and Materials (ASTM), West Conshohocken, PA.

This paper summarizes how deflection data are incorporated into the MEPDG and describes two case studies – one a flexible pavement and on a rigid pavement. Significant findings and recommendations from the evaluated flexible pavement case study include that surface-down cracking is critical in the design of the hot mix asphalt (HMA) overlay, correction factors recommended by Von Quintus and Killingsworth(1998) should be used for adjusting backcalculated layer moduli to laboratory determined values until additional guidance become available, and an FWD testing frequency of 30Hz should be used for estimating the existing HMA modulus. For rigid pavements, the case study found that the thinnest overlay produced from the MEPDG was a bonded PCC overlay while the HMA overlay was unreasonably thick. Within the design procedure, the manually entered k-value is used for unbounded and bonded jointed plain concrete pavements, but does not appear to be used by the program in the HMA overlay design. The backcalculated dynamic (or static) elastic modulus should be used for the PCC layer and the dynamic k-value should be used for the supporting layers. Backcalculated k-value representing the composite stiffness of all layers beneath the slab does not appear to have significant influence on the design thickness for the pavement structure analyzed.

Prozzi J. and Banerjee A., 2012, Quantification of the Effect of Maintenance Activities on Texas Road Network, Texas A&M Transportation Institute, College Station, TX.

Pavement structures are designed for a finite life, usually referred to as performance period. This performance period is typically between 20 to 25 years for flexible pavements and between 25 and 40 years for rigid pavements. After this period, the pavement is predicted to reach a terminal level in terms of several preset criteria. This performance period can be reached by designing a structure that will withstand the effects of traffic and the environment through the design period or by planning a series of maintenance and rehabilitation activities that will keep the structure above the present terminal levels until the end of the design life is reached. The objective of this study is to gather data on pavement performance from FHWA's Long-Term Pavement Performance (LTPP) study. The sections will be selected such that they provide enough time-series information to obtain reliable pavement performance trends. Once the data are collected, the various pavement sections will be modeled using mechanistic-empirical principles and their performance will be predicted. The Mechanistic Empirical Pavement Design Guide (MEPDG) will be used for this purpose. In addition, empirical performance models will be developed to capture the performance (and in particular the differential performance) of the various sections. Once these two types of performance models are available, we will compare the effectiveness of the three types of sections.

Rao C., Titus-Glover L., Bhattacharya B., and Darter M.I., 2012, User's Guide: Estimation of Key PCC, Base, Subbase, and Pavement Engineering Properties from Routine Tests and Physical Characteristics, Report FHWA-HRT-12-031, Federal Highway Administration, McLean, VA.

Material characterization is a critical component of modern day pavement analysis, design, construction, quality control/quality assurance, management, and rehabilitation. At each stage during the life of a project, the influence of several fundamental engineering material parameters on the long-term performance of the pavement can be predicted using advanced tools like the American Association of State Highway and Transportation Officials Mechanistic Empirical Pavement Design Guide (MEPDG). Consequently, there is a need for more information about material properties, which are addressed only to a limited extent with currently available resources for performing laboratory and field testing. Reliable correlations between material parameters and index properties offer a cost-effective alternative and are equivalent to the level 2 MEPDG inputs. The Long-Term Pavement Performance (LTPP) database provides data suitable for developing predictive models for Portland cement concrete (PCC) materials, stabilized materials, and unbound materials, as well as other design-related inputs for the MEPDG. This user's guide provides a summary of the models developed, describes their applications for specific project conditions, and lists their limitations. The following models are included: PCC materials: Compressive strength, flexural strength, elastic modulus, tensile strength, and coefficient of thermal expansion, Stabilized materials: Elastic modulus of lean concrete base. Unbound materials: Resilient modulus of fine-grained and coarse-grained materials, Rigid pavement design features: Pavement curl/wrap effective temperature difference for jointed plain concrete pavement and continuously reinforced concrete pavement designs.

Sachs, Steven; Vandenbossche, Julie M; Snyder, Mark B. Calibration of National Rigid Pavement Performance Models for the Pavement Mechanistic–Empirical Design Guide. Transportation Research Record: Journal of the Transportation Research Board, Issue 2524, 2015, pp 59–67

AASHTOWare Pavement ME Design, software developed from the AASHTO Mechanistic–Empirical Pavement Design Guide (MEPDG), uses performance data extracted primarily from the long-term pavement performance database to calibrate the performance prediction models for rigid pavements. In this study, factorial designs were generated as a subset of the national rigid pavement database for calibration of the MEPDG rigid pavement performance models. Three separate factorial designs were included for each rigid pavement performance model for (a) jointed plain concrete pavement (JPCP) transverse cracking, (b) JPCP faulting (doweled and undoweled), and (c) continuously reinforced concrete pavement punchouts. Experimental design variables for each model were selected to provide the broadest possible representation of key design, construction, and environmental features. The three performance models were then calibrated with the developed factorial matrices. The results were presented along with the calibration procedure. A validation of the calibrated models was then conducted with sites not included in the factorial matrices. An evaluation compared design slab thicknesses required to meet specified performance criteria determined with these and other previously established calibration coefficients. Finally, conclusions and recommendations based on the experiences gained conducting this study are provided.

Schmalzer, P.N. Long-Term Pavement Performance Program Manual for Falling Weight Deflectometer Measurements. Report FHWA-HRT-06-132, Federal Highway Administration, McLean, VA, 2006.

This document provides background information and field operations guidelines for the collection of Falling Weight Deflectometer (FWD) data on Long Term Pavement Performance (LTPP) test sections. It includes equipment setup, equipment calibration, test locations, and test procedures.

Selezneva O. and von Quintus H., 2014, Traffic Load Spectra for Implementing and Using the Mechanistic-Empirical Pavement Design Guide in Georgia, Report FHWA-GA-14-1009, Georgia Department of Transportation, Forest Park, GA.

The GDOT is preparing for implementation of the Mechanistic-Empirical Pavement Design Guide (MEPDG). As part of this preparation, a statewide traffic load spectra program is being developed for gathering truck axle loading data. This final report presents the results of a comprehensive research effort that culminated in recommendations for a statewide Traffic Load Spectra Program for collecting and processing truck axle loading data to support MEPDG implementation in Georgia. The recommendations include an optimal axle loading data collection plan that balances pavement design data needs, cost and number of WIM sites, and types of equipment used in obtaining the data. The report also shows how the available GDOT traffic data and other applicable data resources were used to develop traffic loading inputs and defaults to support local calibration of MEPDG models in Georgia. The available axle loading data were analyzed and the interim traffic loading defaults were developed for different groups of roads designed and maintained by GDOT, along with the recommendations for future updates of the defaults. In addition, user guidelines, decision trees, and software tools were developed to facilitate using the traffic loading defaults in MEPDG applications.

Selezneva O.I. and Hallenbeck M., 2013, Long-Term Pavement Performance Pavement Loading User Guide (LTPP PLUG), Report FHWA-HRT-13-089, Federal Highway Administration, McLean, VA.

This guide addresses the selection and use of axle loading defaults for Mechanistic-Empirical Pavement Design Guide (MEPDG) applications. The defaults were developed based on weigh-in-motion (WIM) data from the Long Term Pavement Performance (LTPP) Special Pavement Study (SPS) Transportation Pooled Fund Study (TPF). The guide consists of two parts. The first part provides guidelines for selecting and using LTPP SPS TPF axle loading defaults with the MEPDG and DARWin-ME software. These defaults provide a source of axle loading information for pavement analysis for locations where site-specific axle load spectra are not available. The second part of the guide provides practical guidelines that States and LTPP can use to generate additional MEPDG traffic loading defaults based on their own WIM data or for specific analysis purposes. In addition, this guide contains an operator's manual that supports the use of the LTPP PLUG software. This software helps users select site-specific or default axle loading conditions from its traffic loading library and produces axle load distribution input files for use with the MEPDG or DARWin-ME software. The software can be used to store, view, and group multiple normalized axle load spectra (NALS) and to develop MEPDG inputs and defaults using agency-provided data.

Stubstad, R.N., Y.J. Jiang, M.L. Clevenson, and E.O. Lukanen, 2006, Review of the Long-Term Pavement Performance Backcalculation Results—Final Report. Report FHWA-HRT-05-150, Federal Highway Administration, McLean, VA.

A new approach to determine layered elastic moduli from in situ load-deflection data was developed. This "forward calculation" approach differs from backcalculation in that modulus estimates come directly from the load and deflection data using closed-form formulae rather iteration. The forward calculation equations are used for the subgrade and the bound surface course for both flexible and rigid pavement falling weight deflectometer (FWD) data. Intermediate layer moduli are estimated through commonly used modular ratios between adjacent layers. The entire LTPP set of backcalculated parameters was screened using forwardcalculated moduli. Any assumed or fixed modulus value was left as is and not further screened (e.g., hard bottom). Further, any back- or forwardcalculated values outside a broad range of reasonable values were not further screened, but flagged as unreasonable. Finally, a set of broad range convergence flags (0 = acceptable, 1 = marginal, 2 = questionable, and 3 = unacceptable) were applied to the backcalculated dataset, depending on how closely the pairs of back- and forwardcalculated moduli matched. Since both techniques used identical FWD load-deflection data as input, the moduli derived from each approach should be reasonably close to each other (within a factor of 1.5 to qualify as acceptable, for example).

Although backcalculated values cannot be rejected merely because they are outside a reasonable or acceptable range, the complementary forwardcalculated values were usually more stable on a section-by-section basis. The exception was the portion of the database based on slab-on-dense-liquid or slab-on-elastic-solid theory, where the correspondence between the two approaches was excellent and very stable. Therefore, it is recommended that the backcalculated database be retained as is, with the addition of checks and flags so the database user can choose the best method, depending on the application.

Tarefder R. and Rodriguez-Ruiz J., 2013, Local Calibration of MEPDG for Flexible Pavements in New Mexico, Journal of Transportation Engineering, 139(10), 981–991.

Local calibration of the mechanistic-empirical pavement design guide (MEPDG) is performed by determining the pavement-performance model coefficients to minimize the difference between the measured and predicted distresses of New Mexico department of transportation (NMDOT) pavements. A total of 24 New Mexico pavement sections, which have all the MEPDG inputs and quantitative-distress values required for MEPDG calibration, were used for calibration. Pavement-performance models such as rutting, alligator cracking, longitudinal cracking, and roughness models were calibrated by an error-minimization algorithm. In the calibration methodology, the target was fixed to reduce the sum of squared errors, defined by the square of the difference between predicted and measured distress, so that any bias was eliminated and precision was increased. The optimized calibration coefficients are: $\beta r1=1.1$, $\beta r2=1.1$, $\beta r3=0.8$, $\beta GB=0.8$, and $\beta SG=1.2$ for the rutting model; C1=0.625, C2=0.25, and C3=6,000 for alligator cracking; C1=3, C2=0.3, and C3=1,000 for longitudinal cracking; and site factor = 0.015 for roughness. The results show that these calibration coefficients reduce error in the MEPDG prediction and assist better design of flexible pavements using MEPDG in New Mexico.

Velasquez, R., Hoegh, K., Yut, I, Funk, N., Cochran, G., Marasteanu, M., Khazanovich, L., 2009, Implementation of the MEPDG for New and Rehabilitated Pavement Structures for Design of Concrete and Asphalt Pavements in Minnesota, Minnesota Department of Transportation, St. Paul, MN.

The recently introduced Mechanistic-Empirical Pavement Design Guide (MEPDG) and related software provide capabilities for the analysis and performance prediction of different types of flexible and rigid pavements. An important aspect of this process is the evaluation of the performance prediction models and sensitivity of the predicted distresses to various input parameters for local conditions and, if necessary, re-calibration of the performance prediction models. To achieve these objectives, the Minnesota Department of Transportation (MnDOT) and the Local Road Research Board (LRRB) initiated a study "Implementation of the MEPDG for New and Rehabilitated Pavement Structures for Design of Concrete and Asphalt Pavements in Minnesota." This report presents the results of the evaluation of default inputs, identification of deficiencies in the software, sensitivity analysis, and comparison of results to the expected limits for typical Minnesota site conditions, a wide range of pavement design features (e.g. layer thickness, material properties, etc), and the effects of different parameters on predicted pavement distresses. Since the sensitivity analysis was conducted over a span of several years and the MEPDG software underwent significant modifications, especially for flexible pavements, various versions of the MEPDG software were run. Performance prediction models of the latest version of the MEPDG 1.003 were evaluated and modified or recalibrated to reduce bias and error in performance prediction for Minnesota conditions.

Von Quintus, H.L., and A. L. Simpson, 2002, Back-Calculation of Layer Parameters for LTPP Test Sections, Volume II: Layered Elastic Analysis for Flexible and Rigid Pavements. Report FHWA-RD-01-113, Federal Highway Administration, McLean, VA.

This report documents the procedure and steps used to back-calculate the layered elastic properties (Young's modulus and the coefficient and exponent of the nonlinear constitutive equation) from deflection basin measurements for all of the LTPP test sections with a level E data status. The back-calculation process was completed with MDOCOMP4 for both flexible and rigid pavement test sections in the LTPP program. The report summarizes the reasons why MODCOMP4 was selected for the computations and analyses of the deflection data, provides a summary of the results using the linear elastic module (Young's modulus) for selected test sections, and identifies those factors that can have a significant effect on the results. Results from this study do provide elastic layer properties that are consistent with previous experience and laboratory material studies related to the effect of temperature, stress-state, and season on material load-response behavior. In fact, over 75 percent of the deflection basins analyzed with the linear elastic module of MODCOMP4 resulted in solutions with an RMS error less than 2.5

percent. Those pavements exhibiting deflection-softening behavior with Type II deflections basins were the most difficult to analyze and were generally found to have RMS errors greater than 2 percent. In summary, the nonlinear

module of MODCOMP did not significantly improve on the number of reasonable solutions, and it is recommended that nonlinear constitutive equations not be used in a batch mode basis.

Von Quintus H. and Moulthrop J., 2007, Mechanistic-Empirical Pavement Design Guide Flexible Pavement Performance Prediction Models for Montana, Volume III: Field Guide, Report FHWA/MT-07-008/8158-3, Montana department of Transportation, Helena, MT.

The objective of this research study was to develop performance characteristics or variables (e.g., ride quality, rutting, fatigue cracking, transverse cracking) of flexible pavements in Montana, and to use these characteristics in the implementation of the distress prediction models or transfer functions included in the Mechanistic-Empirical Pavement Design Guide (MEPDG) software that was developed under NCHRP Project 1-37A. Reliable distress prediction models will enable the Montana Department of Transportation (MDT) to use Mechanistic-Empirical (ME) based principles for flexible pavement design and in managing their highway network. The work conducted within this study included using the MEPDG software to develop local calibration factors in the use of that software for Montana climate, structures, and materials for flexible pavements. The report is comprised of three volumes: Volume I – Executive Research Summary; Volume II – Reference Manual (which includes Selection of Distress Prediction Models, Traffic Characterization and Analyses, and Database for Calibration of ME Distress Prediction Models); and Volume III – Field Guide – Calibration and User's Guide for the Mechanistic-Empirical Pavement Design Guide.

Von Quintus, Harold L; Darter, Michael I; Bhattacharya, Biplab; Titus-Glover, Leslie. Implementation and Calibration of the MEPDG in Georgia. Applied Research Associates; Georgia Department of Transportation; Federal Highway Administration, 2016, 237p

Abstract: The Georgia Department of Transportation (GDOT) currently uses the empirical 1972 American Association of State Highway and Transportation Officials (AASHTO) Interim Guide for Design of Pavement Structures as their standard pavement design procedure. However, GDOT plans to transition to the Mechanistic Empirical Pavement Design Guide (MEPDG) for designing new and rehabilitated pavements. As a part of the transition process, GDOT has sponsored an implementation project. One objective of the implementation project was to calibrate the MEPDG global distress transfer functions to local conditions. The Georgia Long-Term Pavement Performance (LTPP) and non-LTPP roadway segments were used for the verification-calibration-validation process. One of the first activities of the implementation project was to verify or confirm that the MEPDG transfer functions and global calibration coefficients derived from National Cooperative Highway Research Program (NCHRP) project 1-40D reasonably predict distresses and smoothness in Georgia. The Task Order 1, Task 2 interim report focused on using the Georgia LTPP test sections to confirm the applicability of the global calibration coefficients. The interim report concluded some of the transfer functions exhibited significant bias between the measured and predicted distress and require local calibration. The Task Order 2, Task 5 Interim Report documented the local calibration of the transfer functions using LTPP and non-LTPP roadway segments. The calibration process followed the procedure presented in the 2010 AASHTO MEPDG Local Calibration Guide. GDOT calibration coefficients were derived to remove bias for the rutting, fatigue cracking, and thermal cracking transfer functions of flexible pavements, and the faulting and fatigue cracking transfer functions of rigid pavements. The global coefficients of the smoothness degradation regression equation for flexible and rigid pavements were also checked and calibrated as needed for their applicability to Georgia conditions. This report summarizes all calibration-validation activities completed within this implementation project.

Walubita L., Lee, S., Faruk A.N., Hoeffner J., scullion T., Abdallah I., and Nazarian S., 2013, Texas Flexible Pavements and Overlays: Calibration Plans for M-E Models and Related Software, FHWA/TX-13/0-6658-P4, Texas Department of Transportation, Austin, TX.

This five-year project was initiated to collect materials and pavement performance data on a minimum of 100 highway test sections around the State of Texas, incorporating flexible pavements and overlays. Besides being used to calibrate and validate mechanistic-empirical (M-E) design models, the data collected will also serve as an ongoing reference data source and/or diagnostic tool for TxDOT engineers and other transportation professionals. Towards

this goal, this interim report provides a documentation of the comprehensive work plans and strategies that were developed to calibrate and validate the M-E models and the associated software. As a minimum, the calibration and validation plans cover the following M-E models and associated software: The FPS, The TxACOL, The TxM-E., The M-E PDG. As discussed in this interim report, these strategic work plans were devised on the premise that data for calibrating and validating these M-E models/software will predominantly come from the Project 0-6658 MS Access Data Storage System (DSS). Accordingly, the DSS is also discussed in this interim report. Demonstration examples of the software (FPS, TxACOL, and M-E PDG) runs are also included in the report.

Williams R. and Shaidur R., 2013, Mechanistic-Empirical Pavement Design Guide Calibration for Pavement Rehabilitation, Report No. FHWA-OR-RD-13-10, Oregon Department of Transportation, Salem, OR.

This study conducted work to calibrate the design process for rehabilitation of existing pavement structures. Forty-four pavement sections throughout Oregon were included. A detailed comparison of predictive and measured distresses was made using MEPDG software Darwin M-E (Version 1.1). It was found that Darwin M-E predictive distresses did not accurately reflect measured distresses, calling for a local calibration of performance prediction models. Darwin M-E over predicted total rutting compared to the measured total rutting and most of the rutting predicted by Darwin M-E occurs in the subgrade. For alligator (bottom-up) and thermal cracking, Darwin M-E underestimated the amount of cracking considerably as compared to in-field measurements. A high amount of variability between predicted and measured values was observed for longitudinal (top-down) cracking. The performance (punch-out) model was also assessed for continuously reinforced concrete pavement (CRCP) using Darwin M-E's default (nationally calibrated) coefficients. Four distress prediction models (rutting, alligator, longitudinal, and thermal cracking) of the HMA overlays were calibrated for Oregon conditions. It was found that the locally calibrated models for rutting, alligator, and longitudinal cracking provided better predictions with lower bias and standard error than the nationally (default) calibrated models. However, there was a high degree of variability between the predicted and measured distresses, especially for longitudinal and transverse cracking, even after the calibration. It is believed that there is a significant lack-of-fit modeling error for the occurrence of longitudinal cracks. The Darwin M-E calibrated models of rutting and alligator cracking can be implemented, however, it is recommended that additional sites be established and included in the future calibration efforts to improve the accuracy of the prediction models.

Wu Z. and Yang X., 2012, Evaluation of Current Louisiana Flexible Pavement Structures Using PMS Data and New Mechanistic-Empirical Pavement Design Guide, Report FHWA/LA.11/482, Louisiana Department of Transportation, Baton Rouge, LA.

The objectives of this study were to use the MEPDG design software (version 1.1) to evaluate the performance of typical Louisiana flexible pavement types, materials, and structures as compared with the pavement performance data from the pavement management system (PMS) and identify the areas for further local calibration of the MEPDG in Louisiana. In this study, a total of 40 asphalt concrete (AC) pavement projects were strategically selected throughout Louisiana with different design traffic and subgrade properties. The selected projects included five typical Louisiana flexible pavement structure types: AC over AC base, AC over rubblized Portland cement concrete (RPCC) base, AC over crushed stone, AC over soil cement base, and AC over stone interlayer pavements. The original pavement structural design information as well as network-level PMS data for the selected projects were retrieved from multiple LADOTD data sources, including the Louisiana pavement management system (LA-PMS) and other project tracking databases. Based on the sensitivity analyses and available pavement design information, a set of Louisiana-condition-based design inputs (i.e., materials, climate, and traffic inputs) for the MEPDG flexible pavement design was developed, and the results were stored in a database named LAMEPDG along with the pavement performance data retrieved from the LA-PMS for all the projects evaluated in this study. The comparison results between the MEPDG-predicted and the LA-PMS-measured distresses indicated that the MEPDG rutting model tended to over-predict the total rutting for AC over RPCC base, AC over crushed stone, and AC over soil cement base pavements in Louisiana. However, it seemed to be adequate for those AC over AC base pavements selected. Meanwhile, the MEPDG load-related fatigue cracking models were found to be adequate for Louisiana's AC over AC base, AC over RPCC base, and AC over crushed stone pavements. However, for AC over soil cement base pavements in Louisiana, the MEPDG-predicted fatigue cracking was considerably less than the wheel-path cracking reported in the LA-PMS. Further statistical analyses generally indicated that the MEPDG prediction errors for both the rutting and the load-related fatigue cracking models could be significantly influenced by different design factors, such as pavement type, traffic volume, subgrade modulus, and project location. Finally,

based on the available data, a preliminary local calibration of the MEPDG rutting model was conducted for the selected AC over RPCC base and AC over soil cement base pavements, respectively. A set of local calibration factors was proposed for different pavement materials. On the other hand, further local calibration of the MEPDG fatigue cracking models was recommended before using the MEPDG for the AC over soil cement based pavement design in Louisiana.

Wu, Zhong; Xiao, Danny X. Development of DARWin-ME Design Guideline for Louisiana Pavement Design. Louisiana Transportation Research Center; Louisiana Department of Transportation and Development; Federal Highway Administration, 2016, 202p

The AASHTOWare Pavement ME™ Design is the next generation of the American Association of State Highway and Transportation Officials (AASHTO) pavement design software, which builds upon the newly developed National Cooperative Highway Research Program (NCHRP) Mechanistic-Empirical Pavement Design Guide (MEPDG). Pavement ME™ reflects a major change in the methods and procedures engineers use to design pavement structure and represents the most current advancements in pavement design. In preparation for Louisiana Department of Transportation and Development (DOTD) to adopt the new design guide, there is an urgent need to evaluate the MEPDG pavement design software based on typical Louisiana pavement structures and local conditions. This study selected a total of 162 projects (pavement sections) from the existing DOTD highway network for the evaluation of MEPDG pavement design, local calibration, and validation of Pavement ME in Louisiana. The selected projects consisted of flexible pavements with five types of base (asphalt concrete base, rubblized Portland Cement Concrete (PCC) base, crushed stone or recycled PCC base, soil cement base, and stabilized base with a stone interlayer), rigid pavements with three types of base (unbound granular base, stabilized base, and asphalt mixture blanket), and hot mix asphalt (HMA) overlay on top of existing flexible pavements. Pavement design information including structure, materials, and traffic were retrieved from multiple network-level data sources at DOTD. A Louisiana default input strategy of Pavement ME that reflects Louisiana's condition and practice was developed from results of sensitivity analysis. In addition, based on a consensus distress survey and pavement management system (PMS) distress triggers, the design reliability and performance criteria were established for different highway classes in Louisiana. The predicted performance from the Pavement ME was then compared with the corresponding measured performance retrieved from PMS. The analysis results indicate that the Pavement ME's nationally-calibrated distress models generally under-predict alligator cracking, but over-predict rutting for DOTD's flexible pavement types. For rigid pavements, Pavement ME over-predicts slab cracking but under-predicts joint faulting. For those nationally-calibrated distress models that showed constant bias and large variation, local calibration was carried out against the performance data retrieved from PMS. After the local calibration, the Pavement ME designs were verified by additional projects outside of the evaluation projects' pool. Based on the results of this study, an implementation guideline document was prepared. The document contains all necessary design input information and calibration coefficients for DOTD to use the latest MEPDG software on a day-to-day basis for design and analysis of new and rehabilitated pavement structures in Louisiana.

Yu H and Shen S., 2012, An Investigation Of Dynamic Modulus and Flow Number Properties of Asphalt Mixtures in Washington State, Report TNW2012-02, U.S. Department of Transportation, Washington, D.C.

Pavement design is now moving toward more mechanistic based design methodologies for the purpose of producing long lasting and higher performance pavements in a cost-effective manner. The recent Mechanistic-Empirical pavement design guide (MEPDG) is a product under such direction and is making progresses in improving current design methods. Dynamic Modulus is proposed by the MEPDG as an important material characterization property and key input parameter, which correlates material properties to field fatigue cracking and rutting performance. Washington State has strong background and they have put many efforts in moving toward the M-E based design procedures. In addition, Washington State has developed comprehensive PMS database, which makes it possible to use local pavement performance data to calibrate design models and optimize pavement design. However, there is still one important thing missing in this implementation step, which is a comprehensive local material database. Given the limited resources (equipment and time), such database will help the designer to select material properties that are more applicable to local materials and thus develop more reasonable level III design. Therefore, the objectives of this study are to conduct dynamic modulus (E*) tests on asphalt mixtures most popularly used in the State of Washington under different climate conditions, generate material database for the implementation of MEPDG design procedure in Washington State, and provide an evaluation method for recommending potential performing mixes by correlating E* test results to field rutting performance using WSPMS data. Both lab prepared

mixtures based on designs typically used in Western, Central, and Eastern Washington region, and field cored samples from representative field sites will be measured for dynamic modulus over a wide time-temperature domain. Results will be correlated to pavement performance, so that desirable material properties and E* values can be recommended for Washington material and climate conditions.

Yut I., Mahoney J., and Zinke S., 2014, Preparation of the Implementation Plan of AASHTO Mechanistic-Empirical Pavement Design Guide (M-EPDG) in Connecticut, Report No. CT-2274-F-13-15, Connecticut Department of Transportation, Newington, CT.

2002 Mechanistic-Empirical Pavement Design Guide is based on mechanistic-empirical (M-E) principles that provide a uniform platform for the design of flexible, rigid, and composite pavements. It considers design parameters for traffic, structure conditions, environment, and allows the user to specify a reliability Level of the predictions. The distress prediction models were originally calibrated to national averages using data from the Long-Term Pavement Performance (LTPP) effort. The distress models need to be recalibrated with data obtained locally in order to be applicable for the particular materials, construction practices, and environmental conditions encountered in Connecticut. Longitudinal (top-down fatigue), alligator (bottom-up fatigue), thermal cracking, asphalt rutting, and total rutting prediction models were analyzed for all pavement designs. Statistical sensitivity analyses were conducted for all of the input ranges identified as pertinent for Connecticut including mix properties, environmental factors, underlying structures etc... All of the inputs were then ranked according to their significance in order to establish target levels of detail as necessary for each input. Because this study only provides analyses based on a limited dataset, it is recommended that all of the M-EPDG models should be calibrated for use throughout the state. An implementation plan is presented along with course/training materials and recommendations for further analysis.

Yut I. and Zofka A., Effect of Asphalt Oxidation on Performance of LTPP SPS-9A Sections in Connecticut, Paper No. 13-2032, TRB 92nd Annual Meeting Compendium of Papers, Washington, D.C.

Six asphalt pavement test sections were constructed in 1997 on Route 2 in Connecticut to conduct the Special Pavement Study (SPS-9A) experiment under the Long Term Pavement Performance (LTPP) program. The SPS-9A experiment lasted 12 years and targeted comparison of long-term performance of SuperPave and Marshall mixes modified with recycled asphalt pavement (RAP). This paper analyses differences in pre-termination distresses and structural capacity in the LTPP SPS-9A sections as related to their asphalt oxidation level after 12 years of service. The distress data was retrieved from videologs collected by an Automated Road Analyzer, while structural capacity was evaluated by elastic moduli backcalculated from deflections measured by a Falling Weight Deflectometer. The oxidation levels were measured by a portable infrared spectrometer on the pre-stored original binders and those extracted from the cores. In addition, direct infrared measurements on asphalt mixtures from the top of the cores were conducted. On average, all RAP-modified mixes yielded lower elastic moduli than non-modified ones. In addition, RAP-modified SuperPave mixes has shown higher severity of surface cracking and a very high level of weathering. The difference in the effect of RAP on structural integrity and distress performance of Superpave and Marshal mixes was attributed to aging susceptibility of their binder constituents.

Yut, I., Nener-Plante D., and Zofka A., 2010, Preservation of Flexible Pavement in Connecticut, Proceedings, First International Conference on Pavement Preservation, Newport Beach, California, April 12-16, 2010.

Route 82 in Connecticut received a 2007 Perpetual Pavement Award from the Asphalt Pavement Alliance (APA). This paper presents a comprehensive look at this pavement, including the construction details from 1971, historical and current traffic volumes, up-to-date performance, and preservation activities applied since the original construction. Pavement performance is shown in terms of the annual trends for cracking collected by the Automatic Road Analyzer (ARAN). The historical trends in pavement deterioration are analyzed and compared with those of similar pavement sections in Connecticut (Route 9) to determine the major factor(s) that contributed the most to the long-lasting service of Route 82. Special emphasis is made on the pavement preservation techniques and their timing.

Zapata C., 2010, A National Catalog of Subgrade Soil-Water Characteristic Curve (SWCC) Default Inputs and Selected Soil Properties for Use with the MEPDG, NCHRP 09-23A Final Report, Transportation Research Board, Washington, D.C.

The results of this project effort will provide the user with an extremely easy implementable approach to extract unbound material property input data required for the new MEPDG. It contains a full set of Level 3 data and most Level 1 and 2 information, including soil water characteristic curve parameters and saturated hydraulic conductivity. In addition, the information collected allowed for predictions of typical resilient modulus and CBR values based on soil index properties. This information has been provided in the form of a National Database that is implemented via GIS Soil Unit Maps for the entire United States and Puerto Rico. The database developed will be a tremendous asset to the implementation of the Mechanistic-Empirical Pavement Design Guide (MEPDG). The Soil-Water characteristic Curve parameters, which are contained in this database, represent the largest database available in the world. This database may also allow further analysis to be conducted in order to better estimate default parameters for the level three analyses. Parameters such as the group index, the complete gradation, and the Atterberg's limits can be used to make further soil classification sub-divisions and hence obtain default parameters to be used in the implementation of the MEPDG. Furthermore, and most important, this database can be used to eventually revise and update the SWCC models currently available in the MEPDG.

Appendix B. Summary of Information for PMIS Validation Sections

Table B1. Section ID, Van, Age, and Pavement Structure

Road Name	Starting Milepost (mile)	CTDOT Van ID	Surface Age 2014	Pavement Type	Layer Thickness** [in]					
					HAC1	HAC2	HACTOT	HPCC	HBASE	TOTAL STRUCTURE
001L***	50.7	7	6	FLEX	2.25	0	2.25	0	7.5	9.75
001L	50.8	7	6	FLEX	2.25	0	2.25	0	7.5	9.75
001L	50.9	7	6	FLEX	2.25	0	2.25	0	7.5	9.75
001L	51	7	0	FLEX	2.25	0	2.25	0	7.5	9.75
001L	51.1	7	0	FLEX	2.25	0	2.25	0	7.5	9.75
005L	41	7	2	COMP	3.25	0	3.25	8.5	na*	na
005L	41.1	7	2	COMP	3.25	0	3.25	8.5	na	na
005L	41.2	7	2	COMP	3.25	0	3.25	8.5	na	na
005L	41.3	7	2	COMP	3.25	0	3.25	8.5	na	na
005L	41.4	7	2	COMP	3.25	0	3.25	8.5	na	na
007L	4.1	8	3	FLEX	2.25	2	4.25	0	6.5	10.75
007L	4.2	8	3	FLEX	2.25	2	4.25	0	6.5	10.75
007L	4.3	8	3	FLEX	2.25	2	4.25	0	6.5	10.75
007L	8	8	5	FLEX	4	4	8	0	12	20
007L	8.1	8	5	FLEX	4	4	8	0	12	20
007L	8.2	8	5	FLEX	4	4	8	0	12	20
007L	8.3	8	5	FLEX	4	4	8	0	12	20
007L	12.7	8	11	COMP	5.75	0	5.75	9.5	na	na
007L	12.8	8	11	COMP	5.75	0	5.75	9.5	na	na
007L	12.9	8	11	COMP	5.75	0	5.75	9.5	na	na
007L	32.2	8	5	FLEX	3.6	6	9.6	0	12	21.6
007L	32.3	8	5	FLEX	3.6	6	9.6	0	12	21.6
007L	32.4	8	5	FLEX	3.6	6	9.6	0	12	21.6
007L	32.5	8	5	FLEX	3.6	6	9.6	0	12	21.6
007L	32.6	8	5	FLEX	3.6	6	9.6	0	12	21.6
007L	32.7	8	5	FLEX	3.6	6	9.6	0	12	21.6
007L	32.8	8	5	FLEX	3.6	6	9.6	0	12	21.6
007L	32.9	8	5	FLEX	3.6	6	9.6	0	12	21.6
008L	38.7	8	3	COMP	3.25	0	3.25	9.5	6	18.75
008L	38.8	8	3	COMP	3.25	0	3.25	9.5	6	18.75
008L	38.9	8	3	COMP	3.25	0	3.25	9.5	6	18.75
009L	34.8	8	2	COMP	0	0	0	9.5	na	na
009L	34.9	8	2	COMP	0	0	0	9.5	na	na
009L	35	8	2	COMP	0	0	0	9.5	na	na
010L	26.8	8	11	FLEX	4	2.4	6.4	0	10.4	16.8
010L	26.9	8	11	COMP	4	2.4	6.4	0	10.4	16.8
010L	27	8	11	COMP	4	2.4	6.4	0	10.4	16.8
010L	27.1	8	11	COMP	4	2.4	6.4	0	10.4	16.8
010L	27.2	8	11	COMP	4	2.4	6.4	0	10.4	16.8
010L	27.3	8	11	COMP	4	2.4	6.4	0	10.4	16.8
012L	3.9	7	2	FLEX	2.75	2.75	5.5	0	6.5	12

Table B1. Section ID, Van, Age, and Pavement Structure (Cont.)

Road Name	Starting Milepost (mile)	CTDOT Van ID	Surface Age 2014	Pavement Type	Layer Thickness [in]					
					HAC1	HAC2	HACTOT	HPCC	HBASE	TOTAL STRUCTURE
012L	4	7	2	FLEX	2.75	2.75	5.5	0	6.5	12
012L	4.1	7	2	FLEX	2.75	2.75	5.5	0	6.5	12
012L	4.2	7	2	FLEX	2.75	2.75	5.5	0	6.5	12
014AL	5.2	7	10	FLEX	4	0	4	0	16	20
014AL	5.3	7	10	FLEX	4	0	4	0	16	20
014AL	5.4	7	10	FLEX	4	0	4	0	16	20
014AL	5.5	7	10	FLEX	4	0	4	0	16	20
015L	42.2	7	13	COMP	3.5	0	3.5	8.5	na	na
015L	42.3	7	13	COMP	3.5	0	3.5	8.5	na	na
015L	42.4	7	13	COMP	3.5	0	3.5	8.5	na	na
015L	42.5	7	13	COMP	3.5	0	3.5	8.5	na	na
015L	42.6	7	13	COMP	3.5	0	3.5	8.5	na	na
017L	0.8	7	7	COMP	2.25	2.75	5	8.5	na	na
017L	0.9	7	7	COMP	2.25	2.75	5	8.5	na	na
017L	1	7	7	COMP	2.25	2.75	5	8.5	na	na
020L	26.5	8	14	FLEX	4.25	0	4.25	0	13.5	17.75
020L	26.6	8	14	FLEX	4.25	0	4.25	0	13.5	17.75
022L	9.2	7	17	FLEX	2.25	0.75	3	0	7.5	10.5
022L	9.3	7	17	FLEX	2.25	0.75	3	0	7.5	10.5
032L	22.2	7	0	COMP	2.25	2.25	4.5	9.5	na	na
032L	22.3	7	0	COMP	2.25	2.25	4.5	9.5	na	na
032L	22.4	7	0	COMP	2.25	2.25	4.5	9.5	na	na
032L	22.5	7	0	COMP	2.25	2.25	4.5	9.5	na	na
034L	8.8	8	14	FLEX	2.25	0.75	3	0	6.5	9.5
034L	8.9	8	14	FLEX	2.25	0.75	3	0	6.5	9.5
034L	9	8	14	FLEX	2.25	0.75	3	0	6.5	9.5
034L	9.1	8	14	FLEX	2.25	0.75	3	0	6.5	9.5
034L	9.2	8	14	FLEX	2.25	0.75	3	0	6.5	9.5
034L	17	8	17	COMP	2.25	0	2.25	10.5	na	na
034L	17.1	8	17	COMP	2.25	0	2.25	10.5	na	na
034L	17.2	8	17	COMP	2.25	0	2.25	10.5	na	na
035L	2.5	8	4	COMP	4.25	0	4.25	8.25	na	na
035L	2.6	8	4	COMP	4.25	0	4.25	8.25	na	na
044L	7.9	7	16	COMP	6.25	0	6.25	10.5	na	na
044L	8	7	16	COMP	6.25	0	6.25	10.5	na	na
044L	8.1	7	16	COMP	6.25	0	6.25	10.5	na	na
049L	21	7	16	FLEX	3.75	0	3.75	0	6.5	10.25
049L	21.1	7	16	FLEX	3.75	0	3.75	0	6.5	10.25
066L	1.7	7	9	FLEX	3	6	9	0	10	19
066L	1.8	7	9	FLEX	3	6	9	0	10	19
066L	1.9	7	9	FLEX	3	6	9	0	10	19
066L	2	7	9	FLEX	3	6	9	0	10	19

Table B1. Section ID, Van, Age, and Pavement Structure (Cont.)

Road Name	Starting Milepost (mile)	CTDOT Van ID	Surface Age 2014	Pavement Type	Layer Thickness [in]					
					HAC1	HAC2	HACTOT	HPCC	HBASE	TOTAL STRUCTURE
066L	2.1	7	9	FLEX	3	6	9	0	10	19
075L	6.5	8	17	FLEX	3.25	0	3.25	0	6.5	9.75
075L	6.6	8	17	FLEX	3.25	0	3.25	0	6.5	9.75
075L	6.7	8	17	FLEX	3.25	0	3.25	0	6.5	9.75
080L	5.2	7	7	FLEX	3.6	6	9.6	0	10	19.6
080L	5.3	7	7	FLEX	3.6	6	9.6	0	10	19.6
080L	5.4	7	7	FLEX	3.6	6	9.6	0	10	19.6
084L	1.6	7	5	COMP	0	0	0	9.5	6	15.5
084L	1.7	7	5	COMP	0	0	0	9.5	6	15.5
084L	36.1	7	6	COMP	4	1	5	9.75	6	20.75
084L	36.2	7	6	COMP	4	1	5	9.75	6	20.75
084L	36.3	7	6	COMP	4	1	5	9.75	6	20.75
084L	36.4	7	6	COMP	4	1	5	9.75	6	20.75
084L	36.5	7	6	COMP	4	1	5	9.75	6	20.75
084L	36.6	7	6	COMP	4	1	5	9.75	6	20.75
084L	36.7	7	6	COMP	4	1	5	9.75	6	20.75
084L	94.3	7	6	COMP	4.75	0	4.75	10	6	20.75
084L	94.4	7	6	COMP	4.75	0	4.75	10	6	20.75
084L	94.5	7	6	COMP	4.75	0	4.75	10	6	20.75
084L	94.6	7	6	COMP	4.75	0	4.75	10	6	20.75
084L	94.7	7	6	COMP	4.75	0	4.75	10	6	20.75
084L	94.8	7	6	COMP	4.75	0	4.75	10	6	20.75
084R	6.2	7	13	COMP	4.25	0	4.25	9.5	6	19.75
084R	6.3	7	13	COMP	4.25	0	4.25	9.5	6	19.75
084R	6.4	7	13	COMP	4.25	0	4.25	9.5	6	19.75
084R	6.5	7	13	COMP	4.25	0	4.25	9.5	6	19.75
084R	6.6	7	13	COMP	4.25	0	4.25	9.5	6	19.75
084R	6.7	7	13	COMP	4.25	0	4.25	9.5	6	19.75
091L	3.6	7	2	COMP	3	0	3	9	6	18
091L	3.7	7	2	COMP	3	0	3	9	6	18
091L	3.8	7	2	COMP	3	0	3	9	6	18
091L	3.9	7	2	COMP	3	0	3	9	6	18
091L	4	7	2	COMP	3	0	3	9	6	18
091L	51.7	7	0	COMP	4	1	5	9	6	20
091L	51.8	7	0	COMP	4	1	5	9	6	20
091L	51.9	7	0	COMP	4	1	5	9	6	20
091L	52	7	0	COMP	4	1	5	9	6	20
091L	52.1	7	0	COMP	4	1	5	9	6	20
095L	12.4	7	9	COMP	5	1	6	9.5	na	na
095L	12.5	7	9	COMP	5	1	6	9.5	na	na
095L	12.6	7	9	COMP	5	1	6	9.5	na	na
095L	12.7	7	9	COMP	5	1	6	9.5	na	na

Table B1. Section ID, Van, Age, and Pavement Structure (Cont.)

Road Name	Starting Milepost (mile)	CTDOT Van ID	Surface Age 2014	Pavement Type	Layer Thickness [in]					
					HAC1	HAC2	HACTOT	HPCC	HBASE	TOTAL STRUCTURE
095L	12.8	7	9	COMP	5	1	6	9.5	na	na
095L	92.6	7	12	COMP	4	1	5	9.5	6	20.5
095L	92.7	7	12	COMP	4	1	5	9.5	6	20.5
095L	92.8	7	12	COMP	4	1	5	9.5	6	20.5
095L	92.9	7	12	COMP	4	1	5	9.5	6	20.5
095L	93	7	12	COMP	4	1	5	9.5	6	20.5
101L	8.6	7	3	FLEX	4.25	0	4.25	0	6.5	10.75
101L	8.7	7	3	FLEX	4.25	0	4.25	0	6.5	10.75
101L	8.8	7	3	FLEX	4.25	0	4.25	0	6.5	10.75
101L	8.9	7	3	FLEX	4.25	0	4.25	0	6.5	10.75
101L	9	7	3	FLEX	4.25	0	4.25	0	6.5	10.75
101L	9.1	7	3	FLEX	4.25	0	4.25	0	6.5	10.75
110L	2.5	8	9	COMP	1.75	2.25	4	8.5	na	na
110L	2.6	8	9	COMP	1.75	2.25	4	8.5	na	na
113L	4.9	8	17	FLEX	3	6	9	0	10	19
113L	5	8	17	FLEX	3	6	9	0	10	19
113L	5.1	8	17	FLEX	3	6	9	0	10	19
113L	5.2	8	17	FLEX	3	6	9	0	10	19
113L	5.3	8	17	FLEX	3	6	9	0	10	19
113L	5.4	8	17	FLEX	3	6	9	0	10	19
113L	5.5	8	17	FLEX	3	6	9	0	10	19
148L	8.8	7	13	FLEX	2.25	0.75	3	0	6.5	9.5
148L	8.9	7	13	FLEX	2.25	0.75	3	0	6.5	9.5
161L	2.9	7	23	FLEX	3.5	na	3.5	0	na	na
161L	3	7	23	FLEX	3.5	na	3.5	0	na	na
161L	3.1	7	23	FLEX	3.5	na	3.5	0	na	na
187L	6.4	8	17	FLEX	2	4	6	0	12	18
187L	6.5	8	17	FLEX	2	4	6	0	12	18
187L	6.6	8	17	FLEX	2	4	6	0	12	18
187L	6.7	8	17	FLEX	2	4	6	0	12	18
202L	25.5	8	13	COMP	4.5	0	4.5	8.25	na	na
202L	25.6	8	13	COMP	4.5	0	4.5	8.25	na	na
202L	25.7	8	13	COMP	4.5	0	4.5	8.25	na	na
202L	25.8	8	13	COMP	4.5	0	4.5	8.25	na	na
202L	25.9	8	13	COMP	4.5	0	4.5	8.25	na	na
254L	7.4	8	17	FLEX	3.25	0	3.25	0	8.25	11.5
254L	7.5	8	17	FLEX	3.25	0	3.25	0	8.25	11.5
254L	7.6	8	17	FLEX	3.25	0	3.25	0	8.25	11.5
272L	12	8	16	FLEX	4.25	0	4.25	0	7.5	11.75
272L	12.1	8	16	FLEX	4.25	0	4.25	0	7.5	11.75
341L	1.4	8	8	FLEX	4.25	0	4.25	0	7.5	11.75
341L	1.5	8	8	FLEX	4.25	0	4.25	0	7.5	11.75

Table B1. Section ID, Van, Age, and Pavement Structure (Cont.)

Road Name	Starting Milepost (mile)	CTDOT Van ID	Surface Age 2014	Pavement Type	Layer Thickness [in]					
					HAC1	HAC2	HACTOT	HPCC	HBASE	TOTAL STRUCTURE
341L	1.6	8	8	FLEX	4.25	0	4.25	0	7.5	11.75
341L	1.7	8	8	FLEX	4.25	0	4.25	0	7.5	11.75
341L	1.8	8	8	FLEX	4.25	0	4.25	0	7.5	11.75
341L	1.9	8	8	FLEX	4.25	0	4.25	0	7.5	11.75
501L	0.2	8	13	COMP	2	1	3	na	na	na
501L	0.3	8	13	COMP	2	1	3	na	na	na
501L	0.4	8	13	COMP	2	1	3	na	na	na
501L	0.5	8	13	COMP	2	1	3	na	na	na
805L	1.2	8	9	COMP	4	0	4	8.25	na	na
805L	1.3	8	9	COMP	4	0	4	8.25	na	na

*na = not available

**HAC1=thickness of AC layer 1 in inches
HAC2=thickness of AC layer 2 in inches
HACTOT=thickness of total AC layer in inches
HPCC=thickness of PCC layer in inches
HBASE-thickness of base layer in inches
TOTALStructure=thickness of total structure in inches

***L=log direction
R=reverse direction

Table B2. Section ID, Site Factors, Structure Type, and Construction Type

Road Section Name	Starting Milepost (mile)	Climate Zone	Traffic Level	Subgrade Type	Structure Type	Construction Type
001L	50.7	Shore	3	A-4	ThickAC	New
001L	50.8	Shore	3	A-4	ThickAC	New
001L	50.9	Shore	3	A-4	ThickAC	New
001L	51	Shore	3	A-4	ThickAC	New
001L	51.1	Shore	3	A-4	ThickAC	New
005L	41	Inland	2	A-1	ACPCC	Rehab
005L	41.1	Inland	2	A-1	ACPCC	Rehab
005L	41.2	Inland	2	A-1	ACPCC	Rehab
005L	41.3	Inland	2	A-1	ACPCC	Rehab
005L	41.4	Inland	2	A-1	ACPCC	Rehab
007L	4.1	Shore	3	A-4	ThickAC	Rehab
007L	4.2	Shore	3	A-4	ThickAC	Rehab
007L	4.3	Shore	3	A-4	ThickAC	Rehab
007L	8	Inland	2	A-4	ThickAC	New
007L	8.1	Inland	2	A-4	ThickAC	New
007L	8.2	Inland	2	A-4	ThickAC	New
007L	8.3	Inland	2	A-4	ThickAC	New
007L	12.7	Hills	2	A-4	ACPCC	Rehab
007L	12.8	Hills	2	A-4	ACPCC	Rehab
007L	12.9	Hills	2	A-4	ACPCC	Rehab
007L	32.2	Hills	3	A-2-4	ThickAC	New
007L	32.3	Hills	3	A-2-4	ThickAC	New
007L	32.4	Hills	3	A-2-4	ThickAC	New
007L	32.5	Hills	3	A-2-4	ThickAC	New
007L	32.6	Hills	3	A-2-4	ThickAC	New
007L	32.7	Hills	3	A-2-4	ThickAC	New
007L	32.8	Hills	3	A-2-4	ThickAC	New
007L	32.9	Hills	3	A-2-4	ThickAC	New
008L	38.7	Hills	3	A-4	ACACPCC	None
008L	38.8	Hills	3	A-4	ACACPCC	None
008L	38.9	Hills	3	A-4	ACACPCC	None
009L	34.8	Inland	3	A-4	ACACPCC	None
009L	34.9	Inland	3	A-4	ACACPCC	None
009L	35	Inland	3	A-4	ACACPCC	None
010L	26.8	Inland	3	A-4	ThickAC	New
010L	26.9	Inland	3	A-4	ThickAC	New
010L	27	Inland	3	A-4	ThickAC	New
010L	27.1	Inland	3	A-4	ThickAC	New
010L	27.2	Inland	3	A-4	ThickAC	New
010L	27.3	Inland	3	A-4	ThickAC	New
012L	3.9	Shore	2	A-4	ThickAC	New
012L	4	Shore	2	A-4	ThickAC	New
012L	4.1	Shore	2	A-4	ThickAC	New

Table B2. Section ID, Site Factors, Structure Type, and Construction Type (Cont.)

Road Section Name	Starting Milepost (mile)	Climate Zone	Traffic Level	Subgrade Type	Structure Type	Construction Type
012L	4.2	Shore	2	A-4	ThickAC	New
014AL	5.2	Inland	2	A-4	ThickAC	New
014AL	5.3	Inland	2	A-4	ThickAC	New
014AL	5.4	Inland	2	A-4	ThickAC	New
014AL	5.5	Inland	2	A-4	ThickAC	New
015L	42.2	Shore	3	A-2-4	ACACPCC	None
015L	42.3	Shore	3	A-2-4	ACACPCC	None
015L	42.4	Shore	3	A-2-4	ACACPCC	None
015L	42.5	Shore	3	A-2-4	ACACPCC	None
015L	42.6	Shore	3	A-2-4	ACACPCC	None
017L	0.8	Shore	2	A-4	ACPCC	Rehab
017L	0.9	Shore	2	A-4	ACPCC	Rehab
017L	1	Shore	2	A-4	ACPCC	Rehab
020L	26.5	Inland	3	A-2	ThinAC	Rehab
020L	26.6	Inland	3	A-2	ThinAC	Rehab
022L	9.2	Shore	2	A-4	ThinAC	Rehab
022L	9.3	Shore	2	A-4	ThinAC	Rehab
032L	22.2	Shore	2	A-4	ACPCC	Rehab
032L	22.3	Shore	2	A-4	ACPCC	Rehab
032L	22.4	Shore	2	A-4	ACPCC	Rehab
032L	22.5	Shore	2	A-4	ACPCC	Rehab
034L	8.8	Inland	2	A-4	ThickAC	Rehab
034L	8.9	Inland	2	A-4	ThickAC	Rehab
034L	9	Inland	2	A-4	ThickAC	Rehab
034L	9.1	Inland	2	A-4	ThickAC	Rehab
034L	9.2	Inland	2	A-4	ThickAC	Rehab
034L	17	Shore	3	A-2-4	ACPCC	New
034L	17.1	Shore	3	A-2-4	ACPCC	New
034L	17.2	Shore	3	A-2-4	ACPCC	New
035L	2.5	Hills	2	A-4	ACPCC	Rehab
035L	2.6	Hills	2	A-4	ACPCC	Rehab
044L	7.9	Hills	2	A-4	ACPCC	Rehab
044L	8	Hills	2	A-4	ACPCC	Rehab
044L	8.1	Hills	2	A-4	ACPCC	Rehab
049L	21	Inland	1	A-4	ThinAC	Rehab
049L	21.1	Inland	1	A-4	ThinAC	Rehab
066L	1.7	Inland	3	A-4	ThickAC	New
066L	1.8	Inland	3	A-4	ThickAC	New
066L	1.9	Inland	3	A-4	ThickAC	New
066L	2	Inland	3	A-4	ThickAC	New
066L	2.1	Inland	3	A-4	ThickAC	New
075L	6.5	Inland	2	A-2	ThinAC	Rehab
075L	6.6	Inland	2	A-2	ThinAC	Rehab

Table B2. Section ID, Site Factors, Structure Type, and Construction Type (Cont.)

Road Section Name	Starting Milepost (mile)	Climate Zone	Traffic Level	Subgrade Type	Structure Type	Construction Type
075L	6.7	Inland	2	A-2	ThinAC	Rehab
080L	5.2	Shore	3	A-4	ThickAC	New
080L	5.3	Shore	3	A-4	ThickAC	New
080L	5.4	Shore	3	A-4	ThickAC	New
084L	1.6	Hills	4	A-4	ACACPCC	None
084L	1.7	Hills	4	A-4	ACACPCC	None
084L	36.1	Inland	4	A-4	ACACPCC	None
084L	36.2	Inland	4	A-4	ACACPCC	None
084L	36.3	Inland	4	A-4	ACACPCC	None
084L	36.4	Inland	4	A-4	ACACPCC	None
084L	36.5	Inland	4	A-4	ACACPCC	None
084L	36.6	Inland	4	A-4	ACACPCC	None
084L	36.7	Inland	4	A-4	ACACPCC	None
084L	94.3	Hills	4	A-4	ACACPCC	None
084L	94.4	Hills	4	A-4	ACACPCC	None
084L	94.5	Hills	4	A-4	ACACPCC	None
084L	94.6	Hills	4	A-4	ACACPCC	None
084L	94.7	Hills	4	A-4	ACACPCC	None
084L	94.8	Hills	4	A-4	ACACPCC	None
084R	6.2	Hills	4	A-4	ACACPCC	None
084R	6.3	Hills	4	A-4	ACACPCC	None
084R	6.4	Hills	4	A-4	ACACPCC	None
084R	6.5	Hills	4	A-4	ACACPCC	None
084R	6.6	Hills	4	A-4	ACACPCC	None
084R	6.7	Hills	4	A-4	ACACPCC	None
091L	3.6	Shore	4	A-4	ACACPCC	None
091L	3.7	Shore	4	A-4	ACACPCC	None
091L	3.8	Shore	4	A-4	ACACPCC	None
091L	3.9	Shore	4	A-4	ACACPCC	None
091L	4	Shore	4	A-4	ACACPCC	None
091L	51.7	Inland	4	A-1	ACACPCC	None
091L	51.8	Inland	4	A-1	ACACPCC	None
091L	51.9	Inland	4	A-1	ACACPCC	None
091L	52	Inland	4	A-1	ACACPCC	None
091L	52.1	Inland	4	A-1	ACACPCC	None
095L	12.4	Shore	4	A-4	ACACPCC	None
095L	12.5	Shore	4	A-4	ACACPCC	None
095L	12.6	Shore	4	A-4	ACACPCC	None
095L	12.7	Shore	4	A-4	ACACPCC	None
095L	12.8	Shore	4	A-4	ACACPCC	None
095L	92.6	Shore	3	A-4	ACACPCC	None
095L	92.7	Shore	3	A-4	ACACPCC	None
095L	92.8	Shore	3	A-4	ACACPCC	None

Table B2. Section ID, Site Factors, Structure Type, and Construction Type (Cont.)

Road Section Name	Starting Milepost (mile)	Climate Zone	Traffic Level	Subgrade Type	Structure Type	Construction Type
095L	92.9	Shore	3	A-4	ACACPCC	None
095L	93	Shore	3	A-4	ACACPCC	None
101L	8.6	Hills	2	A-4	ThickAC	New
101L	8.7	Hills	2	A-4	ThickAC	New
101L	8.8	Hills	2	A-4	ThickAC	New
101L	8.9	Hills	2	A-4	ThickAC	New
101L	9	Hills	2	A-4	ThickAC	New
101L	9.1	Hills	2	A-4	ThickAC	New
110L	2.5	Shore	2	A-2-4	ACPCC	Rehab
110L	2.6	Shore	2	A-2-4	ACPCC	Rehab
113L	4.9	Shore	2	A-4	ThickAC	New
113L	5	Shore	2	A-4	ThickAC	New
113L	5.1	Shore	2	A-4	ThickAC	New
113L	5.2	Shore	2	A-4	ThickAC	New
113L	5.3	Shore	2	A-4	ThickAC	New
113L	5.4	Shore	2	A-4	ThickAC	New
113L	5.5	Shore	2	A-4	ThickAC	New
148L	8.8	Shore	2	A-4	ThinAC	Rehab
148L	8.9	Shore	2	A-4	ThinAC	Rehab
161L	2.9	Shore	3	A-2-4	ThickAC	New
161L	3	Shore	3	A-2-4	ThickAC	New
161L	3.1	Shore	3	A-2-4	ThickAC	New
187L	6.4	Inland	2	A-2	ThickAC	New
187L	6.5	Inland	2	A-2	ThickAC	New
187L	6.6	Inland	2	A-2	ThickAC	New
187L	6.7	Inland	2	A-2	ThickAC	New
202 L	25.5	Hills	2	A-4	ACPCC	Rehab
202 L	25.6	Hills	2	A-4	ACPCC	Rehab
202 L	25.7	Hills	2	A-4	ACPCC	Rehab
202 L	25.8	Hills	2	A-4	ACPCC	Rehab
202 L	25.9	Hills	2	A-4	ACPCC	Rehab
254L	7.4	Hills	2	A-4	ThinAC	Rehab
254L	7.5	Hills	2	A-4	ThinAC	Rehab
254L	7.6	Hills	2	A-4	ThinAC	Rehab
272L	12	Hills	2	A-4	ThinAC	Rehab
272L	12.1	Hills	2	A-4	ThinAC	Rehab
341L	1.4	Hills	2	A-4	ThickAC	Rehab
341L	1.5	Hills	2	A-4	ThickAC	Rehab
341L	1.6	Hills	2	A-4	ThickAC	Rehab
341L	1.7	Hills	2	A-4	ThickAC	Rehab
341L	1.8	Hills	2	A-4	ThickAC	Rehab
341L	1.9	Hills	2	A-4	ThickAC	Rehab
501L	0.2	Inland	2	A-4	ACPCC	New

Table B2. Section ID, Site Factors, Structure Type, and Construction Type

Road Section Name	Starting Milepost (mile)	Climate Zone	Traffic Level	Subgrade Type	Structure Type	Construction Type
501L	0.3	Inland	2	A-4	ACPCC	New
501L	0.4	Inland	2	A-4	ACPCC	New
501L	0.5	Inland	2	A-4	ACPCC	New
805L	1.2	Hills	2	A-4	ACPCC	Rehab
805L	1.3	Hills	2	A-4	ACPCC	Rehab

Table B3. Section ID and WiseCrax™ Crack Lengths in ft/10m/lane-width

Road Section Name	L_TOTAL*	T_TOTAL	L_WP	L_NWP	T_WP	T_NWP
001L	0	0	0	0	0	0
001L	57	14	40	17	7	7
001L	60	37	40	19	19	19
001L	34	37	18	17	19	18
001L	54	3	29	26	1	2
005L	1	5	0	0	3	3
005L	2	7	0	2	4	3
005L	3	10	1	2	5	5
005L	6	8	4	2	4	4
005L	22	7	14	8	3	4
007L	33	9	13	20	5	4
007L	46	11	13	33	6	6
007L	31	10	7	24	5	6
007L	49	4	12	36	2	2
007L	86	12	22	64	6	5
007L	75	5	17	58	3	2
007L	87	5	22	65	3	2
007L	86	79	32	54	36	42
007L	65	63	27	39	33	30
007L	94	117	50	44	55	63
007L	15	1	3	11	1	1
007L	23	5	8	15	2	3
007L	38	6	12	26	3	3
007L	29	3	4	25	1	2
007L	52	4	6	46	2	2
007L	59	3	6	54	2	1
007L	47	2	6	42	1	0
007L	54	4	4	50	2	2
008L	20	11	5	14	5	6
008L	60	21	25	34	9	12
008L	51	11	24	27	4	7
009L	27	7	3	24	4	3
009L	18	5	0	18	3	2
009L	17	5	1	16	2	3
010L	61	26	22	39	12	14
010L	36	30	13	24	15	14
010L	50	65	28	22	32	33
010L	75	40	37	38	19	20
010L	173	55	96	77	24	31
010L	93	64	62	30	35	29
012L	37	1	2	35	0	1
012L	23	0	1	21	0	0
012L	28	0	1	26	0	0

Table B3. Section ID and WiseCrax™ Crack Lengths in ft/10m/lane-width (Cont.)

Road Section Name	L_TOTAL	T_TOTAL	L_WP	L_NWP	T_WP	T_NWP
012L	11	1	1	11	0	0
014AL	28	1	1	27	0	0
014AL	24	1	2	22	0	0
014AL	11	3	3	9	1	2
014AL	32	2	2	30	1	1
015L	36	47	25	11	21	26
015L	43	55	23	19	25	30
015L	40	56	13	26	24	32
015L	65	27	15	51	11	16
015L	42	25	15	27	10	15
017L	42	39	5	37	18	21
017L	40	22	4	36	11	12
017L	50	34	4	45	18	16
020L	107	58	14	93	23	35
020L	64	54	12	52	23	31
022L	131	164	58	74	83	81
022L	49	97	15	34	47	50
032L	18	31	11	7	14	16
032L	16	27	10	6	14	13
032L	17	19	11	6	10	10
032L	19	47	5	15	25	22
034L	135	19	75	60	9	10
034L	219	38	112	107	18	20
034L	176	39	63	113	20	19
034L	121	32	81	40	16	17
034L	204	49	102	102	26	24
034L	127	36	55	72	17	19
034L	107	31	59	48	15	16
034L	136	31	71	66	16	15
035L	18	9	9	9	3	5
035L	22	21	12	10	10	11
044L	187	49	103	84	25	24
044L	122	91	58	65	45	45
044L	118	79	62	55	37	42
049L	35	3	16	19	2	1
049L	65	3	47	18	2	2
066L	87	1	4	83	0	1
066L	57	2	3	53	1	1
066L	53	30	9	44	14	16
066L	74	8	4	71	3	5
066L	63	3	8	55	1	2
075L	129	146	49	80	74	72
075L	68	72	29	39	32	40

Table B3. Section ID and WiseCrax™ Crack Lengths in ft/10m/lane-width (Cont.)

Road Section Name	L_TOTAL	T_TOTAL	L_WP	L_NWP	T_WP	T_NWP
075L	81	70	41	40	35	35
080L	155	72	62	93	37	36
080L	194	84	102	92	41	43
080L	156	87	85	70	42	44
084L	17	12	9	8	6	6
084L	19	14	1	18	7	7
084L	0	18	0	0	10	9
084L	0	14	0	0	6	8
084L	1	23	0	1	12	11
084L	0	4	0	0	2	2
084L	2	1	0	2	0	0
084L	1	6	0	1	3	3
084L	9	0	2	7	0	0
084L	2	2	0	2	1	1
084L	3	2	0	3	1	1
084L	7	3	0	7	1	2
084L	2	2	0	2	1	1
084L	0	2	0	0	1	1
084L	10	1	0	10	0	1
084R	9	53	5	3	26	27
084R	5	58	0	5	27	31
084R	1	50	1	1	23	26
084R	4	49	1	3	22	27
084R	3	59	1	2	26	33
084R	1	53	0	0	24	29
091L	1	11	0	1	5	6
091L	0	2	0	0	1	1
091L	0	1	0	0	0	0
091L	1	0	0	1	0	0
091L	1	1	0	0	0	0
091L	35	22	0	35	9	13
091L	49	15	0	49	7	9
091L	46	37	1	45	17	20
091L	28	24	0	28	11	13
091L	26	37	1	25	15	22
095L	19	59	1	18	24	36
095L	6	45	1	5	19	26
095L	3	38	1	2	15	23
095L	23	54	2	21	23	31
095L	8	56	1	7	24	31
095L	21	26	8	12	12	15
095L	15	35	2	13	15	20
095L	39	44	3	37	19	24

Table B3. Section ID and WiseCrax™ Crack Lengths in ft/10m/lane-width (Cont.)

Road Section Name	L_TOTAL	T_TOTAL	L_WP	L_NWP	T_WP	T_NWP
095L	16	49	1	15	21	28
095L	26	43	3	23	19	24
101L	4	16	2	3	8	8
101L	3	5	1	2	2	3
101L	5	2	1	4	1	1
101L	7	1	1	5	0	1
101L	2	10	1	1	5	5
101L	1	2	0	1	1	1
110L	60	36	21	38	17	19
110L	52	40	18	34	18	22
113L	132	77	61	71	37	40
113L	118	59	59	59	29	30
113L	107	121	45	62	57	64
113L	82	127	43	39	56	71
113L	209	105	122	87	52	54
113L	272	141	141	131	70	71
113L	99	24	49	50	12	12
148L	80	66	44	37	34	32
148L	58	51	34	23	26	25
161L	31	15	13	18	7	9
161L	51	36	25	26	18	18
161L	59	34	26	33	18	16
187L	139	116	73	66	56	60
187L	98	55	39	58	27	28
187L	103	47	29	74	22	25
187L	129	67	44	84	31	37
202L	32	38	5	27	17	20
202L	82	60	25	57	27	33
202L	106	56	56	51	29	27
202L	66	41	22	44	20	21
202L	45	35	1	44	16	19
254L	188	104	106	82	53	51
254L	173	80	106	67	42	38
254L	203	110	110	93	55	55
272L	86	56	43	43	26	29
272L	84	65	47	37	31	34
341L	23	38	8	15	18	20
341L	62	33	44	17	14	19
341L	14	17	6	7	7	10
341L	15	38	9	6	17	22
341L	21	21	8	12	10	12
341L	19	13	4	15	6	7
501L	163	85	38	125	35	50

Table B3. Section ID and WiseCrax™ Crack Lengths in ft/10m/lane-width (Cont.)

Road Section Name	L_TOTAL	T_TOTAL	L_WP	L_NWP	T_WP	T_NWP
501L	117	73	60	57	34	39
501L	115	63	24	91	27	36
501L	100	36	50	50	17	19
805L	146	36	89	57	16	20
805L	129	12	34	95	5	7

*L_TOTAL = total length of longitudinal cracks
T_TOTAL = total length of transverse cracks
L_WP = length of longitudinal cracks within wheelpaths (left and right)
L_NWP = length of longitudinal cracks outside wheelpaths (edges and center)
T_WP = length of transverse cracks within wheelpaths (left and right)
T_NWP = length of transverse cracks outside wheelpaths (edges and center)

Appendix C. PMIS Performance Data for Validation

Table C1. Wisecrax Pavement Performance Data for 2014

Road Name	From	Ptype	CONSTRUCT AGE	SURFACE AGE	L_TOT	L_WP	L_NWP	T_TOT	T_WP	T_NWP	NWP_TOT	WP_TOT	IRI_AVG	RUT_AVG
005L	41	COMP	55	2	0.6	0.1	0.5	5.3	2.6	2.8	3.2	2.7	84.6	0.09
005L	41.1	COMP	55	2	2.0	0.1	1.8	7.1	3.7	3.4	5.2	3.9	77.7	0.09
005L	41.2	COMP	55	2	3.2	0.8	2.4	9.8	4.9	4.9	7.2	5.7	71.7	0.08
005L	41.3	COMP	55	2	5.5	3.7	1.8	7.6	3.6	4.0	5.8	7.3	69.4	0.12
005L	41.4	COMP	55	2	22.1	14.4	7.7	6.9	3.2	3.7	11.4	17.7	85.9	0.12
007L	4.1	FLEX	26	3	32.8	13.2	19.6	9.1	5.0	4.1	23.7	18.2	181.2	0.14
007L	4.2	FLEX	26	3	46.4	13.5	32.9	11.3	5.5	5.8	38.7	19.0	159.5	0.16
007L	4.3	FLEX	26	3	31.5	7.0	24.4	10.4	4.8	5.6	30.0	11.8	150.9	0.24
007L	8	COMP	5	5	48.6	12.2	36.4	3.8	2.0	1.7	38.1	14.3	126.6	0.10
007L	8.1	COMP	5	5	85.8	21.7	64.1	11.8	6.4	5.4	69.4	28.1	156.5	0.11
007L	8.2	COMP	5	5	74.8	16.7	58.1	5.1	2.7	2.4	60.5	19.4	133.1	0.12
007L	8.3	COMP	5	5	87.1	22.5	64.6	5.0	2.7	2.3	66.9	25.2	112.7	0.11
007L	12.7	COMP	35	11	86.0	31.8	54.1	78.8	36.5	42.3	96.5	68.3	148.7	0.18
007L	12.8	COMP	35	11	65.2	26.5	38.7	62.9	32.6	30.3	69.1	59.1	227.3	0.22
007L	12.9	COMP	35	11	94.2	50.3	43.8	117.3	54.7	62.6	106.4	105.0	136.6	0.16
007L	32.2	FLEX	5	5	14.5	3.4	11.1	1.4	0.8	0.7	11.8	4.2	105.9	0.15
007L	32.3	FLEX	5	5	23.3	8.1	15.2	5.0	2.2	2.8	18.0	10.2	115.4	0.14
007L	32.4	FLEX	5	5	38.1	11.9	26.1	6.3	2.9	3.4	29.5	14.8	109.3	0.14
007L	32.5	FLEX	5	5	28.7	3.6	25.1	3.0	1.2	1.8	26.9	4.8	123.5	0.13
007L	32.6	FLEX	5	5	52.2	5.9	46.3	4.2	1.8	2.4	48.6	7.8	110.3	0.17
007L	32.7	FLEX	5	5	59.0	5.5	53.5	2.8	1.6	1.2	54.7	7.1	111.5	0.15
007L	32.8	FLEX	5	5	47.4	5.8	41.6	1.7	1.4	0.4	42.0	7.2	91.9	0.15
007L	32.9	FLEX	5	5	54.3	3.9	50.4	3.8	1.7	2.1	52.6	5.6	98.4	0.14
008L	38.7	COMP	47	3	19.5	5.5	14.1	10.7	4.7	5.9	20.0	10.2	92.1	0.06
008L	38.8	COMP	47	3	59.7	25.3	34.4	21.0	8.7	12.3	46.7	34.0	65.0	0.06
008L	38.9	COMP	47	3	50.8	24.3	26.5	10.9	3.9	7.0	33.6	28.1	67.6	0.08
009L	34.8	COMP	45	2	26.7	2.7	24.0	7.0	3.5	3.4	27.4	6.2	59.2	0.06
009L	34.9	COMP	36	2	18.4	0.3	18.1	4.5	2.5	2.0	20.1	2.9	61.4	0.06
009L	35	COMP	36	2	17.4	1.0	16.5	4.6	1.7	2.8	19.3	2.7	50.7	0.06
010L	26.8	FLEX	51	11	61.0	21.8	39.2	25.7	11.9	13.7	52.9	33.7	235.1	0.34
010L	26.9	COMP	42	11	36.3	12.5	23.8	29.5	15.1	14.5	38.2	27.6	376.3	0.32
010L	27	COMP	42	11	49.9	28.4	21.6	64.8	32.0	32.8	54.4	60.3	267.0	0.27
010L	27.1	COMP	42	11	75.2	36.8	38.4	39.5	19.1	20.4	58.8	56.0	262.3	0.21
010L	27.2	COMP	42	11	172.8	95.5	77.2	54.8	24.0	30.8	108.1	119.5	182.3	0.20
010L	27.3	COMP	42	11	92.6	62.4	30.1	63.6	35.0	28.5	58.7	97.4	297.4	0.24
012L	3.9	FLEX	71	2	36.8	1.7	35.1	0.5	0.0	0.5	35.6	1.7	100.8	0.05
012L	4	FLEX	71	2	22.5	1.4	21.1	0.5	0.1	0.4	21.5	1.5	161.9	0.06

012L	4.1	FLEX	71	2	27.7	1.5	26.3	0.3	0.0	0.3	26.5	1.5	78.6	0.05

Table C1. Wisecrax Pavement Performance Data for 2014 (Cont.)

Road Name	From	Ptype	CONSTRUCT AGE	SURFACE AGE	L_TOT	L_WP	L_NWP	T_TOT	T_WP	T_NWP	NWP_TOT	WP_TOT	IRI_AVG	RUT_AVG
012L	4.2	FLEX	71	2	11.4	0.5	10.8	0.8	0.4	0.5	11.3	0.9	92.5	0.07
014	5.2	FLEX	10	10	27.8	0.6	27.1	0.7	0.4	0.2	27.4	1.1	107.4	0.11
014	5.3	FLEX	10	10	24.2	1.7	22.5	0.8	0.4	0.5	22.9	2.1	122.4	0.17
014	5.4	FLEX	10	10	11.3	2.8	8.5	2.9	1.3	1.6	10.1	4.0	120.5	0.13
014	5.5	FLEX	10	10	31.9	2.1	29.8	1.9	0.9	1.0	30.8	3.0	149.8	0.15
015L	42.2	COMP	38	13	36.3	24.9	11.4	47.1	21.0	26.1	37.4	46.0	73.2	0.15
015L	42.3	COMP	38	13	42.6	23.3	19.3	54.5	24.9	29.7	48.9	48.2	74.0	0.15
015L	42.4	COMP	38	13	39.5	13.3	26.3	55.8	24.1	31.8	58.0	37.4	68.6	0.13
015L	42.5	COMP	38	13	65.4	14.8	50.6	27.4	11.3	16.1	66.7	26.1	122.2	0.16
015L	42.6	COMP	38	13	42.2	14.8	27.4	25.1	10.2	14.9	42.3	25.0	82.9	0.15
017L	0.8	COMP	44	7	42.0	5.2	36.8	39.0	18.1	20.9	57.7	23.4	127.2	0.14
017L	0.9	COMP	44	7	39.6	3.7	35.9	22.1	10.6	11.6	47.5	14.2	110.4	0.13
017L	1	COMP	44	7	49.8	4.5	45.4	34.1	17.6	16.5	61.8	22.1	112.2	0.13
020L	26.5	FLEX	14	14	107.2	14.1	93.1	57.9	22.9	35.0	128.1	36.9	110.9	0.27
020L	26.6	FLEX	14	14	64.0	12.0	52.0	53.8	22.8	31.0	83.0	34.9	119.6	0.34
022L	9.2	FLEX	74	17	131.2	57.6	73.7	164.3	82.9	81.4	155.1	140.4	153.5	0.14
022L	9.3	FLEX	74	17	48.9	14.6	34.3	97.2	47.0	50.2	84.5	61.6	100.0	0.14
034L	8.8	FLEX	76	14	134.7	74.9	59.8	18.9	8.8	10.1	69.9	83.7	146.4	0.20
034L	8.9	FLEX	76	14	219.2	112.3	106.9	38.0	17.6	20.3	127.2	129.9	136.1	0.17
034L	9	FLEX	76	14	176.3	63.1	113.2	38.8	19.6	19.2	132.3	82.7	116.3	0.16
034L	9.1	FLEX	76	14	121.3	81.3	40.0	32.1	15.5	16.5	56.5	96.8	113.1	0.16
034L	9.2	FLEX	76	14	203.6	101.8	101.8	49.2	25.5	23.7	125.5	127.3	106.1	0.20
034L	17	COMP	33	17	126.9	55.2	71.6	36.2	17.4	18.8	90.4	72.6	144.2	0.27
034L	17.1	COMP	33	17	107.4	59.0	48.4	31.3	14.9	16.3	64.8	73.9	215.9	0.32
034L	17.2	COMP	33	17	136.2	70.6	65.6	30.7	16.0	14.7	80.4	86.6	234.8	0.32
035L	2.5	COMP	87	4	18.0	9.0	9.0	8.6	3.4	5.2	14.2	12.4	142.7	0.09
035L	2.6	COMP	87	4	21.6	11.8	9.8	20.9	10.1	10.8	20.6	21.8	110.3	0.07
044L	7.9	COMP	35	16	186.5	102.7	83.8	49.0	24.6	24.4	108.2	127.3	156.0	0.23
044L	8	COMP	35	16	122.3	57.7	64.7	90.5	45.5	45.1	109.7	103.1	170.5	0.15
044L	8.1	COMP	35	16	117.7	62.4	55.3	78.7	36.5	42.1	97.4	99.0	207.9	0.18
049L	21	FLEX	73	16	34.9	16.3	18.6	3.0	1.8	1.2	19.8	18.1	173.2	0.22
049L	21.1	FLEX	73	16	65.1	47.1	18.0	3.2	1.6	1.6	19.6	48.7	175.2	0.25
066L	1.7	FLEX	9	9	87.1	3.9	83.2	1.0	0.4	0.6	83.8	4.3	90.1	0.13
066L	1.8	FLEX	9	9	56.6	3.3	53.3	2.5	1.3	1.2	54.5	4.6	85.8	0.12
066L	1.9	FLEX	9	9	52.8	8.7	44.1	30.1	13.9	16.2	60.3	22.5	180.0	0.14
066L	2	FLEX	9	9	74.4	3.9	70.5	7.8	3.1	4.7	75.2	7.0	146.7	0.14
066L	2.1	FLEX	9	9	63.1	7.8	55.3	2.7	1.0	1.7	57.0	8.8	107.8	0.16
075L	6.5	FLEX	33	17	128.7	48.6	80.2	145.9	73.8	72.1	152.2	122.4	123.0	0.27

Table C1. Wisecrax Pavement Performance Data for 2014 (Cont.)

Road Name	From	Ptype	CONSTRUCT AGE	SURFACE AGE	L_TOT	L_WP	L_NWP	T_TOT	T_WP	T_NWP	NWP_TOT	WP_TOT	IRI_AVG	RUT_AVG
075L	6.6	FLEX	33	17	68.4	29.1	39.3	72.3	31.9	40.4	79.7	61.0	156.3	0.29
075L	6.7	FLEX	33	17	81.0	41.2	39.8	69.9	35.3	34.6	74.4	76.5	217.0	0.23
084L	1.6	COMP	53	5	16.9	9.1	7.9	12.3	6.0	6.3	14.1	15.0	53.5	0.11
084L	1.7	COMP	53	5	19.1	1.5	17.6	14.1	6.9	7.2	24.9	8.4	61.6	0.12
084L	36.1	COMP	53	6	0.0	0.0	0.0	18.4	9.5	8.9	8.9	9.5	106.6	0.10
084L	36.2	COMP	53	6	0.3	0.2	0.1	13.8	6.2	7.7	7.8	6.3	72.0	0.11
084L	36.3	COMP	53	6	0.9	0.4	0.5	23.1	11.7	11.4	11.9	12.1	73.4	0.09
084L	36.4	COMP	53	6	0.1	0.1	0.0	4.3	1.8	2.4	2.4	2.0	121.5	0.09
084L	36.5	COMP	53	6	2.1	0.1	2.0	0.8	0.3	0.5	2.4	0.5	71.3	0.09
084L	36.6	COMP	53	6	0.7	0.0	0.7	5.7	2.7	3.0	3.7	2.7	93.4	0.08
084L	36.7	COMP	53	6	9.0	1.6	7.4	0.3	0.2	0.1	7.5	1.8	82.1	0.08
084L	94.3	COMP	38	2	1.7	0.2	1.5	2.0	0.9	1.1	2.6	1.1	50.0	0.11
084L	94.4	COMP	38	2	2.7	0.1	2.6	2.5	1.2	1.3	3.9	1.3	49.2	0.12
084L	94.5	COMP	38	2	7.2	0.4	6.8	3.2	1.5	1.8	8.5	1.9	71.5	0.13
084L	94.6	COMP	38	2	1.7	0.0	1.7	2.5	1.5	1.0	2.7	1.5	52.5	0.11
084L	94.7	COMP	38	2	0.4	0.2	0.3	1.9	1.0	0.9	1.2	1.2	58.4	0.12
084L	94.8	COMP	38	2	10.0	0.0	10.0	1.3	0.2	1.1	11.1	0.2	54.1	0.12
084R	6.2	COMP	52	13	8.6	5.2	3.5	53.1	25.8	27.4	30.8	31.0	126.3	0.23
084R	6.3	COMP	52	13	4.6	0.0	4.6	57.9	27.0	30.9	35.6	27.0	146.0	0.25
084R	6.4	COMP	52	13	1.3	0.8	0.5	49.5	23.2	26.3	26.8	24.0	183.2	0.28
084R	6.5	COMP	52	13	4.2	0.9	3.3	49.1	22.3	26.8	30.0	23.3	164.8	0.30
084R	6.6	COMP	52	13	3.3	1.2	2.1	59.4	26.2	33.2	35.3	27.4	108.2	0.21
084R	6.7	COMP	52	13	0.9	0.5	0.4	52.8	23.6	29.2	29.6	24.1	133.4	0.21
091L	3.6	COMP	49	2	0.8	0.0	0.8	11.0	4.8	6.1	6.9	4.8	56.0	0.13
091L	3.7	COMP	49	2	0.4	0.0	0.4	2.1	0.8	1.3	1.7	0.8	44.3	0.12
091L	3.8	COMP	49	2	0.2	0.0	0.2	0.5	0.3	0.3	0.5	0.3	47.4	0.12
091L	3.9	COMP	49	2	1.3	0.0	1.3	0.3	0.2	0.2	1.5	0.2	51.5	0.12
091L	4	COMP	49	2	0.7	0.3	0.4	0.7	0.4	0.3	0.7	0.7	51.0	0.13
095L	12.4	COMP	41	9	19.2	0.9	18.3	59.2	23.7	35.5	53.8	24.6	79.0	0.23
095L	12.5	COMP	41	9	5.8	0.5	5.3	45.1	19.1	26.0	31.3	19.6	74.3	0.23
095L	12.6	COMP	41	9	3.1	0.7	2.5	38.4	15.4	22.9	25.4	16.1	76.0	0.23
095L	12.7	COMP	41	9	23.3	2.5	20.8	54.2	23.4	30.8	51.5	25.9	79.7	0.25
095L	12.8	COMP	41	9	7.6	0.8	6.8	55.6	24.2	31.4	38.2	25.0	84.5	0.25
095L	92.6	COMP	45	12	20.8	8.3	12.5	26.3	11.5	14.7	27.2	19.9	86.9	0.15
095L	92.7	COMP	45	12	15.3	2.5	12.8	35.4	15.4	20.0	32.8	17.8	77.2	0.16
095L	92.8	COMP	39	12	39.2	2.5	36.7	43.5	19.2	24.3	61.0	21.7	76.8	0.14
095L	92.9	COMP	39	12	16.5	1.4	15.0	48.9	20.7	28.2	43.3	22.1	81.5	0.15
095L	93	COMP	39	12	25.9	3.4	22.6	42.6	18.6	23.9	46.5	22.0	78.4	0.16

Table C1. Wisecrax Pavement Performance Data for 2014 (Cont.)

Road Name	From	Ptype	CONSTRUCT AGE	SURFACE AGE	L_TOT	L_WP	L_NWP	T_TOT	T_WP	T_NWP	NWP_TOT	WP_TOT	IRI_AVG	RUT_AVG
101L	8.6	FLEX	79	3	4.5	1.8	2.7	16.2	8.2	8.1	10.8	9.9	113.8	0.08
101L	8.7	FLEX	79	3	2.7	0.8	1.9	4.7	1.7	3.0	4.9	2.5	90.2	0.07
101L	8.8	FLEX	79	3	5.2	1.5	3.7	1.6	0.8	0.8	4.5	2.3	87.8	0.07
101L	8.9	FLEX	79	3	6.5	1.5	5.1	1.2	0.4	0.8	5.8	1.9	85.1	0.07
101L	9	FLEX	79	3	1.5	0.7	0.9	10.3	5.5	4.9	5.7	6.2	95.2	0.08
101L	9.1	FLEX	79	3	0.9	0.2	0.7	2.3	1.1	1.2	1.9	1.3	80.7	0.07
110L	2.5	COMP	87	9	59.8	21.4	38.3	36.2	17.0	19.3	57.6	38.4	87.2	0.14
110L	2.6	COMP	87	9	52.3	18.3	34.1	40.2	18.1	22.1	56.2	36.4	93.4	0.13
113L	4.9	FLEX	17	17	131.7	61.1	70.6	76.6	36.9	39.7	110.4	98.0	172.9	0.19
113L	5	FLEX	17	17	117.8	58.8	59.0	59.1	29.0	30.1	89.1	87.8	208.0	0.20
113L	5.1	FLEX	17	17	106.7	45.1	61.6	120.9	56.6	64.3	125.8	101.7	277.2	0.24
113L	5.2	FLEX	17	17	82.3	43.1	39.3	126.9	56.1	70.8	110.0	99.2	228.8	0.22
113L	5.3	FLEX	17	17	208.5	121.7	86.9	105.3	51.6	53.6	140.5	173.3	291.3	0.21
113L	5.4	FLEX	17	17	271.7	140.8	130.8	141.5	70.4	71.0	201.9	211.3	240.2	0.17
113L	5.5	FLEX	17	17	98.9	48.6	50.3	24.4	12.5	11.9	62.2	61.1	206.0	0.15
148L	8.8	FLEX	72	13	80.5	43.8	36.6	66.0	34.0	32.0	68.6	77.9	131.2	0.12
148L	8.9	FLEX	72	13	57.6	34.4	23.2	50.7	26.0	24.6	47.8	60.4	106.7	0.10
187L	6.4	FLEX	17	17	138.6	72.6	66.0	116.0	55.9	60.1	126.1	128.4	136.7	0.25
187L	6.5	FLEX	17	17	97.5	39.4	58.1	54.8	27.2	27.5	85.7	66.7	134.1	0.25
187L	6.6	FLEX	17	17	103.4	29.0	74.4	47.3	22.5	24.9	99.3	51.5	142.8	0.26
187L	6.7	FLEX	17	17	128.7	44.4	84.4	67.3	30.7	36.6	120.9	75.1	103.3	0.25
202L	25.5	COMP	83	13	32.2	5.2	27.0	38.0	17.5	20.5	47.5	22.6	92.0	0.14
202L	25.6	COMP	83	13	82.2	25.5	56.7	60.0	27.5	32.6	89.3	53.0	111.7	0.14
202L	25.7	COMP	83	13	106.4	55.8	50.7	55.9	29.0	26.9	77.5	84.8	126.1	0.17
202L	25.8	COMP	83	13	66.0	21.8	44.3	40.7	19.9	20.8	65.1	41.6	135.7	0.15
202L	25.9	COMP	83	13	45.3	1.5	43.9	35.0	16.2	18.8	62.6	17.7	119.9	0.14
254L	7.4	FLEX	31	17	188.1	105.7	82.3	104.0	52.9	51.1	133.4	158.6	182.0	0.16
254L	7.5	FLEX	31	17	172.8	105.6	67.2	80.1	42.0	38.1	105.2	147.6	192.4	0.17
254L	7.6	FLEX	31	17	203.3	109.9	93.4	110.1	54.8	55.3	148.7	164.7	153.1	0.15
272L	12	FLEX	89	16	86.1	42.7	43.4	55.6	26.4	29.1	72.5	69.2	188.8	0.26
272L	12.1	FLEX	89	16	84.4	47.3	37.1	64.7	30.6	34.1	71.2	78.0	173.1	0.26
341L	1.4	FLEX	74	8	23.0	8.0	15.0	37.8	18.3	19.5	34.6	26.3	154.7	0.13
341L	1.5	FLEX	74	8	61.8	44.3	17.5	33.1	14.3	18.9	36.3	58.5	187.8	0.15
341L	1.6	FLEX	74	8	13.7	6.3	7.4	17.2	7.3	9.9	17.3	13.6	144.5	0.12
341L	1.7	FLEX	74	8	14.9	8.9	5.9	38.4	16.9	21.5	27.4	25.8	226.0	0.13
341L	1.8	FLEX	74	8	20.6	8.3	12.3	21.1	9.6	11.5	23.8	17.9	185.8	0.13
341L	1.9	FLEX	74	8	18.9	4.4	14.5	12.6	5.6	7.0	21.5	10.0	150.5	0.12
501L	0.2	COMP	49	13	162.7	37.8	124.9	84.9	35.4	49.6	174.4	73.2	106.2	0.21
501L	0.3	COMP	49	13	117.0	60.0	56.9	73.3	33.8	39.5	96.4	93.8	181.1	0.21

Table C1. Wisecrax Pavement Performance Data for 2014 (Cont.)

Road Name	From	Ptype	CONSTRUCT AGE	SURFACE AGE	L_TOT	L_WP	L_NWP	T_TOT	T_WP	T_NWP	NWP_TOT	WP_TOT	IRI_AVG	RUT_AVG
501L	0.4	COMP	49	13	115.5	24.4	91.1	62.7	26.5	36.2	127.3	51.0	82.4	0.16
501L	0.5	COMP	49	13	100.3	50.3	50.1	35.8	17.0	18.8	68.9	67.3	81.0	0.20
805L	1.2	COMP	86	9	146.3	89.4	56.8	35.8	15.7	20.1	76.9	105.2	144.9	0.17
805L	1.3	COMP	86	9	129.0	33.9	95.1	11.8	5.2	6.6	101.6	39.1	171.7	0.18
Outlier Sections														
001L	50.7	FLEX	31	6	0.0	0.0	0.0	0.0	0.0	0.0	0.0	0.0	130.1	0.13
001L	50.8	FLEX	6	6	57.5	40.4	17.1	24.2	14.1	7.0	7.1	47.4	136.0	0.16
001L	50.9	FLEX	6	6	59.5	40.2	19.3	38.1	37.5	18.7	18.8	58.9	183.3	0.22
001L	51	FLEX	6	0	34.4	17.6	16.8	34.9	37.3	19.3	18.0	36.8	172.0	0.14
001L	51.1	FLEX	6	0	54.4	28.7	25.7	27.4	3.1	1.3	1.7	30.1	132.7	0.12
032L	22.2	COMP	33	0	18.0	10.7	7.2	23.7	30.7	14.3	16.4	25.0	103.7	0.18
032L	22.3	COMP	33	0	15.8	9.9	6.0	18.5	26.7	14.2	12.5	24.0	105.5	0.20
032L	22.4	COMP	33	0	16.8	11.3	5.5	15.2	19.2	9.6	9.7	20.8	91.1	0.20
032L	22.5	COMP	33	0	19.3	4.7	14.6	36.4	47.0	25.2	21.8	29.8	97.0	0.16
080L	5.2	FLEX	7	7	154.9	62.4	92.6	128.3	72.4	36.7	35.7	99.1	87.0	0.17
080L	5.3	FLEX	7	7	193.8	102.0	91.9	134.4	83.9	41.4	42.6	143.3	83.4	0.20
080L	5.4	FLEX	7	7	155.6	85.5	70.1	114.2	86.5	42.5	44.0	127.9	123.0	0.18
091L	51.7	COMP	55	0	34.8	0.1	34.7	47.8	21.9	8.8	13.1	9.0	94.2	0.18
091L	51.8	COMP	55	0	49.5	0.0	49.5	58.0	15.3	6.7	8.5	6.7	61.1	0.17
091L	51.9	COMP	55	0	45.5	0.7	44.8	64.9	36.9	16.8	20.0	17.5	76.8	0.18
091L	52	COMP	55	0	27.8	0.3	27.5	40.5	23.9	10.9	12.9	11.2	77.0	0.17
091L	52.1	COMP	55	0	25.6	0.9	24.7	46.4	37.0	15.3	21.8	16.1	72.1	0.16
161L	2.9	FLEX	55	23	31.4	13.3	18.1	26.9	15.3	6.6	8.7	19.9	183.2	0.22
161L	3	FLEX	63	23	51.2	25.4	25.9	43.5	35.8	18.2	17.6	43.6	178.7	0.28
161L	3.1	FLEX	63	23	59.3	26.1	33.3	49.2	33.6	17.6	16.0	43.7	169.2	0.24

*L_TOT = total longitudinal crack length in ft/10m/lane-width
L_WP = longitudinal wheelpath crack length in ft/10m/lane-width
L_NWP = longitudinal non-wheelpath crack length in ft/10m/lane-width
T_TOT = total transverse crack length in ft/10m/lane-width
T_WP = transverse wheelpath crack length in ft/10m/lane-width
T_NWP = transverse non-wheelpath crack length in ft/10m/lane-width
NWP_TOT = total non-wheelpath crack length in ft/10m/lane-width
WP_TOT =wheelpath crack length in ft/10m/lane-width
IRI_AVG = average IRI in in/mi
RUT_AVG = average rut depth in inches

Table C2. Summary of distresses from visual Photolog and automated WiseCrax™ evaluations per 10m/lane-width

Road Name	From	Direction	Van	Surface Age	Visual from Photolog				Automated from WiseCrax™		
					Longitudinal [ft/10m]	Transverse [ft/10m]	L+T * [ft/10m]	Alligator [%Area]	Longitudinal [ft/10m]	Transverse [ft/10m]	L+T [ft/10m]
005L	41	N	8	0	0	0	0	0%	2	1	2
005L	41.1	N	8	0	0	0	0	0%	1	1	1
005L	41.2	N	8	0	0	0	0	0%	1	2	3
005L	41.3	N	8	0	0	0	0	0%	9	2	11
005L	41.4	N	8	0	0	0	0	0%	4	0	4
007L	4.1	N	8	1	0	0	0	0%	10	9	18
007L	4.2	N	8	1	0	0	0	0%	25	0	25
007L	4.3	N	8	1	0	0	0	0%	16	13	29
007L	8	N	8	3	10	0	10	0%	34	3	37
007L	8.1	N	8	3	18	2	21	0%	42	6	47
007L	8.2	N	8	3	14	0	14	0%	36	3	39
007L	8.3	N	8	3	21	0	21	0%	34	2	35
007L	12.7	N	8	9	37	13	50	16%	73	26	100
007L	12.8	N	8	9	20	7	27	10%	53	10	63
007L	12.9	N	8	9	29	12	42	8%	76	24	100
007L	32.2	N	8	3	0	0	0	0%	10	1	10
007L	32.3	N	8	3	0	1	1	0%	12	4	16
007L	32.4	N	8	3	2	1	3	0%	13	6	18
007L	32.5	N	8	3	10	0	10	0%	22	3	25
007L	32.6	N	8	3	19	0	19	0%	29	2	31
007L	32.7	N	8	3	18	0	18	0%	37	1	39
007L	32.8	N	8	3	3	0	3	0%	26	0	27
007L	32.9	N	8	3	10	0	10	0%	33	6	39
008L	38.7	N	7	1	0	0	0	0%	7	10	17
008L	38.8	N	7	1	0	0	0	0%	5	4	8
008L	38.9	N	7	1	0	0	0	0%	3	3	6
010L	26.8	N	8	9	10	1	11	0%	27	14	40
010L	26.9	N	8	9	11	6	17	1%	31	23	55
010L	27	N	8	9	33	7	40	1%	48	16	65
010L	27.1	N	8	9	35	9	44	0%	52	35	87
010L	27.2	N	8	9	62	20	83	6%	89	50	139
010L	27.3	N	8	9	46	13	59	8%	75	33	109

Table C2. Summary of distresses from visual Photolog and automated WiseCrax™ evaluations per 10m/lane-width (Cont.)

Road Name	From	Direction	Van	Surface Age	Visual from Photolog				Automated from WiseCrax™		
					Longitudinal [ft/10m]	Transverse [ft/10m]	L+T [ft/10m]	Alligator [%Area]	Longitudinal [ft/10m]	Transverse [ft/10m]	L+T [ft/10m]
014AL	5.2	E	7	8	15	1	16	0%	30	3	33
014AL	5.3	E	7	8	17	0	17	0%	24	0	24
014AL	5.4	E	7	8	4	0	4	0%	1	1	2
014AL	5.5	E	7	8	18	1	19	0%	19	0	19
015L	42.2	N	7	11	26	11	37	10%	38	59	97
015L	42.3	N	7	11	35	8	43	12%	22	46	69
015L	42.4	N	7	11	32	9	41	10%	11	46	56
015L	42.5	N	7	11	37	12	49	12%	63	48	111
015L	42.6	N	7	11	27	11	37	3%	46	47	93
017L	0.8	N	7	5	5	9	14	0%	4	18	21
017L	0.9	N	7	5	2	12	14	0%	5	19	25
017L	1	N	7	5	1	9	10	0%	3	8	11
020L	26.5	E	8	12	34	19	52	7%	81	45	126
020L	26.6	E	8	12	38	18	56	7%	49	37	86
022L	9.2	E	7	15	64	29	93	12%	126	157	284
022L	9.3	E	7	15	15	16	31	3%	48	52	100
034L	8.8	E	8	12	52	6	58	16%	80	20	100
034L	8.9	E	8	12	81	6	87	20%	147	14	161
034L	9	E	8	12	52	11	63	10%	103	28	131
034L	9.1	E	8	12	42	9	51	7%	90	18	108
034L	9.2	E	8	12	67	13	80	11%	136	33	169
034L	17	E	8	15	29	11	41	4%	67	27	94
034L	17.1	E	8	15	30	11	41	1%	60	19	80
034L	17.2	E	8	15	51	6	57	4%	93	23	116
035L	2.5	N	8	2	0	0	0	0%	5	17	22
035L	2.6	N	8	2	0	2	2	0%	8	3	11
044L	7.9	E	8	14	89	10	99	10%	150	33	183
044L	8	E	8	14	61	12	74	7%	106	35	142
044L	8.1	E	8	14	51	17	68	6%	75	27	102

*L+T = longitudinal +transverse

Table C3. Summary of distresses by visual Photolog and automated WiseCraxTM per route in ft/mi

Road Name	From	Van	Surface Age	Visual from Photolog				Automated from WiseCrax™		
				Longitudinal [ft/mi]	Transverse [ft/mi]	L+T [ft/mi]	Alligator [%Area]	Longitudinal [ft/mi]	Transverse [ft/mi]	L+T [ft/mi]
005L	41.4	7	0	0	0	0	0.0%	527	143	670
007L	4.3	8	1	0	0	0	0.0%	2711	1150	3860
007L	8.3	8	3	2522	109	2631	0.0%	5818	522	6340
007L	12.9	8	9	4582	1741	6323	11.6%	10809	3220	14029
007L	32.9	8	3	1267	34	1301	0.0%	3629	456	4085
008L	38.9	8	1	0	0	0	0.0%	788	880	1668
010L	27.3	8	9	5233	1525	6758	2.7%	8615	4563	13178
014AL	5.5	7	8	2153	75	2229	0.0%	2919	182	3101
015L	42.6	7	11	5003	1626	6629	9.4%	5773	7880	13653
017L	1	7	5	437	1608	2045	0.0%	642	2414	3056
020L	26.6	8	12	5709	2938	8647	7.0%	10404	6517	16921
022L	9.3	7	15	6316	3643	9959	7.3%	13987	16720	30707
034L	9.2	8	12	9413	1440	10853	12.8%	17779	3642	21421
034L	17.2	8	15	5845	1510	7356	3.2%	11751	3674	15425
035L	2.6	8	2	16	164	180	0.0%	1052	1605	2657
044L	8.1	7	14	10745	2073	12818	7.7%	17692	5051	22744

*L+T = longitudinal +transverse

Appendix D. Summary of Pavement-ME Validation Inputs and Outputs

Table D1. Road ID Design Life, Climate, Traffic, and Pavement Type Inputs

Road Name	From	File Name	Design Life [years]	Climate	AADTT	Structure	Construction
005L	41.4	L5	2	WILLIMANTIC, CT	400	ACPCC	Rehab
007L	4.3	L7_4	3	BRIDGEPORT, CT	1000	ThickAC	Rehab
007L	8.3	L7_8	5	WILLIMANTIC, CT	400	ThickAC	New
007L	12.9	L7	11	WESTFIELD/SPRINGFIELD, MA	400	ACPCC	Rehab
007L	32.9	L7_32	5	WESTFIELD/SPRINGFIELD, MA	1000	ThickAC	New
008L	38.9	L8	3	WESTFIELD/SPRINGFIELD, MA	1000	ACACPCC	None
010L	27.3	L10	11	WILLIMANTIC, CT	1000	ThickAC	New
012L	4.2	L12	2	BRIDGEPORT, CT	400	ThickAC	New
014AL	5.5	L14A	10	WILLIMANTIC, CT	400	ThickAC	New
015L	42.6	L15_42	17	BRIDGEPORT, CT	1000	ACPCC	None
017L	1	L17	7	BRIDGEPORT, CT	400	ACACPCC	Rehab
020L	26.6	L20	14	WILLIMANTIC, CT	1000	ThinAC	Rehab
022L	9.3	L22	17	BRIDGEPORT, CT	400	ThinAC	Rehab
034L	9.2	L34_8	14	WILLIMANTIC, CT	400	ThinAC	Rehab
034L	17.2	L34_17	17	BRIDGEPORT, CT	1000	ACPCC	New
035L	2.6	L35	4	WESTFIELD/SPRINGFIELD, MA	400	ACPCC	Rehab
044L	8.1	L44	16	WESTFIELD/SPRINGFIELD, MA	400	ACPCC	Rehab
049L	21.1	L49	16	WILLIMANTIC, CT	400	ThinAC	Rehab
066L	2.1	L66	9	WILLIMANTIC, CT	1000	ThickAC	New
075L	6.7	L75	17	WILLIMANTIC, CT	400	ThinAC	Rehab
084L	1.7	L84_1	5	WESTFIELD/SPRINGFIELD, MA	2500	ACACPCC	None
084L	36.7	L84_36	6	WILLIMANTIC, CT	2500	ACACPCC	None
084L	94.8	L84_94	2	WESTFIELD/SPRINGFIELD, MA	2500	ACACPCC	None
091L	4	L91_3	2	BRIDGEPORT, CT	2500	ACPCC	None
095L	12.8	L95_12	9	BRIDGEPORT, CT	2500	ACACPCC	None
095L	93	L95_92	12	BRIDGEPORT, CT	1000	ACACPCC	None
101L	9.1	L101	3	WESTFIELD/SPRINGFIELD, MA	400	ThickAC	New
110L	2.6	L110	9	BRIDGEPORT, CT	400	ACACPCC	Rehab
113L	5.5	L113	17	BRIDGEPORT, CT	400	ThickAC	New
148L	8.9	L148	13	BRIDGEPORT, CT	400	ThinAC	Rehab
187L	6.7	L187	17	WILLIMANTIC, CT	400	ThickAC	New
202L	25.9	L202	13	WESTFIELD/SPRINGFIELD, MA	400	ACPCC	Rehab
254L	7.6	L254	17	WESTFIELD/SPRINGFIELD, MA	400	ThinAC	Rehab
272L	12.1	L272	16	WESTFIELD/SPRINGFIELD, MA	400	ThinAC	Rehab
341L	1.9	L341	8	WESTFIELD/SPRINGFIELD, MA	400	ThinAC	Rehab
501L	0.5	L501	13	WILLIMANTIC, CT	400	ACPCC	Rehab
805L	1.3	L805	9	WESTFIELD/SPRINGFIELD, MA	400	ACPCC	Rehab

Table D2. Road ID and Asphalt Layer Data

Road Name	From	Top AC Layer						Bottom AC Layer					
		hac1	p34	p38	p4	p200	acbind1	hac2	2p34	2p38	2p4	2p200	acbind2
005L	41.4	3.3	100	95	75	6	64-22	na*	na	na	na	na	na
007L	4.3	2.3	100	77	60	6	64-22	2	100	77	60	6	AC 20
007L	8.3	4	100	77	60	6	64-22	4	100	77	60	6	64-22
007L	12.9	5.8	100	95	75	6	64-28	na	na	na	na	na	na
007L	32.9	3.6	100	77	60	6	64-22	6	100	77	60	6	64-22
008L	38.9	3.3	100	95	75	6	64-22	na	na	na	na	na	na
010L	27.3	4	100	77	60	6	64-28	2.4	100	77	60	6	AC20
012L	4.2	2.8	100	77	60	6	64-22	2.8	100	77	60	6	AC 20
014AL	5.5	4	100	77	60	6	64-28	na	na	na	na	na	na
015L	42.6	2.3	100	95	75	6	64-28	na	na	na	na	na	na
017L	1	2.3	100	95	75	6	64-28	2.8	100	77	60	6	AC 20
020L	26.6	2	100	77	60	6	64-28	2.3	100	77	60	6	AC 20
022L	9.3	2	100	77	60	6	64-28	1	100	77	60	6	AC 20
034L	9.2	2	100	77	60	6	64-28	1	100	77	60	6	AC 20
034L	17.2	2.3	100	95	75	6	64-28	na	na	na	na	na	na
035L	2.6	4.3	100	95	75	6	64-22	na	na	na	na	na	na
044L	8.1	6.3	100	95	75	6	AC 20	na	na	na	na	na	na
049L	21.1	2	100	77	60	6	AC 20	1.8	100	77	60	6	AC 20
066L	2.1	3	100	77	60	6	AC 20	6	100	77	60	6	AC 20
075L	6.7	2.3	100	77	60	6	AC 20	1	100	77	60	6	AC 20
084L	1.7	3.3	100	95	75	6	64-22	na	na	na	na	na	na
084L	36.7	4	100	95	75	6	64-28	1	100	77	60	6	AC 20
084L	94.8	4.8	100	95	75	6	64-28	na	na	na	na	na	na
091L	4	3	100	95	75	6	64-22	na	na	na	na	na	na
095L	12.8	1	100	95	75	6	64-28	1	100	77	60	6	AC 20
095L	93	4	100	95	75	6	64-28	1	100	77	60	6	AC 20
101L	9.1	4.3	100	77	60	6	64-22	na	na	na	na	na	na
110L	2.6	1.8	100	95	75	6	64-28	2.3	100	77	60	6	AC 20
113L	5.5	3	100	77	60	6	AC 20	6	100	77	60	6	AC 20
148L	8.9	2	100	77	60	6	64-28	1	100	77	60	6	AC 20
187L	6.7	2	100	77	60	6	AC 20	4	100	77	60	6	AC 20
202L	25.9	4.5	100	95	75	6	64-28	na	na	na	na	na	na
254L	7.6	2	100	77	60	6	64-22	1.3	100	77	60	6	AC 20
272L	12.1	2.3	100	77	60	6	64-22	2	100	77	60	6	AC 20
341L	1.9	2.3	100	77	60	6	64-22	2	100	77	60	6	AC 20
501L	0.5	3	100	95	75	6	64-28	na	na	na	na	na	na
805L	1.3	4	100	95	75	6	64-28	na	na	na	na	na	na

*na=not applicable

hac = AC layer thickness in inches

p34 = percent weight of aggregate passing ¾" sieve

p38 = percent weight of aggregate passing 3/8" sieve

p4 = percent weight of aggregate passing #4 sieve

p200 = percent weight of aggregate passing #200 sieve

acbind = AC binder performance grade

Table D3. Road ID, PCC, and Unbound Layer Data

Road Name	From	hpcc	hbase	es
005L	41.4	8.5	6	17024
007L	4.3	na	6.5	15740
007L	8.3	na	12	15740
007L	12.9	9.5	6	15740
007L	32.9	na	12	21112
008L	38.9	9.5	6	15740
010L	27.3	na	10.4	15740
012L	4.2	na	6.5	15740
014AL	5.5	na	16	15741
015L	42.6	10.3	6	21112
017L	1	8.5	6	32000
020L	26.6	na	13.5	10872
022L	9.3	na	7.5	15740
034L	9.2	na	6.5	15740
034L	17.2	10.3	6	21112
035L	2.6	8.3	6	15740
044L	8.1	10.5	6	15740
049L	21.1	na	6.5	15740
066L	2.1	na	10	15741
075L	6.7	na	6.5	10873
084L	1.7	9.5	6	15740
084L	36.7	9.8	6	32000
084L	94.8	10	6	15740
091L	4	9	6	15740
095L	12.8	9.5	6	32000
095L	93	9.5	6	32000
101L	9.1	na	6.5	15740
110L	2.6	8.5	6	32000
113L	5.5	na	10	15740
148L	8.9	na	6.5	15740
187L	6.7	na	12	10873
202L	25.9	8.3	6	15740
254L	7.6	na	8.5	15740
272L	12.1	na	7.5	15740
341L	1.9	na	7.5	15740
501L	0.5	8.3	6	15740
805L	1.3	8.3	6	15740

*na=not applicable

hpcc = PCC slab thickness in inches

hbase = granular base layer thickness in inches

es = subgrade resilient modulus in psi

Table D4. Road ID and Pavement-ME Outputs at 90% Reliability

Road Name	From	ESALs [mln]	IRI [in/mi]	TOT RUT [in]	TOT CRACK [%Area]	TRANS CRACK [ft/mi]	JPCP CRACK [ft/mi]	ALLIG CRACK [%Area]	LONG CRACK [ft/mi]	AC RUT [in]
005L	41.4	0.15	102	0.04	7.18	217	19.87	1.45	257	0.04
007L	4.3	0.59	112	0.54	23.59	27	na	1.45	3384	0.17
007L	8.3	0.40	106	0.37	1.50	27	na	1.50	610	0.11
007L	12.9	0.93	113	0.10	7.56	217	24.08	1.45	289	0.10
007L	32.9	0.99	106	0.35	22.40	26	na	1.49	914	0.16
008L	38.9	0.59	104	0.07	7.34	217	20.09	1.45	261	0.07
010L	27.3	2.31	131	0.63	3.50	27	na	3.50	2774	0.25
012L	4.2	0.15	102	0.35	5.08	27	na	1.45	1466	0.07
014AL	5.5	0.83	125	0.54	na	27	na	12.24	2235	0.19
015L	42.6	2.78	117	0.13	7.33	217	19.88	1.45	269	0.13
017L	1	0.57	107	0.07	7.34	217	19.98	1.45	260	0.07
020L	26.6	3.02	147	0.83	33.22	27	na	1.45	3605	0.34
022L	9.3	1.51	155	0.81	20.13	27	na	1.45	5455	0.27
034L	9.2	1.21	148	0.82	19.61	27	na	1.45	5583	0.28
034L	17.2	3.77	122	0.11	7.33	217	19.87	1.45	257	0.11
035L	2.6	0.32	104	0.06	7.33	217	19.87	1.45	260	0.06
044L	8.1	1.41	121	0.10	7.34	218	19.98	1.45	305	0.10
049L	21.1	1.41	150	0.74	31.03	27	na	1.45	5869	0.26
066L	2.1	1.86	120	0.49	1.60	27	na	1.60	666	0.20
075L	6.7	1.51	162	0.94	22.40	26	na	1.55	7140	0.31
084L	1.7	2.49	108	0.13	7.34	217	19.97	1.45	273	0.13
084L	36.7	3.01	110	0.15	7.46	217	22.20	1.45	297	0.15
084L	94.8	0.97	105	0.11	4.88	217	23.52	1.45	298	0.11
091L	4	0.97	103	0.07	7.18	217	19.87	1.45	258	0.07
095L	12.8	4.65	110	0.09	7.33	217	19.88	1.45	257	0.09
095L	93	2.55	116	0.14	7.57	217	24.16	1.45	285	0.14
101L	9.1	0.23	108	0.44	na	26	na	1.99	2503	0.10
110L	2.6	0.74	110	0.09	7.33	217	19.87	1.45	266	0.09
113L	5.5	1.51	136	0.45	1.55	27	na	1.55	456	0.16
148L	8.9	1.11	143	0.77	18.73	27	na	1.45	5166	0.24
187L	6.7	1.51	146	0.63	22.40	27	na	2.74	2387	0.21
202L	25.9	1.11	116	0.11	7.33	217	19.88	1.45	269	0.11
254L	7.6	1.51	157	0.84	25.71	33	na	1.45	5572	0.31
272L	12.1	1.41	150	0.74	31.36	41	na	1.45	5348	0.27
341L	1.9	0.65	124	0.61	29.54	28	na	1.45	3593	0.19
501L	0.5	1.11	115	0.09	7.33	217	19.88	1.45	258	0.09
805L	1.3	0.74	111	0.09	7.33	217	19.87	1.45	263	0.09

*na=not applicable

Table D5. Road ID and WiseCrax™ Performance Data

Road Name	From	L_TOT [ft/mi]	T_TOT [ft/mi]	L_WP [ft/mi]	L_NWP [ft/mi]	T_WP [ft/mi]	T_NWP [ft/mi]	TOTCRACK [ft/mi]	IRI_AVG [in/mi]	RUT_AVG [in]
005L	41.4	1069	1173	615	454	576	597	2242	78	0.10
007L	4.3	5898	1646	1796	4103	820	826	7545	164	0.18
007L	8.3	11850	1027	2924	8926	557	470	12878	132	0.11
007L	12.9	13086	13812	9870	12150	1673	2136	26897	171	0.19
007L	32.9	6351	564	964	5387	269	295	6915	108	0.15
008L	38.9	6934	2274	1660	1507	1077	1279	9208	75	0.07
010L	27.3	13657	8070	7540	6117	4004	4066	21727	270	0.26
012L	4.2	3939	83	205	3734	19	64	4022	108	0.06
014AL	5.5	3807	251	289	3518	119	131	4058	125	0.14
015L	42.6	7233	6717	2916	4316	2927	3790	13950	84	0.15
017L	1	7012	5080	714	6298	2470	2610	12092	117	0.13
020L	26.6	13695	8937	2089	11606	3654	5283	22632	115	0.31
022L	9.3	14411	20918	5772	8639	10392	10526	35329	127	0.14
034L	9.2	27363	5659	13868	13495	2787	2873	33023	124	0.18
034L	17.2	19760	5237	9856	9904	2580	2656	24997	198	0.30
035L	2.6	3167	2356	3509	7122	3520	3823	5523	127	0.08
044L	8.1	22749	11638	5795	7291	6599	7212	34387	178	0.19
049L	21.1	8007	495	5075	2932	272	222	8502	174	0.24
066L	2.1	10689	1406	883	9806	626	781	12095	122	0.14
075L	6.7	14833	15366	6340	8493	7523	7844	30200	165	0.26
084L	1.7	2884	2112	11882	10867	5688	5950	4996	58	0.12
084L	36.7	420	2124	78	342	1036	1088	2544	89	0.09
084L	94.8	633	359	2934	4000	924	1351	992	56	0.12
091L	4	112	468	9	103	208	260	579	50	0.12
095L	12.8	1888	8077	172	1716	3386	4691	9965	79	0.24
095L	93	3766	6293	580	3186	2734	3559	10060	80	0.15
101L	9.1	569	969	168	401	472	497	1538	92	0.07
110L	2.6	8969	6116	3175	5794	2808	3307	15085	90	0.14
113L	5.5	23262	14962	11867	11395	7158	7804	38224	232	0.20
148L	8.9	11046	9336	6257	4789	4806	4529	20382	119	0.11
187L	6.7	18730	11418	7415	11315	5453	5965	30148	129	0.25
202L	25.9	10632	7343	231	383	3949	4634	17975	117	0.15
254L	7.6	30085	15688	17130	12955	7982	7705	45773	176	0.16
272L	12.1	13642	9621	7204	6438	4566	5056	23264	181	0.26
341L	1.9	4078	4274	2141	1937	1918	2356	8352	175	0.13
501L	0.5	19818	10271	6901	12917	4507	5764	30089	113	0.20
805L	1.3	22020	3809	23	611	165	193	25828	158	0.18

Appendix E. Summary Material Property Inputs for Sensitivity Runs

Table E1. Baseline pavement structures and mix properties

Design Parameter	Structure I (3+5+0)	Structure II (4+6+0)	Structure III (3+3+6)
HMA Layer Thicknesses [in]			
Surface	3	4	3
Binder	5	6	3
Base	0	0	6
Asphalt Binder Inputs			
Surface AC Binder PG	64-22	64-22	64-22
Binder AC Binder PG	64-22	64-22	64-22
Base AC Binder PG	64-22	64-22	64-22
HMA Mix Properties[1]			
Surface AC Mix Type/ NMAS	S0.375	S0.375	S0.375
Binder AC Mix Type	S0.5	S0.5	S0.5
Base AC Mix Type	Granular Base A[2] + 2% PG 64-22		
Air Voids [percent]	4 (for all AC layers)		
Asphalt Binder Content[3] **[percent]**			
Surface AC	5.4-5.5	5.4-5.5	5.4-5.5[3]
Binder AC	4.8-4.9	4.8-4.9	4.8-4.9
Base AC	2	2	2

[1]See Figure E1 for gradation and volumetrics

[2]See Table E2 for granular base properties

[3]Depends on traffic level (See Figures E2 and E3)

Table E2. Basic granular base material properties (after CTDOT Division 400)

Input	Grading A	Grading B	Grading C
Aggregate Gradation (Percent Passing Sieve)			
125 mm (5 in)	100	100	
90 mm (3.6 in)		90-100	
37.5 mm(1 ½ in)	55-100	55-95	100
19 mm(3/4 in)			15-80
6.3 mm(1/4 in)	25-60	25-40	25-60
4.15 mm (#4)	20-52	20-52	20-52
2 mm (#10)	15-45	15-45	15-45
0.425 mm (#40)	5-25	5-25	5-25
0.15 mm (#100)	0-10	0-10	0-10
0.075 mm (#200)	0-5	0-5	0-5
Plasticity Index	1	1	1
Assigned Modulus [psi]	30,000	25,000	20,000

Notes: (1) Minimum Pb as specified in Table M.04.02-5. (2) Voids in Mineral Aggregates shall be computed as specified in AASHTO R 35. (3) Control point range is also defined as the master range for that mix. (4) Dust is considered to be the percent of materials passing the #200 sieve. (5) For WMA, lower minimum aggregate temperature will require Engineer's approval. (6) For WMA and PMA, the mix temperature shall meet manufacturer's recommendations.

	S0.25		S0.375		S0.5		S1	
Sieve	CONTROL POINTS (3)		CONTROL POINTS(3)		CONTROL POINTS(3)		CONTROL POINTS(3)	
inches	Min (%)	Max (%)	Min (%)	Max (%)	Min (%)	Max (%)	Min (%)	Max (%)
2.0	-	-	-	-	-	-	-	-
1.5	-	-	-	-	-	-	100	-
1.0	-	-	-	-	-	-	90	100
3/4	-	-	-	-	100	-	-	90
1/2	100	-	100	-	90	100	-	-
3/8	97	100	90	100	-	90	-	-
#4	-	90	-	90	-	-	-	-
#8	32	67	32	67	28	58	19	45
#16	-	-	-	-	-	-	-	-
#30	-	-	-	-	-	-	-	-
#50	-	-	-	-	-	-	-	-
#100	-	-	-	-	-	-	-	-
#200	2.0	10.0	2.0	10.0	2.0	10.0	1.0	7.0
Pb (1)	-	-	-	-	-	-	-	-
VMA (2) (%)	16.0 ± 1		16.0 ± 1		15.0 ± 1		13.0 ± 1	
VA (%)	4.0 ± 1		4.0 ± 1		4.0 ± 1		4.0 ± 1	
Gse	JMF value		JMF value		JMF value		JMF value	
Gmm	JMF ± 0.030		JMF ± 0.030		JMF ± 0.030		JMF ± 0.030	
Dust/Pbe(4)	0.6 – 1.2		0.6 – 1.2		0.6 – 1.2		0.6 – 1.2	
Agg. Temp(5)	280 – 350°F		280 – 350°F		280 – 350°F		280 – 350°F	
Mix Temp(6)	265 – 325°F		265 – 325°F		265 – 325°F		265 – 325°F	
Design TSR	≥ 80%		≥ 80%		≥ 80%		≥ 80%	
T-283 Stripping	Minimal, as determined by the Engineer							

Figure E1. Superpave Master Range for Bituminous Concrete Mixture Design Criteria (after Table M.04.02–2, CTDOT Section M.04 – Bituminous Concrete)

Traffic Level	Design ESALs (million)	Number of Gyrations by Superpave Gyratory Compactor	
		Nini	Ndes
1*	< 0.3	6	50
2	0.3 to < 3.0	7	75
3	≥3.0	8	100

Figure E2. Superpave Master Range for Traffic Levels and Design Volumetric Properties (after Table M.04.03– 6, CTDOT Section M.04 – Bituminous Concrete)

Mix Type	Level	Binder Content Minimum (1)
S0.25	1*	5.6
S0.25	2	5.5
S0.25	3	5.4
S0.375	1*	5.6
S0.375	2	5.5
S0.375	3	5.4
S0.5	1*	5.0
S0.5	2	4.9
S0.5	3	4.8
S1	1*	4.6
S1	2	4.5
S1	3	4.4

Figure E3. Superpave Minimum Binder Content by Mix Type and Traffic Level (after Table M.04.02–5, CTDOT Section M.04 – Bituminous Concrete)